

Introductory visual lecture on QCD at large- N_c : bound states, chiral models, and phase diagram

FRANCESCO GIACOSA

Institute of Physics, Jan Kochanowski University,
ul. Uniwersytecka 7, 25-406, Kielce, Poland

Institute for Theoretical Physics, Johann Wolfgang Goethe University,
Max-von-Laue-Str. 1, 60438, Frankfurt am Main, Germany

In these lectures, we present the behavior of conventional $\bar{q}q$ mesons, glueballs, and hybrids in the large- N_c limit of QCD. To this end, we use an approach based on rather simple “NJL-like” bound-state equations. The obtained large- N_c scaling laws are general and coincide with the known results. A series of consequences, such as the narrowness of certain mesons and interaction types, the behavior of chiral and dilaton models at large- N_c , and the relation to the compositeness condition and the standard derivation of large- N_c results, are explained. The bound-state formalism shows also that mesonic molecular and dynamically generated states do not form in the large- N_c limit. The same fate seems to apply also for tetraquark states, but here further studies are needed. Next, following the same approach, baryons are studied as bound states of a generalized diquark ($N_c - 1$ antisymmetric object) and a quark. Similarities and differences with regular mesons are discussed. All the standard scaling laws for baryons and their interaction with mesons are correctly reproduced. The behavior of chiral models involving baryons and describing chirally invariant mass generation is investigated. Finally, properties of QCD in the medium at large- N_c are studied: the deconfinement phase transition is investigated along the temperature and the chemical potential directions, respectively. While the critical temperature for deconfinement T_{dec} is N_c independent, the critical chemical potential is not and increases for growing N_c , thus for very large N_c one has confined matter below T_{dec} and deconfined above. Yet, in the confined phase but for large densities, one has a stiff-matter phase whose pressure is proportional to N_c (just as a gas of quarks would do) in agreement with a quarkyonic phase. Within the QCD phase diagrams, the features of different models at large- N_c are reviewed and the location of the critical endpoint is discussed. In the end, the very existence of nuclei and the implications of large- N_c arguments for neutron stars are outlined.

1. Introduction

In Quantum Chromodynamics (QCD) each quark can appear in three charges denoted as colors: red (R), green (G), and blue (B). This applies for any of the six quark flavors present in Nature (the light quarks flavors u, d, s and the heavy quark flavors c, b, t [1]). The force carriers, the gluons, can be thought as color-anticolor objects, for a total of $9 - 1 = 8$ combinations [2, 3].

The origin of colors can be better understood by looking at the fundamental properties of QCD, which is a gauge theory built under local invariance of the color group $SU(3)$. The quarks transform under the fundamental representation and the gluons under the adjoint representation.

Why QCD has 3 colors ($N_c = 3$, where N_c stands for the number of colors) and not, e.g. 7? At present, there is no compelling answer for that, at least not within the Standard Model (SM). One may eventually ask if the choice $N_c \neq 3$ would allow for stable nuclei, and if this is not the case [4], resort to a kind of anthropic argument.

Yet, here we are not interested in this type of questions, but rather in the study of N_c different from 3, and in particular the study of the limit in which N_c is a ‘large’ number, in order to understand better our world with $N_c = 3$. This is indeed the so-called QCD in the large- N_c limit, initiated by ‘t Hooft [5] and further investigated in several review papers and lectures [6, 7, 8, 9, 10, 11, 12] (and refs. therein).

At first, the idea to consider an expansion along N_c may sound as strange: how could *anything* valid for, say, $N_c = 101$, be also somewhat relevant for the physical case $N_c = 3$? In other words, how can $N_c = 3$ be considered a ‘large’ number [6]? As we shall see, that depends. In some (indeed the majority of) cases, the number 3 turns out to be large.

In particular, in these lectures we intend to revisit the behavior of bound states of QCD in the large- N_c limit. To this end, we recall that quarks and gluons are confined in hadrons, further classified as mesons (bosonic hadrons) and baryons (baryonic hadrons).

Mesons can be divided into conventional ones corresponding to quark-antiquark states (quarkonia), and to exotic or non-conventional types, such as glueballs, hybrids but also mesonic molecules, dynamically generated states, and compact tetraquark states (bound states of diquarks). Quite interestingly, quarkonia, glueballs, and hybrids ‘survive’ in the large- N_c limit: this means that their masses are N_c -independent, and their widths decrease with N_c , implying that these objects become stable in the large- N_c limit. We shall revisit these well known results as well as the specific scaling laws in a novel fashion, that involves the study of bound-state equations. For the latter, we chose the easiest possible approach that describes bound-state

equations similar to the ones found in the Nambu Jona-Lasinio (NJL) model [13, 14, 15] (technically, the kernel is separable). Indeed, these bound state equations are also similar to approaches involving the compositeness conditions, e.g. [16, 17, 18, 19]. Yet, it should be stressed that our aim is not to actually solve these equations, but just to discuss their large- N_c behavior. The latter is (thought to be) independent on the particular approach and applies also to more advanced methods for bound states, such as Bethe-Salpeter equations in QCD [20, 21, 22]. Quite interestingly, the proposed large- N_c treatment can also help to understand, from a different perspective, various large- N_c features. Namely, we shall re-derive known results in a different and quite simple way. The coupling of bound objects to their constituents is also an intermediate consequence of the chosen approach.

As additional applications, we shall present the large- N_c study of the linear sigma model (LSM) [23, 24], the dilaton [25, 26, 27, 28], and their interconnection. Many other properties (weak decay constant, decay chains, etc.) shall be discussed as well. The connection of our bound-state approach to the commonly implemented one that uses correlators and currents is also shown.

The fate of mesonic molecular and dynamically generated states is different: they fade away in the large- N_c limit. Indeed, we shall recover this result within the bound state approach. A peculiar case, not yet fully solved, is if all tetraquark types (among which molecules are only a specific example) fade out as well. It was long believed that this is the case, but this conclusion was revisited by Weinberg in 2013 [29], in which he argued that certain tetraquarks could exist in the large- N_c and, if that is the case, their mass scale as N_c^0 and their width as N_c^{-1} , just as regular quarkonia. The work [29] was followed by a series of papers on the subject [12, 30, 31, 32, 33, 34]. Up to now, the existence of such peculiar tetraquarks in the large- N_c limit is not settled. We shall discuss what the bound-state approach has to say for tetraquarks as well.

Baryons will be also briefly discussed in this work. We shall concentrate on conventional baryons, which for $N_c = 3$ are made by 3 quarks and for an arbitrary N_c by N_c quarks. We shall present some interesting similarities between conventional baryons and conventional mesons. To this end, we treat baryons in a way similar to conventional mesons: they shall be seen as a bound state of a quark and of a generalized diquark, the latter being the antisymmetric combination of $N_c - 1$ quarks. Within this context, we will re-derive the large- N_c scaling for baryons. As an application, we study chiral models implementing baryonic fields and investigate possible ways to generate their mass in a chiral invariant manner and in agreement with large- N_c expectations.

In the end, we recall -concisely- some relevant facts concerning the large-

N_c behavior of QCD at finite temperature and density, concentrating on the phase diagram and the quarkyonic phase [35, 36, 37, 38], chiral models in the medium [24, 39], nuclear matter [4, 40], and neutron stars [41, 42].

The style of these lectures is focused on the conceptual and qualitative features of QCD at large- N_c . Moreover, many pictures shall be presented for a better visualization of the scaling properties. These lectures on large- N_c complete previous lectures on chiral models mesons beyond the quark-antiquark picture given few years ago [43].

The article is organized as follows. In Sec. 2 we introduce QCD for an arbitrary number of colors together with the double-line notation and the groups $SU(N)$ and $U(N)$, we discuss the QCD running coupling in the framework of the 't Hooft large- N_c limit, and we qualitatively argue that the main features of the propagators of quarks and gluons are N_c -independent. Next, in Sec. 3 we study mesons in the large- N_c limit, first the conventional ones (quarkonia) and related topics (chiral models,...), then the exotic glueballs (together with the dilaton), hybrids, and four-quark objects. In Sec. 4 we present conventional baryons and their implementation in chiral models. In Sec. 5 we discuss the main properties of QCD matter at nonzero temperature and chemical potential for large N_c . In Sec. 6 conclusions are summarized.

2. QCD for arbitrary N_c

2.1. QCD Lagrangian of any N_c

We present the Lagrangian of QCD for an arbitrary number of colors N_c and quark flavors N_f (see, for instance, [2, 3]):

$$\begin{aligned} \mathcal{L}_{QCD} = \text{Tr} \left[\bar{q}_i (i\gamma^\mu D_\mu - m_i) q_i - \frac{1}{2} G_{\mu\nu} G^{\mu\nu} \right], \quad D_\mu = \partial_\mu - ig_0 A_\mu, \\ G_{\mu\nu}^a = \partial_\mu A_\nu - \partial_\nu A_\mu - ig_0 [A_\mu, A_\nu], \quad A_\mu = A_\mu^a t^a. \end{aligned} \quad (1)$$

Above, a is the color index with $a = 1, \dots, N_c^2 - 1$, t^a are $N_c \times N_c$ matrix generators of the group $SU(N_c)$ (see below), f_{abc} are the structure constants of $SU(N_c)$, and $i = 1, \dots, N_f$ is the flavor index (N_f is the number of quark flavors). Moreover, the coupling constant g_0 is an adimensional parameter of the classical Lagrangian and m_i is the bare mass of the i -th quark flavor. Note, in the chiral limit ($m_i = 0$, for each i) the Lagrangian is invariant under dilatation transformation, since no dimensionful parameter is present in the classical theory. This symmetry is broken by quantum fluctuations (trace anomaly, see Sec. 3.2).

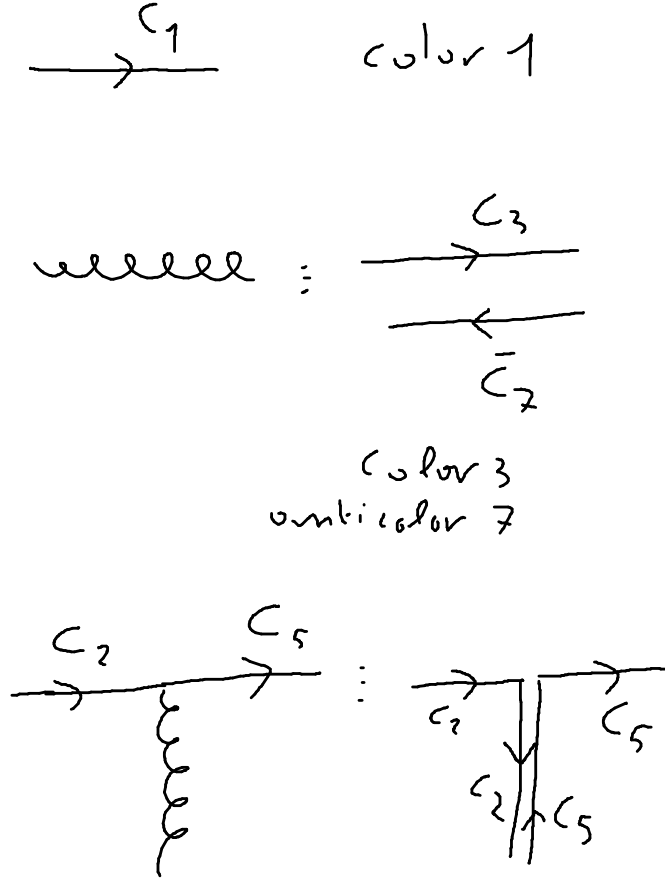


Fig. 1. Free quark, free gluon, and quark-gluon vertex. The double-line notation for the gluons is also shown. The specific choice of colors refers to illustrative examples: the free quark is taken with color C_1 , the free gluon carries \bar{C}_7C_3 , and the vertex shows how a quark C_2 changes into C_5 via the interaction with a \bar{C}_2C_5 gluon.

The part of Eq. (1) containing only gluons is called the Yang-Mills (YM) Lagrangian:

$$\mathcal{L}_{YM} = \text{Tr} \left[-\frac{1}{2} G_{\mu\nu} G^{\mu\nu} \right] = -\frac{1}{4} G_{\mu\nu}^a G^{a,\mu\nu}. \quad (2)$$

For $N_c > 1$, the YM Lagrangian contains 3-gluon and 4-gluon vertices. The

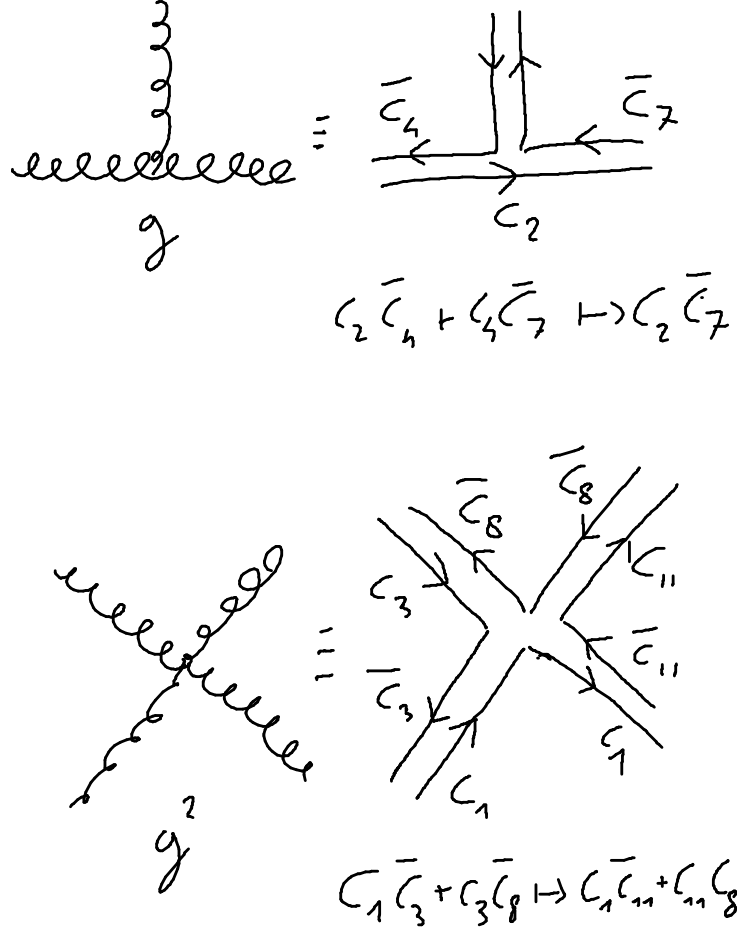


Fig. 2. Three-leg and four-leg in the standard and double-line notation. The specific choice of colors on the right part refers to examples.

gluonic self-interactions are a fundamental property of nonabelian theories. In turn, this feature implies that gluonic bound states, called glueballs, are possible [44, 45, 46], see also Sec. 3.2.

In Nature, $N_c = 3$ and $N_f = 6$. However, depending on the problem, one can consider different values for N_c and N_f . For instance, low-energy QCD is realized for $N_c = 3$ and $N_f = 3$, i.e. only light quarks are retained. Moreover, varying N_c is the main goal of large- N_c studies.

In Figs. 1 and 2 we present the Feynman diagrams that follow from the QCD Lagrangian. In particular, in Fig. 1 the fundamental quark-gluon

vertex is depicted, while in Fig. 2 the gluonic self-interactions are shown. In both cases, gluons are also represented via the so-called double line notation, that ‘naively speaking’ corresponds to a quark and an antiquark. In order to understand this point better, we need to have a closer look at the gluon field.

The Yang-Mills field $A_\mu(x)$ is a $N_c \times N_c$ matrix that can be expressed as:

$$A_\mu(x) = \sum_{a=1}^{N_c^2-1} A_\mu^a(x) t^a, \quad (3)$$

where t^a is a set of $N_c^2 - 1$ Hermitian and traceless matrices (see below), while the quark field is a vectors in color space with

$$q_i = \begin{pmatrix} q_{1,i} \\ q_{1,i} \\ \dots \\ q_{N_c,i} \end{pmatrix}, \quad (4)$$

where $i = 1, \dots, N_f$ is the flavor index.

Under $SU(N_c)$ local gauge transformations these fields transform as:

$$q_i \rightarrow U(x) q_i, \quad A_\mu(x) \rightarrow A'_\mu(x) = U(x) A_\mu(x) U^\dagger(x) - \frac{i}{g_0} U(x) \partial_\mu U^\dagger(x), \quad (5)$$

with

$$U(x) = e^{i\theta_a(x)t^a}, \quad a = 1, \dots, N_c^2 - 1 \quad (= 8 \text{ for } N_c = 3), \quad (6)$$

where the quantities $\theta_a(x)$ are arbitrary functions of the space-time variable $x \equiv x^\mu \equiv (t, \mathbf{x})$.

The Lagrangian \mathcal{L}_{QCD} has been constructed to be invariant under the local gauge transformations of Eq. (5).

A particularly useful limit is the one in which $U(x) = U$ is a constant matrix (thus, θ_a are $N_c^2 - 1$ fixed constants). Then:

$$q_i \rightarrow U q_i, \quad A_\mu(x) \rightarrow A'_\mu(x) = U A_\mu(x) U^\dagger. \quad (7)$$

In Figs. 1 and 2 a double-line notation for the gluon is presented, according to which the gluon field is described with the help of two indices

$$A_\mu^{(a,b)}(x) \equiv A_\mu^{(a,b)}(x) \text{ with } a, b = 1, \dots, N_c. \quad (8)$$

This point reflects the adjoint Nature of the gluon field that, for what concerns color, can be seen (besides the singlet colorless configuration that is not present) as a quark-antiquark object. For instance:

$$A^{(2,5)} \equiv \bar{C}_2 C_5, \quad (9)$$

implying that this gluon configuration contains the color C_5 and the anti-color \bar{C}_2 .

Indeed, this choice corresponds to a specific choice for the basis:

$$A_\mu(x) \equiv \sum_{a=1}^{N_c} \sum_{b=1}^{N_c} A_\mu^{(a,b)} t^{(a,b)} \quad (10)$$

where the N_c^2 matrices $t^{(a,b)}$ are given by:

$$\left(t^{(a,b)} \right)_{c,d} = \delta_{ac} \delta_{bd} \quad (11)$$

Note, there is above a matrix ‘too much’. One should remove the color singlet (traceless) configuration. Yet, for large- N_c this additional contribution is negligible, so we will not bother to subtract it. Note, also the tensor $G_{\mu\nu}$ can be expressed in this basis as

$$G_{\mu\nu} = \sum_{a=1}^{N_c} \sum_{b=1}^{N_c} G_{\mu\nu}^{(a,b)} t^{(a,b)} . \quad (12)$$

Indeed, while this choice for the matrices t^a may be useful to realize the double-line idea for a gluon, it is not what is usually employed for the specific cases of $N_c = 2$ or $N_c = 3$, see the next subsection.

2.2. Brief recall of $SU(N)$

Before we continue, it is important to recall some basic properties of the groups $U(N)$ and $SU(N)$ (see e.g. Ref. [47]). An element of the group $U(N)$ is a complex $N \times N$ matrix such that:

$$U^\dagger U = U U^\dagger = 1_N , \quad (13)$$

thus U can be expressed as:

$$U = e^{i\theta_a t^a}, \quad a = 0, 1, \dots, N^2 - 1 , \quad (14)$$

where the matrices t^a are N^2 linearly independent $N \times N$ Hermitian matrices, implying that Eq. (13) is fulfilled. A specific example for such matrices has been encountered in Eq. (11), but this is not the most convenient choice. Following the usual convention, we set:

$$t^0 = \frac{1}{\sqrt{2N}} 1_N , \quad (15)$$

and for the other matrices, we choose:

$$\text{Tr} [t^a t^b] = \frac{1}{2} \delta^{ab} \text{ with } a, b = 0, 1, \dots, N^2 - 1, \quad (16)$$

then

$$\text{Tr} [t^a] = 0 \text{ for } a = 1, \dots, N^2 - 1. \quad (17)$$

A $N \times N$ matrix U belongs to the group $SU(N)$ if the following two equations are fulfilled:

$$U^\dagger U = U U^\dagger = 1_N, \quad \det U = 1. \quad (18)$$

It is clear that a matrix belonging to $SU(N)$ can be written as $U = e^{i\theta_a t^a}$ with $a = 1, \dots, N^2 - 1$ (the identity matrix, which is not traceless, is left out). Then:

$$\det U = e^{\text{Tr} [i \sum_{a=1}^{N^2-1} \theta_a t^a]} = 1. \quad (19)$$

The matrices t^a with $a = 1, \dots, N^2 - 1$ are the generators of $SU(N)$ and fulfill the algebra:

$$[t^a, t^b] = i f^{abc} t^c \text{ with } a, b, c = 1, \dots, N^2 - 1, \quad (20)$$

where f^{abc} are the corresponding antisymmetric structure constants, see [47] for their explicit form. Namely, the commutator of two Hermitian matrices is anti-Hermitian and traceless, therefore it must be expressed as a sum over t^a for $a = 1, \dots, N^2 - 1$.

For $N = 2$ a useful choice is $t^a = \frac{\tau^a}{2}$ ($a = 1, 2, 3$) with the Pauli-matrices τ^a , while for $N = 3$ one sets $t^a = \frac{\lambda^a}{2}$ ($a = 1, \dots, 8$) with the Gell-Mann matrices λ^a .

Finally, we recall also that there is a subgroup of $SU(N)$, denoted as the center $Z(N)$, whose N elements are given by [3]:

$$Z = Z_n = e^{i \frac{2\pi n}{N}} 1_N, \quad n = 0, 1, 2, \dots, N - 1. \quad (21)$$

Each Z_n corresponds to a proper choice of the parameters θ_a (the case $Z_0 = 1_N$ corresponds to the simple case $\theta_a = 0$, the other elements to more complicated choices). This group plays an important role at nonzero temperature as an indicator of confinement, since the symmetry is realized in the QCD vacuum and in the confined phase (at small T), but is broken in the deconfined one (at large T) [3, 48].

2.3. Running coupling of QCD

The coupling ‘constant’ g_0 entering in the classical QCD Lagrangian of Eq. (1) turns into a running coupling when QCD is quantized. At one-loop level (which is enough for our illustrative purposes here) one has [2]:

$$\mu \frac{dg}{d\mu} = -bg^3, \quad (22)$$

with

$$b = \frac{1}{2} \frac{1}{8\pi^2} \left(\frac{11}{3} N_c - \frac{2}{3} N_f \right) \quad (23)$$

and where

$$g_{QCD} \equiv g \equiv g(\mu) \quad (24)$$

refers to the running QCD coupling. In this work, whenever g will be presented, it always refers to the fundamental QCD coupling. Other coupling constants shall carry an appropriate subscript specifying to what they refer. For a detailed description of the QCD running coupling for $N_c = 3$ we refer to Ref. [49] and refs. therein.

In Nature $N_c = 3$ and N_f ranges from 2 to 6, in dependence on the number of considered quark flavors; in any case, $b > 0$. Note, $b > 0$ is definitely also true in the large- N_c limit upon keeping N_f fixed, as we shall do here. This is the so-called ‘t Hooft large- N_c scheme [5].

Upon fixing g_0 at a certain (large, or ultraviolet (UV)) energy scale Λ_{UV} and by integrating:

$$\int_g^{g_0} dg' \frac{dg'}{g'^3} = - \int_\mu^{\Lambda_{UV}} dg' b \frac{d\mu'}{\mu'} = \left[\frac{g'^{-2}}{-2} \right]_g^{g_0} = -b \ln \frac{\Lambda_{UV}}{\mu} = b \ln \frac{\mu}{\Lambda_{UV}}; \quad (25)$$

$$\frac{1}{g_0^2} - \frac{1}{g^2} = -2b \ln \frac{\mu}{\Lambda_{UV}}; \quad (26)$$

$$\frac{1}{g^2} = \frac{1}{g_0^2} + 2b \ln \frac{\mu}{\Lambda_{UV}} = \frac{1 + 2bg_0^2 \ln \frac{\mu}{\Lambda_{UV}}}{g_0^2}. \quad (27)$$

Hence:

$$g^2 = \frac{g_0^2}{1 + 2bg_0^2 \ln \frac{\mu}{\Lambda_{UV}}}. \quad (28)$$

Then:

$$g^2(\mu) = \frac{g_0^2}{1 + 2bg_0^2 \ln \frac{\mu}{\Lambda_{UV}}} = \frac{g_0^2}{1 + \frac{g_0^2}{8\pi^2} \left(\frac{11}{3} N_c - \frac{2}{3} N_f \right) \ln \frac{\mu}{\Lambda_{UV}}}. \quad (29)$$

One has (by construction):

$$g^2(\mu = \Lambda_{UV}) = g_0^2 . \quad (30)$$

Upon setting the denominator to zero

$$1 + \frac{g_0^2}{8\pi^2} \left(\frac{11}{3} N_c - \frac{2}{3} N_f \right) \ln \frac{\mu}{\Lambda_{UV}} = 0 , \quad (31)$$

we obtain the the so-called Λ_{QCD} scale as a Landau pole of the running coupling:

$$\Lambda_{QCD} = \Lambda_{UV} \exp \left[-\frac{8\pi^2}{g_0^2 \left(\frac{11}{3} N_c - \frac{2}{3} N_f \right)} \right] . \quad (32)$$

The existence of a pole of the coupling is an artifact of the one-loop perturbative approach, but it signalizes that at the energy scale Λ_{QCD} the running coupling becomes large. In Ref. [50], using the FRG approach, it is shown that no infinity of the QCD running coupling takes place.

The value of the bare coupling can be expressed as:

$$g_0^2 = -\frac{1}{\left(\frac{11}{3} N_c - \frac{2}{3} N_f \right) \ln \frac{\Lambda_{QCD}}{\Lambda_{UV}}} \frac{8\pi^2}{\Lambda_{UV}} . \quad (33)$$

Here, we intend to study the limit in which the low-energy scale Λ_{QCD} is independent on N_c ('t Hooft limit). We then require that

$$g_0^2 \propto \frac{1}{N_c} , \quad (34)$$

then

$$g_0 \propto \frac{1}{\sqrt{N_c}} . \quad (35)$$

Next, upon eliminating the UV scale Λ_{UV} we find:

$$\begin{aligned} g^2(\mu) &= \frac{g_0^2}{1 + \frac{g_0^2}{8\pi^2} \left(\frac{11}{3} N_c - \frac{2}{3} N_f \right) \ln \frac{\mu}{\Lambda_{UV}}} \\ &= -\frac{\frac{1}{\left(\frac{11}{3} N_c - \frac{2}{3} N_f \right) \ln \frac{\Lambda_{QCD}}{\Lambda_{UV}}} \frac{8\pi^2}{\Lambda_{UV}}}{1 + \left(-\frac{1}{\left(\frac{11}{3} N_c - \frac{2}{3} N_f \right) \ln \frac{\Lambda_{QCD}}{\Lambda_{UV}}} \frac{8\pi^2}{\Lambda_{UV}} \right) \frac{1}{8\pi^2} \left(\frac{11}{3} N_c - \frac{2}{3} N_f \right) \ln \frac{\mu}{\Lambda_{UV}}} \\ &= \frac{8\pi^2}{\left(\frac{11}{3} N_c - \frac{2}{3} N_f \right) \ln \frac{\mu}{\Lambda_{QCD}}} . \end{aligned} \quad (36)$$

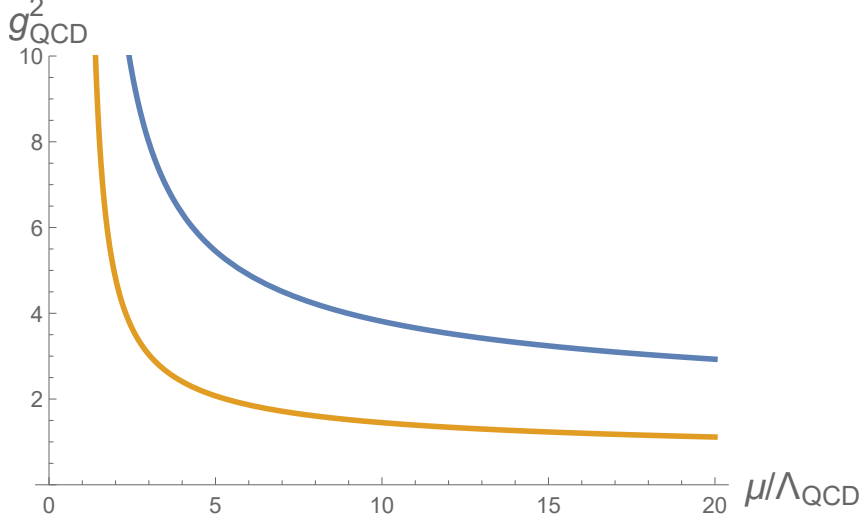


Fig. 3. Running coupling of QCD of Eq. (38) for $N_c = 3$ (upper, blue curve) and for $N_c = 7$ (lower, yellow curve). The Landau pole is the same in both cases, in agreement with the 't Hooft large- N_c limit.

Thus, in terms of μ and Λ_{QCD} the one-loop running coupling can be expressed as:

$$g^2(\mu) = \frac{8\pi^2}{\left(\frac{11}{3}N_c - \frac{2}{3}N_f\right)} \frac{1}{\ln \frac{\mu}{\Lambda_{QCD}}} . \quad (37)$$

For large- N_c we get:

$$g_{QCD}^2 \equiv g^2(\mu) = \frac{8\pi^2}{\left(\frac{11}{3}N_c\right)} \frac{1}{\ln \frac{\mu}{\Lambda_{QCD}}} \propto \frac{1}{N_c} . \quad (38)$$

As for the bare coupling, also the running coupling scales as $1/\sqrt{N_c}$ if Λ_{QCD} and N_f are kept N_c -independent. In Fig. 3 the coupling $g(\mu)$ is plotted for $N_c = 3$ and $N_c = 7$.

The fact that the coupling g is a function of μ is also at the basis of the so-called trace anomaly: the original classical invariance under dilatation symmetry in the chiral limit is broken by the emergence of the energy scale Λ_{QCD} .

The behavior of the running coupling is in agreement with two crucial properties of QCD: asymptotic freedom and confinement. The former is due to the fact that the coupling becomes smaller at large energies, at which quarks and gluons interact perturbatively. The latter implies that quarks and gluons are confined into hadrons. This is not directly provable, but it fits well with the fact that the coupling becomes large at small energies.

The coupling constant becomes also small in the large- N_c limit, but at the same time the number of colors grows. So, at first it is hard to say what it will happen in this regime. It is assumed (and one finds no contradiction) that many of the properties of QCD are still valid in the large- N_c limit, among which confinement, asymptotic freedom, and spontaneous symmetry breaking (SSB).

For completeness, we summarize below also additional symmetries (besides ‘local’ color symmetry) of QCD for $m_i = 0$ (more details in Ref. [43]). To this end, the quark field q_i is split into

$$q_i = q_{i,R} + q_{i,L} \quad (39)$$

with

$$q_{i,L} = \frac{1 - \gamma^5}{2} q_i \text{ and } q_{i,R} = \frac{1 + \gamma^5}{2} q_i . \quad (40)$$

(i) The dilatation transformation ($x^\mu \rightarrow \lambda^{-1} x^\mu$, together with $A_\mu \rightarrow \lambda A_\mu$ and $q_i \rightarrow \lambda^{3/2} q_i$) is a classical symmetry of QCD in the chiral limit, which is broken by quantum fluctuations (trace anomaly), in turn implying the emergence of the energy scale Λ_{QCD} outlined above.

(ii) Chiral symmetry is expressed as

$$U(N_f)_R \times U(N_f)_L \equiv U(1)_V \times SU(N_f)_V \times U(1)_A \times SU(N_f)_A .$$

According to it, quark fields transform as

$$q_i = q_{i,L} + q_{i,R} \rightarrow U_{L,i,j} q_{j,L} + U_{R,i,j} q_{j,R} , \quad (41)$$

where U_L and U_R are 3×3 unitary matrices that mix flavor (but no color!) degrees of freedom. This symmetry undergoes SSB:

$$SU(N_f)_V \times SU(N_f)_A \rightarrow SU(N_f)_V . \quad (42)$$

(iii) The axial symmetry $U(1)_A$ corresponds to the choice $U_L = U_R^\dagger = \exp(-i\alpha/2)$. This symmetry is also broken by quantum fluctuations and the corresponding anomaly is called axial or chiral anomaly.

(iv) There is also an explicit breaking of $U(1)_A$ and $SU(N_f)_A$ through nonzero bare quark masses. An explicit breaking of $SU(N_f)_V$ occurs if the quark masses are different.

In the following, in order to keep the discussion as simple as possible, we will omit -if not stated differently- the flavor index $i = u, d, \dots$. Yet, the main features of QCD at large- N_c are not dependent on the number of flavors. Yet, whenever needed, we will explicitly mention the quark flavors as well.

2.4. Quark and gluon propagators

Here we shall have a quick look at the quark and the gluon propagators. The main message is simple: their main features are retained in the large- N_c limit. It means that they can be “naively” regarded as large- N_c invariant objects.

Let us be more specific. For the quark propagator, there is an infinity class of diagrams which are large- N_c independent. They are depicted in Fig. 4 and 5. These are the famous ‘planar diagrams’ since they can be drawn on a plane without intersection [5, 6]. In Fig. 5 a detailed explanation of the large- N_c counting is presented.

Admittedly, there are also non-planar diagrams which disappear in the large- N_c limit, thus the large- N_c world is slightly simpler than the one for $N_c = 3$. An example of a non-planar diagram for the quark propagator can be found in Fig. 6. Yet, the main features are expected to be contained in the large- N_c dominant terms, which survive the limit $N_c \rightarrow \infty$.

An important consequence is that many features related to low-energy QCD, among which SSB [51], are still valid for large N_c . For instance, the quark u develops a constituent mass due to SSB as [14]:

$$m_u^{\text{bare}} \simeq 3 \text{ MeV} \rightarrow m_u^* \simeq 300 \text{ MeV}, \quad (43)$$

which holds also for arbitrary large values of N_c . Since the main contributions to the quark propagator are large- N_c independent, the constituent mass $m_u^* \simeq 300 \text{ MeV}$ scales as N_c^0 . Then, as a consequence the whole low-energy mesonic phenomenology is quite similar: the pions and kaons are still Goldstone bosons, the vector particles carry a mass of about $2m_u^*$, see later on for more details on mesons. An important exception regards the chiral anomaly, which indeed goes away for $N_c \rightarrow \infty$. In the chiral limit, the mass of the singlet η_0 scales as $m_{\eta_0}^2 \propto N_c^{-1}$ [52], thus for $N_f = 3$ a full nonet of Goldstone bosons is actually realized in the chiral limit for large N_c .

The gluon propagator is dressed by large- N_c independent planar diagrams, that are expected to be responsible for its main properties. In this sense, this feature is analogous to the quark propagator. One may roughly speak about an effective gluon mass of about $m_g^* \simeq 800 \text{ MeV}$ [53], even though the term ‘mass’ should be used with extreme care: one should better refer to an energy scale entering into the propagator without breaking of local color gauge invariance [54]. This effective energy scale is N_c -independent. As a consequence, glueballs carry a mass (starting at) about $2m_g^*$, which is also N_c independent, as we shall discuss in more detail below.

Summarizing, the quark and the gluon propagators contain a class of dominant N_c -independent ($\propto N_c^0$) contributions. For our purposes, these propagators can be seen as independent from the number of colors.

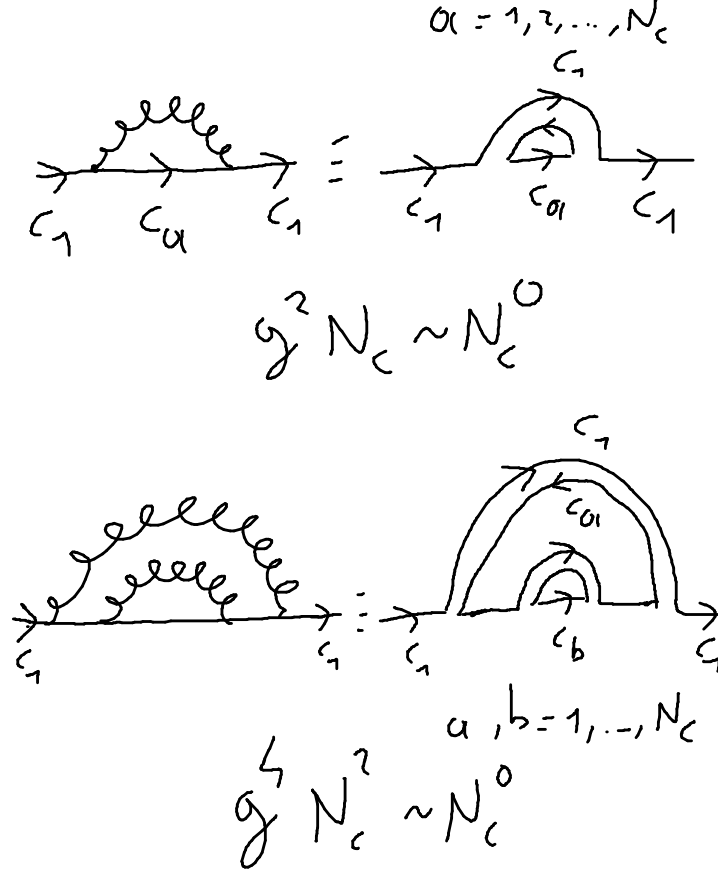


Fig. 4. Two planar diagrams describing the self-energy of the quark (which is taken to have a specific color C_1 for definiteness). Both diagrams are ‘mass contributions’ and scale as N_c^0 . There is an infinity of such planar diagrams.

2.5. Brief recall of mesons and baryons at large- N_c

Quarks and gluons are not the physical states that hit our detectors. They are confined into hadrons, i.e. mesons (integer spin) and baryons (semi-integer spin).

A *conventional meson* is a meson constructed out of a quark and an antiquark. Although it represents only one of (actually infinitely many) possibilities to build a meson, the vast majority of mesons of the PDG [1] can be consistently (and successfully) interpreted as belonging to a quark-

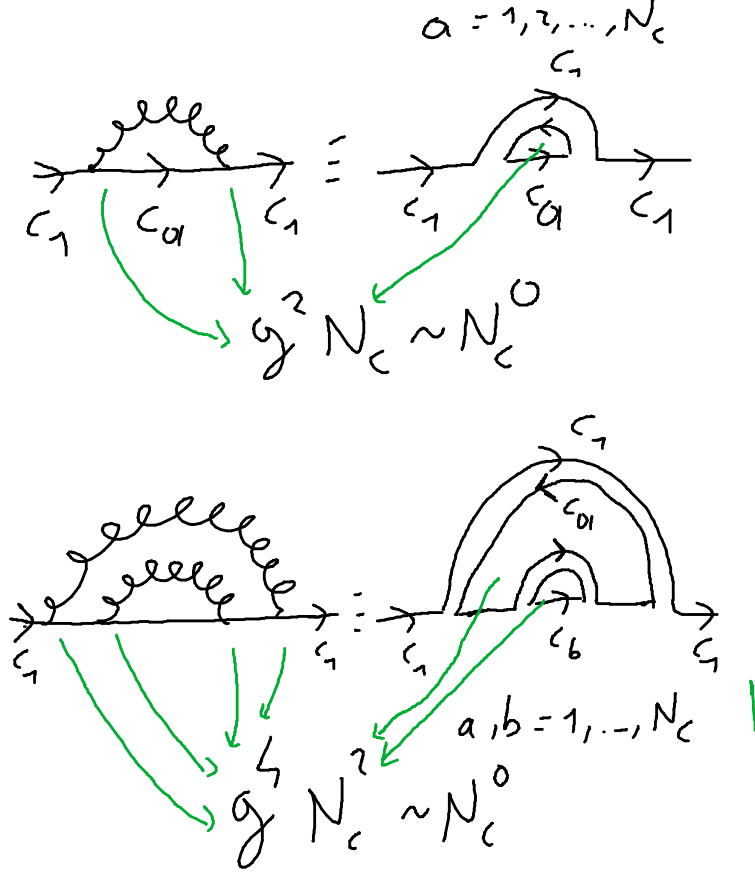


Fig. 5. Same as Fig. 4 with the detailed explanation of the origin of all factors depending on N_c .

antiquark multiplet (see also the results of the quark model [55]). Mesons are classified according to their total spin J , parity P , and charge conjugation C , forming multiplets denoted with J^{PC} .

Moreover, in the quark model one may express a quark-antiquark state Q using the radial quantum number $n = 1, 2, 3, \dots$, the angular quantum number $L = 0, 1, 2, 3, \dots \equiv S, P, D, F, \dots$, the spin part $S = 0, 1$, the flavor composition, and finally the color wave function (that is crucial for this work).

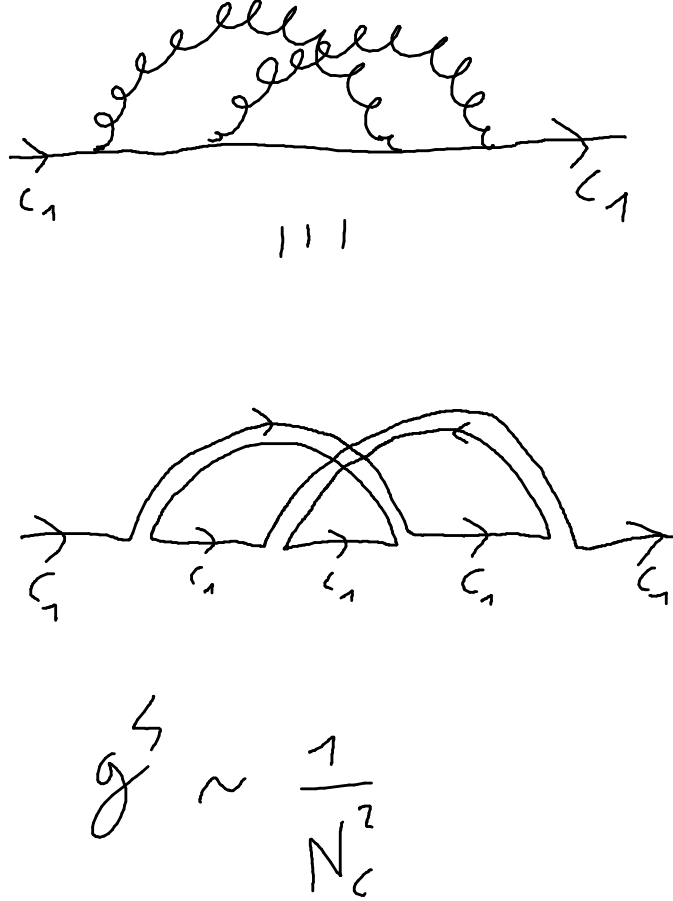


Fig. 6. An example of a non-planar self-energy diagram for the quark propagator. It scales as N_c^{-2} , thus suppressed.

Following this spectroscopic notation a meson is classified as

$$n^{2S+1}L_J , \quad (44)$$

where J is the total spin arising from the proper combination of L and S . We remind that P and C are calculated as:

$$P = (-1)^{L+1} , C = (-1)^{L+S} . \quad (45)$$

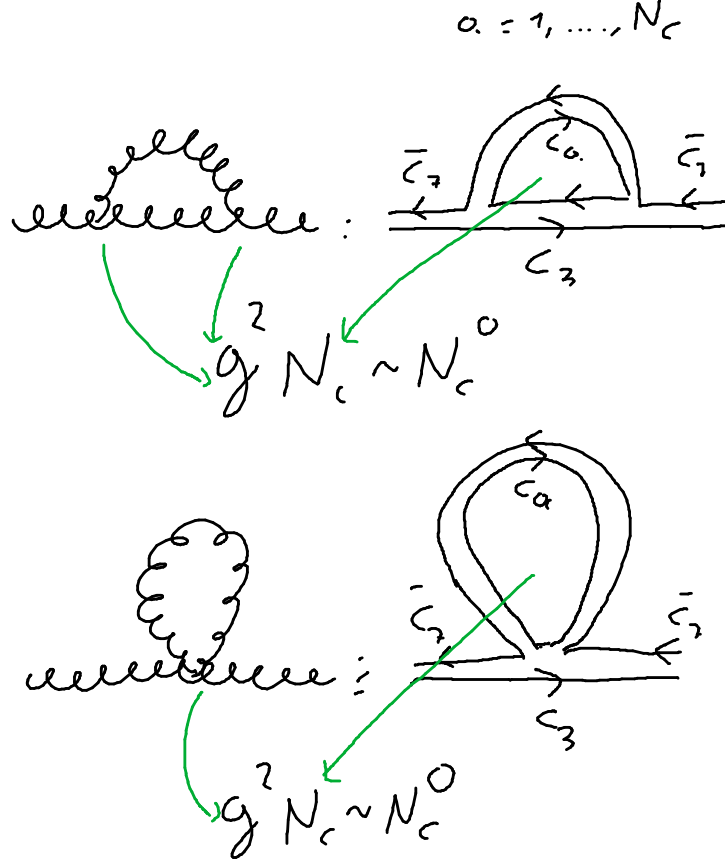


Fig. 7. Two planar diagrams describing the self-energy of the gluon (which is taken to have a specific color $C_3\bar{C}_7$ an explicit example). Both diagrams are ‘mass contributions’ and scale as N_c^0 .

In general, the wave function of a quarkonium state Q takes the form

$$|Q \text{ with } n^{2S+1}L_J \text{ and } J^{PC}\rangle = |\text{radial part } n\rangle |\text{angular part } L\rangle |\text{spin part } S\rangle |\text{flavor}\rangle |\text{color}\rangle. \quad (46)$$

As an example, the wave function of the vector meson $\rho^+ \equiv u\bar{d}$ reads

$$|\rho^+\rangle = N |n=1\rangle |L=0\rangle |S=1(\uparrow\downarrow + \downarrow\uparrow)\rangle |u\bar{d}\rangle |\bar{R}R + \bar{G}G + \bar{B}B\rangle, \quad (47)$$

where N is an overall normalization. The properly normalized color part is

$$|Q\text{-color}\rangle = \frac{1}{\sqrt{3}} |\bar{R}R + \bar{G}G + \bar{B}B\rangle . \quad (48)$$

Interestingly, this is the color wave function of any quarkonium, independently on the other quantum numbers. This combination is colorless, in the sense that it is invariant under any (local) $SU(N_c = 3)$ color transformations.

As we shall prove explicitly later, in the large- N_c limit quark-antiquark mesons retain their mass and become very narrow. For a generic N_c the color wave function takes the form:

$$|Q\text{-color}\rangle = \frac{1}{\sqrt{N_c}} |\bar{C}_1 C_1 + \bar{C}_2 C_2 + \dots + \bar{C}_{N_c} C_{N_c}\rangle , \quad (49)$$

which is invariant under (local) $SU(N_c)$ color transformations. This fact can be easily seen by considering

$$|Q\text{-color}\rangle \simeq \frac{1}{\sqrt{N_c}} \sum_{a=1}^{N_c} \bar{q}_a q_a |0\rangle . \quad (50)$$

A generic color transformation implies:

$$q_a \rightarrow U_{ab} q_b , \quad q_a^\dagger \rightarrow (U_{ac} q_c)^\dagger = q_c^\dagger U_{ac}^* = q_c^\dagger (U^\dagger)_{ca} , \quad (51)$$

thus

$$\bar{q}_a q_a \rightarrow \bar{q}_c (U^\dagger)_{ca} U_{ab} q_b = \bar{q}_a q_a \quad (52)$$

where $(U^\dagger)_{ca} U_{ab} = \delta_{bc}$ follows from $U^\dagger U = 1$ (sum over indices understood).

Other mesons (such as glueballs, hybrids,...) have more complicated wave functions, see later for their detailed study.

The same procedure above can be carried out for conventional baryon states, where a conventional baryon is a three-quark state. Even if the remaining part of their w.f. is more complicated, the normalized color part is pretty simple:

$$|B\text{-color}\rangle = \frac{1}{\sqrt{6}} |RGB + BRG + GBR - GRB - BGR - RBG\rangle , \quad (53)$$

which is invariant under $SU(N_c = 3)$ color transformations. The extension to a generic number of colors gives:

$$|B\text{-color}\rangle = \frac{1}{\sqrt{N_c!}} \varepsilon_{abc} |C_a C_b C_c\rangle \quad (54)$$

or, by using quark fields:

$$|B\text{-color}\rangle \simeq \frac{1}{\sqrt{N_c!}} \varepsilon_{abc} q_a q_b q_c |0\rangle . \quad (55)$$

In fact, under $SU(N_c)$ color transformations:

$$\varepsilon_{abc} q_a q_b q_c \rightarrow \varepsilon_{abc} U_{aa'} U_{bb'} U_{cc'} q_{a'} q_{b'} q_{c'} = \varepsilon_{a'b'c'} q_{a'} q_{b'} q_{c'} \quad (56)$$

where we have used that:

$$\varepsilon_{abc} U_{aa'} U_{bb'} U_{cc'} = \varepsilon_{a'b'c'} , \quad (57)$$

being a consequence of $\det U = 1$, namely:

$$N! \det U = N! = \varepsilon_{abc} U_{aa'} U_{bb'} U_{cc'} \varepsilon_{a'b'c'} = \varepsilon_{a'b'c'} \varepsilon_{a'b'c'} = N! . \quad (58)$$

2.6. Large- N_c : recall of basic results

We present here a short summary of known large- N_c rules [6, 8]. In the next sections we will re-derive them following (relatively simple) bound-state equations forming these states.

1. The masses of quark-antiquark states $Q \equiv \bar{q}q$, glueballs $G \equiv gg$, and hybrids mesons $H \equiv \bar{q}qg$ are constant for $N_c \rightarrow \infty$:

$$M_Q \propto N_c^0 , M_G \propto N_c^0 , M_H \propto N_c^0 . \quad (59)$$

2. The interaction between n_Q quark-antiquark states $Q \equiv |\bar{q}q\rangle$ scales as

$$A_{n_Q Q} \propto \frac{N_c}{N_c^{n_Q/2}} \text{ for } n_Q \geq 1 . \quad (60)$$

This implies that the amplitude for a n_Q -meson scattering process becomes smaller and smaller for increasing N_c . In particular the decay amplitude is realized for $n_Q = 3$, ergo $A_{\text{decay}} \propto N_c^{-1/2}$, implying that the width scales as $\Gamma \propto 1/N_c$. Conventional quarkonia become very narrow for large N_c .

3. The interaction amplitude between n_G glueballs is

$$A_{n_G G} \propto \frac{N_c^2}{N_c^{n_G}} \text{ for } n_G \geq 1 , \quad (61)$$

which is smaller than in the quarkonium case.

4. The interaction amplitude between n_Q quarkonia and n_G glueballs behaves as

$$A_{(n_Q Q)(n_G G)} \propto \frac{N_c}{N_c^{n_Q/2} N_c^{n_G}} \text{ for } n_Q \geq 1, \quad (62)$$

thus the mixing ($n_G = n_Q = 1$) scales as $A_{\text{mixing}} \propto N_c^{-1/2}$. Then, also the glueball-quarkonium mixing is suppressed for $N_c \gg 1$. Note, for $n_G = 0$ one recovers the correct interaction for n_Q quarkonia.

5. The amplitude for n_Q quarkonia and n_H hybrids scales as

$$A_{(n_Q Q)(n_H H)} \propto \frac{N_c}{N_c^{n_Q/2} N_c^{n_H/2}} \text{ for } n_Q + n_H \geq 1. \quad (63)$$

For $n_Q = n_H = 1$ one recovers that the quarkonium-hybrid mixing scales as N_c^0 .

6. For the general case of n_Q quarkonia, n_G glueballs, and n_H hybrids one has:

$$A_{(n_Q Q)(n_G G)(n_H H)} \propto \frac{N_c}{N_c^{n_Q/2} N_c^{n_G} N_c^{n_H/2}} \text{ for } n_Q + n_H \geq 1. \quad (64)$$

7. Four-quark states (both as molecular objects and diquark-anti-diquark objects). A part from (eventually existing, but not proven yet) peculiar tetraquarks [29], these objects typically do not survive in the large- N_c limit.

8. Baryons are made of N_c quarks for an arbitrary N_c . As a consequence

$$M_B \propto N_c. \quad (65)$$

9. Interactions involving baryons: the baryon-baryon-meson interaction scales as $N_c^{1/2}$, while baryon-baryon scattering as N_c . In particular, for an arbitrary number of $\bar{B}B$, as well as n_Q quarkonia, n_G glueballs, and n_H hybrids, one has:

$$A_{(\bar{B}B\dots)(n_Q Q)(n_G G)(n_H H)} \propto \frac{N_c}{N_c^{n_Q/2} N_c^{n_G} N_c^{n_H/2}}. \quad (66)$$

Indeed, the large- N_c limit is a firm theoretical method which explains why the quark model works. In fact, a decay channel for a certain meson causes quantum fluctuations: the propagator of the meson is dressed by

loops of other mesons. For instance, the state ρ^+ decays into $\pi^+\pi^0$, thus the ρ -meson is dressed by loops of pions. In the end, one has schematically that the wave function of the ρ -meson is given by:

$$|\rho^+\rangle = a|u\bar{d}\rangle + b|\pi^+\pi^0\rangle + \dots, \quad (67)$$

where the full expression of $|u\bar{d}\rangle$ is given in Eq. (47). Being $a \propto N_c^0$ and $b \propto N_c^{-1/2}$, we understand why the quark-antiquark configuration dominates. Dots refer to further contributions which are even more suppressed.

Yet, for $N_c = 3$ there are some mesons for which the meson-meson component dominates. These are for instance, the light scalar mesons such as $a_0(980)$, see 3.5.

3. Large- N_c results for mesons

In this Section we deal with mesons. First, we discuss conventional quarkonia states, then various exotic configurations: glueballs, hybrids, and (briefly) four-quark states.

3.1. Quark-antiquark mesons

A quark-antiquark meson has a rather simple color wave function, see eq. (49), that we rewrite here for convenience:

$$|Q\text{-color}\rangle = \frac{1}{\sqrt{N_c}} |\bar{C}_1 C_1 + \bar{C}_2 C_2 + \dots + \bar{C}_{N_c} C_{N_c}\rangle. \quad (68)$$

How does such a bound state emerge? For simplicity, let us consider the processes that mix two elements of the wave function, for instance:

$$\bar{C}_1 C_1 \rightarrow \bar{C}_2 C_2 \quad (69)$$

This particular transition implies that an initial state with color 1 and anticolor 1 transforms into color 2 and anticolor 2. (For $N_c = 3$ that would correspond to e.g. $\bar{R}R$ into $\bar{G}G$.) Of course, any other example, such as $\bar{C}_3 C_3 \rightarrow \bar{C}_7 C_7$, is equally good. The important point is that we start from a possible component of a quarkonium state and end up in another component of its wave function. This is so because an eventual bound state would couple to any color combination $\bar{C}_a C_a$ with the same strength, and would appear as an intermediate state for processes of the type (69). In particular, close to the mass of the quarkonium, the s -channel becomes dominant. Note, for the moment we do not ‘care’ about the normalization $1/\sqrt{N_c}$ entering in eq. (49), but we simply study the transition of Eq. (69).

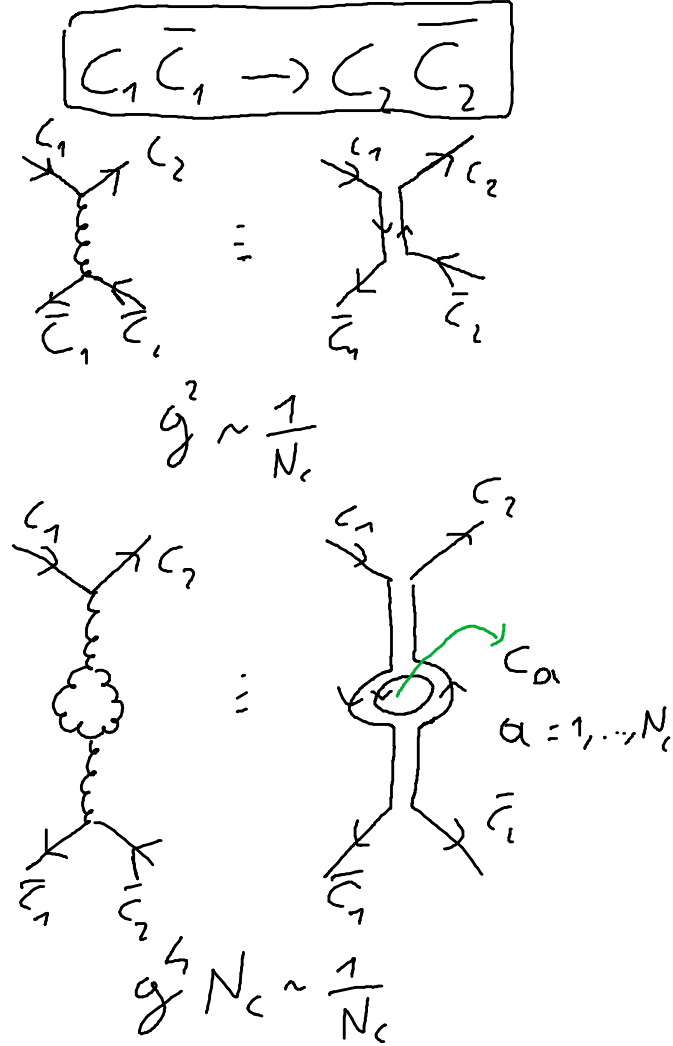
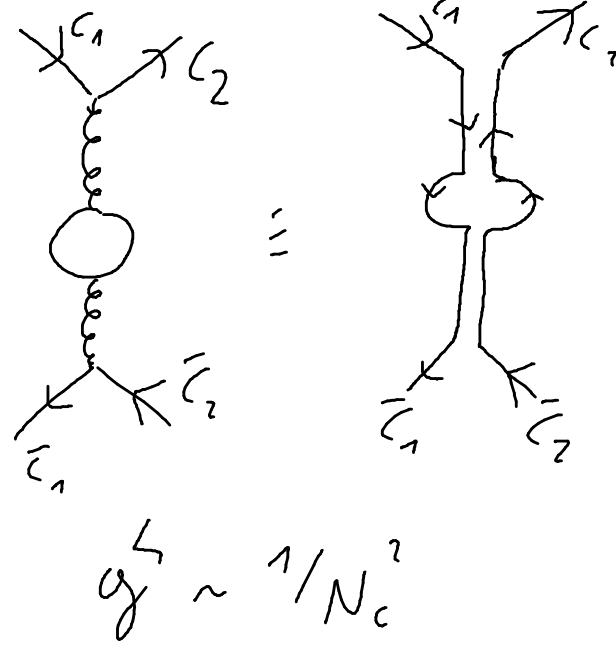


Fig. 8. Examples of dominating diagrams for the scattering process $\bar{C}_1 C_1 \rightarrow \bar{C}_2 C_2$. These diagrams scale as N_c^{-1} . Of course, one could take any other color combination, such as $\bar{C}_7 C_7 \rightarrow \bar{C}_{11} C_{11}$.

The simplest process of this type is depicted in Fig. 8 (upper part), where it is evident that the dominant amplitude for $\bar{C}_1 C_1 \rightarrow \bar{C}_2 C_2$ scales as $1/N_c$. Interestingly, loop processes of the type of Fig. 8 (lower part) also scale in this way. Of course, there are also subleading terms that scale as



This diagram is suppressed

Fig. 9. Example of a subleading diagram for the scattering process $\bar{C}_1 C_1 \rightarrow \bar{C}_2 C_2$. These types of diagram scale as N_c^{-2} .

$1/N_c^2$, see Fig. 9, which can be dismissed in the large- N_c limit. In Fig. 10 we show another type of diagrams, which scales also as N_c^{-1} and displays an intermediate loop with any possible color combination.

How to study the emergence of bound states in this context? Of course, the full problem is complicated and one would need a Bethe-Salpeter approach. Yet, a simple and in many respects successful approach makes use of a quartic separable interaction, such as in the NJL model [14, 15]. As previously mentioned, the large- N_c counting is thought to be independent on the precise approach, thus the results that we will present are general.

Let us consider a generic ‘colorless’ current for an arbitrary quarkonium

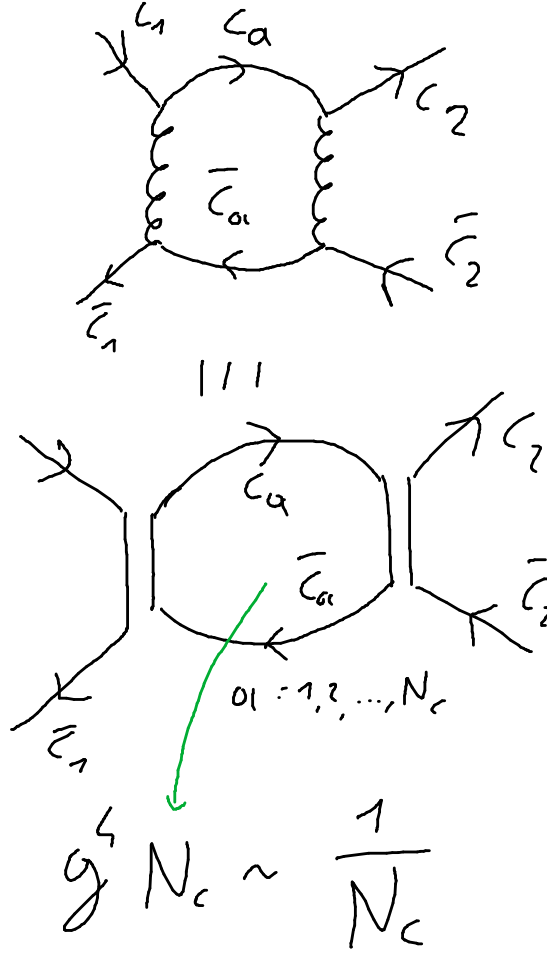
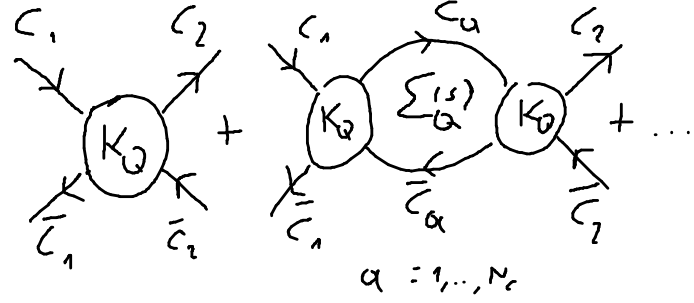


Fig. 10. Another dominating diagram for the scattering process $\bar{C}_1 C_1 \rightarrow \bar{C}_2 C_2$, that involves an intermediate state with an arbitrary color $\bar{C}_a C_a$ for $a = 1, \dots, N_c$. It scales as N_c^{-1} .

meson Q :

$$J_Q(x) = \sum_{a=1}^{N_c} \bar{q}^{(a)} \Gamma q^{(a)} \equiv C_1 \bar{C}_1 + C_2 \bar{C}_2 + \dots + C_{N_c} \bar{C}_{N_c}, \quad (70)$$

where no normalization is considered. The separable interaction term is



$M_Q \sim N_c^0$

$$\frac{1}{K_Q^{-1} - \Sigma_Q^{(s)}} \sim \frac{g_{Q\bar{q}q}}{s - M_Q^2}$$

$K_Q \sim 1/N_c; \Sigma_Q \sim N_c; g_{Q\bar{q}q} \sim 1/\sqrt{N_c}$

Fig. 11. Generation of a quark-antiquark meson (red line) upon resummation of diagrams for the illustrative process $\bar{C}_1 C_1 \rightarrow \bar{C}_2 C_2$.

proportional to J_Q^2 . The corresponding Lagrangian takes the effective form

$$\mathcal{L}_Q = K_Q J_Q^2, \quad (71)$$

where K_Q is a coupling constant. In order to determine the scaling of K_Q , one may consider the illustrative transition $C_1 \bar{C}_1 \rightarrow C_2 \bar{C}_2$ or any other of

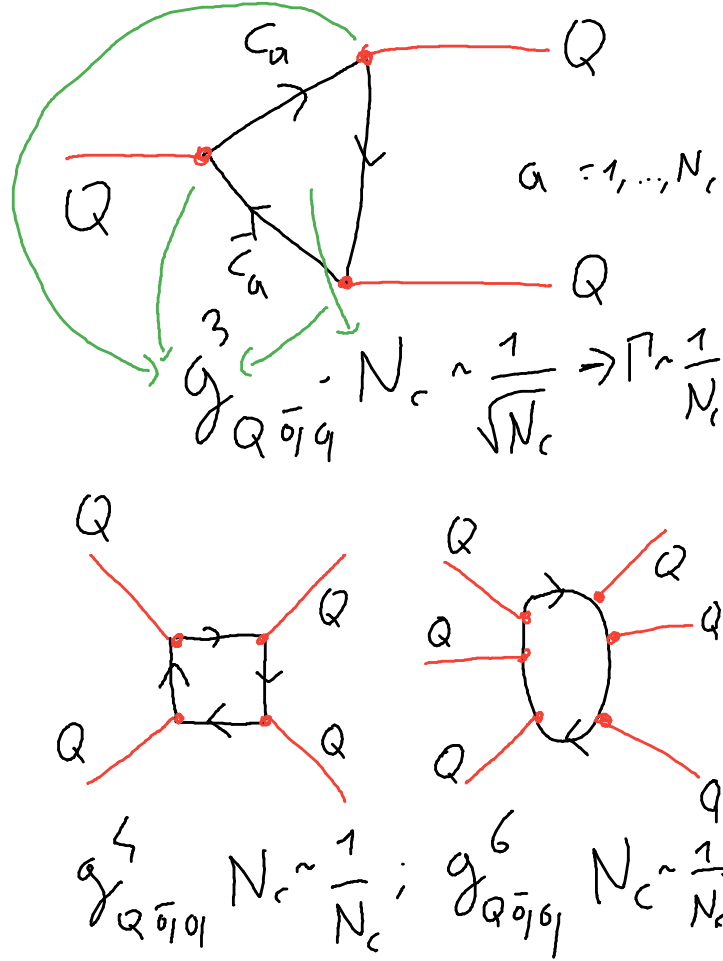


Fig.12. Conventional $\bar{q}q$ mesons Q are in red, quarks in black. Up: decay of a conventional $\bar{q}q$ meson into two conventional $\bar{q}q$ mesons via a loop of quarks. The leading amplitude scales as $N_c^{-1/2}$, hence the decay width scales as N_c^{-1} . Down: scattering process of conventional mesons, whose leading order is N_c^{-1} , thus the cross-section goes as N_c^{-2} .

that type), finding that

$$K_Q \propto g_{QCD}^2 \propto N_c^{-1}. \quad (72)$$

We then introduce a useful notation. We define \bar{K}_Q as a N_c -independent

constant, thus:

$$K_Q = \frac{\bar{K}_Q}{N_c} . \quad (73)$$

In the following, any quantity with ‘bar’ shall be regarded as N_c -independent.

The corresponding T -matrix T_Q is obtained by properly resumming the interactions originated by the Lagrangian of Eq. (71), see Fig. 11 for its pictorial representation. It then takes the form:

$$iT_Q(s) = iK_Q + iK_Q(-i\Sigma_Q(s))iK_Q + iK_Q(-i\Sigma_Q(s))iK_Q(-i\Sigma_Q(s))iK_Q + \dots$$

leading to

$$T_Q(s) = K_Q + K_Q\Sigma_Q(s)K_Q + \dots = \frac{K_Q}{1 - \Sigma_Q(s)K_Q} = \frac{1}{K_Q^{-1} - \Sigma_Q(s)} , \quad (74)$$

where $\Sigma_Q(s)$ is the quark-antiquark loop contribution, which scales as:

$$\Sigma_Q(s) = N_c \bar{\Sigma}_Q(s) . \quad (75)$$

This result is a simple consequence of the N_c possible loops when the quark carries N_c colors. The quantity $\bar{\Sigma}_Q(s)$ is, according to the adopted convention, independent on N_c .

Next, the amplitude $T_Q(s)$ scales as $1/N_c$ (indeed, each terms in the expansion is of order $1/N_c$, as one can easily check). In this specific model, one can also write the explicit form of the loop function $\Sigma_Q(s)$ as

$$\Sigma_Q(s = p^2) = -iN_c \int \frac{d^4k}{(2\pi)^4} \text{Tr} [S_q(p/2 + k) \Gamma S_q(-p/2 + k) \Gamma] f_\Lambda(q) . \quad (76)$$

In this sense, the factor N_c is simply a trace over color d.o.f.: this is indeed a general result that does not depend on the model details. The function $f_\Lambda(q)$ stays for a regulator (in turn, this function may arise from a nonlocal current [18, 19]), but its specification is not needed since no explicit calculation will be performed.

The mass of the quark-antiquark bound states M_Q corresponds to a pole of the resummed amplitude $T_Q(s)$, hence to a zero of its denominator. As such, it is a solution of the equation

$$T_Q(s)^{-1} = 0 \rightarrow K_Q^{-1} - \Sigma_Q(s = M_Q^2) = 0 . \quad (77)$$

Then, upon using $K_Q = \bar{K}_Q/N_c$ and $\Sigma_Q(s) = N_c \bar{\Sigma}_Q(s)$, the previous equation takes the form

$$\frac{N_c}{\bar{K}_Q} - N_c \bar{\Sigma}_Q(s = M_Q^2) = 0 \rightarrow \frac{1}{\bar{K}_Q} - \bar{\Sigma}_Q(s = M_Q^2) = 0 \quad (78)$$

which is N_c independent. Thus, the mass of the mesonic quarkonium state Q scales as

$$M_Q \propto N_c^0 . \quad (79)$$

We were able to reproduce this very well known and general result of the large- N_c phenomenology.

Next, let us expand the denominator T_Q around $s = M_Q^2$, finding:

$$\begin{aligned} K_Q^{-1} - \Sigma_Q(s) &\simeq \underbrace{K_Q^{-1} - \Sigma_Q(M_Q^2)}_{=0} - \left(\frac{\partial \Sigma_Q(s)}{\partial s} \right)_{s=M_Q^2} (s - M_Q^2) + \dots \\ &\simeq -N_c \left(\frac{\partial \bar{\Sigma}_Q(s)}{\partial s} \right)_{s=M_Q^2} (s - M_Q^2) + \dots \end{aligned} \quad (80)$$

Hence, the amplitude becomes:

$$T_Q(s) = \frac{1}{K_Q^{-1} - \Sigma_Q(s)} \simeq \frac{1}{-N_c \left(\frac{\partial \bar{\Sigma}_Q(s)}{\partial s} \right)_{s=M_Q^2} (s - M_Q^2)} = \frac{(ig_{Q\bar{q}q})^2}{s - M_Q^2} , \quad (81)$$

where we identify the coupling of the quarkonium to its constituents, a quark and an antiquark, as:

$$g_{Q\bar{q}q} = \frac{1}{\sqrt{N_c \left(\frac{\partial \bar{\Sigma}_Q(s)}{\partial s} \right)_{s=M_Q^2}}} = \frac{1}{\sqrt{N_c}} \bar{g}_{Q\bar{q}q} . \quad (82)$$

Again, $\bar{g}_{Q\bar{q}q}$ is N_c independent. Thus, the coupling of a conventional meson to a quark-antiquark pair $g_{Q\bar{q}q}$ scales as $1/\sqrt{N_c}$. In terms of the composite field Q and the constituent quark fields, one can write an effective interaction Lagrangian

$$\mathcal{L}_{Q\bar{q}q} = g_{Q\bar{q}q} Q J_Q . \quad (83)$$

Such interactions enter, for example, in meson-quark chiral models [56, 57], in approaches using the Weinberg compositeness condition [16, 17] (sometimes within nonlocal Lagrangians [18, 19]), as well as at intermediate stages of the hadronization process of quark models such as the NJL one [14].

Many results can be obtained from the previous outcomes. Let us first look at 3-leg meson interactions (see Fig. 12), which is proportional to:

$$A_{3Q} \propto g_{Q\bar{q}q}^3 N_c \propto \frac{1}{\sqrt{N_c}} . \quad (84)$$

As a consequence, the decay width of a conventional mesons into two conventional mesons $Q \rightarrow Q_1 Q_2$ scales as:

$$\Gamma_{Q \rightarrow Q_1 Q_2} \propto |A_{3Q}|^2 \propto \frac{1}{N_c}. \quad (85)$$

This is also a very well known result of large- N_c phenomenology. Conventional quark-antiquark mesons become stable for $N_c \rightarrow \infty$ with a scaling of the type N_c^{-1} .

Similarly, the four-leg conventional meson interaction goes as (again Fig. 12):

$$A_{4Q} \propto g_{Q\bar{q}q}^4 N_c \propto \frac{1}{N_c}. \quad (86)$$

For instance, the four-pion interaction term in an effective Lagrangian should scale as $1/N_c$.

In general, the n_Q -th leg meson interaction among convectional mesons scales as ($n_Q \geq 1$)

$$A_{n_Q Q} \propto g_{Q\bar{q}q}^{n_Q} N_c \propto N_c^{-n_Q/2} N_c = \frac{N_c}{N_c^{n_Q/2}}, \quad (87)$$

in agreement with the general result quoted in Sec. 2.6 (point 2). Note, the case $n_Q = 1$ generates $A_Q \sim N_c^{1/2}$, which coincides with the vacuum production amplitude (and also with the weak decay constant), see below. The case $n_Q = 0$ implies $A_0 \sim N_c$ which can be interpreted as the vacuum contribution of quarks. In turn, the pressure generated by quarks scales as N_c , see Sec. 5.

Next, we examine various additional consequences of the obtained large- N_c scaling behavior.

1) Suppressed decays: the example of the j/ψ meson.

The j/ψ meson is the ground-state vector $\bar{c}c$. Its decay width is very small [1]. Can large- N_c help us to understand why? Indeed, it does. The dominant decay of the j/ψ would be the decay into $D^+ D^-$ or into $D^0 \bar{D}^0$. This decay would be of the order of N_c^{-1} , but cannot take place because it is kinematically forbidden since $M_{j/\psi} < 2M_D$. Schematically:

$$\Gamma_{j/\psi \rightarrow \bar{D} D} \propto g_{j/\psi \bar{D} D}^2 \cdot \frac{k_D^3}{M_{j/\psi}^2} \theta(M_{j/\psi} - 2M_D) = 0, \quad (88)$$

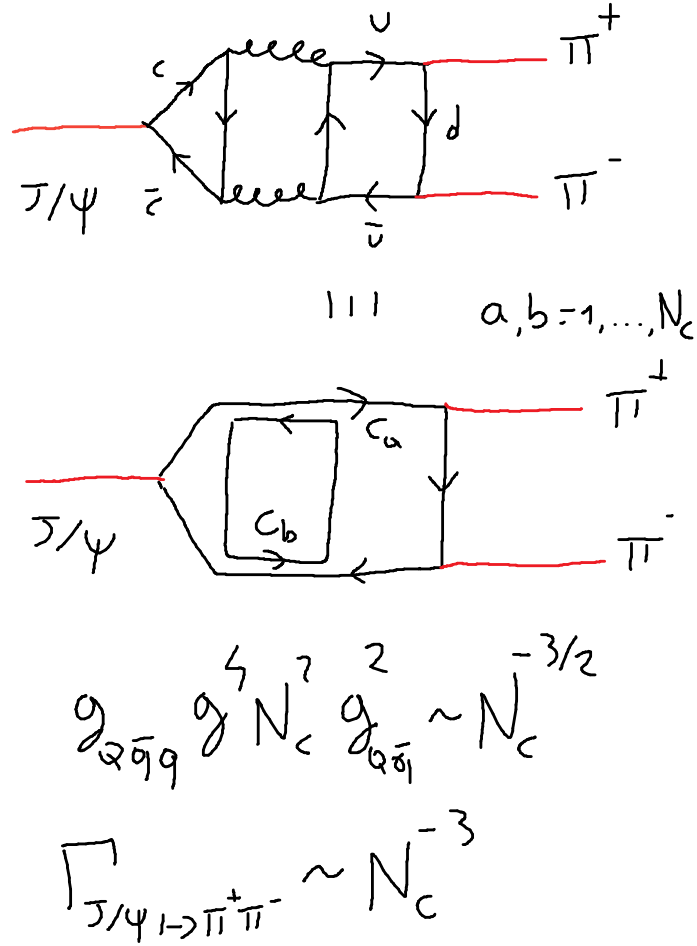


Fig. 13. Decay of the charm-anticharm J/ψ meson (red) into two pions (also red). In this case, the leading decay into $\bar{D}D$ mesons as in Fig. 12 cannot take place because kinematically forbidden. The subleading diagram scales as $N_c^{-3/2}$, thus the decay width goes as N_c^{-3} , explaining why the J/ψ meson is so narrow. Note, the diagrams above also show that the flavor lines (upper part) behave differently than the color ones (lower part).

where $g_{j/\psi \bar{D}D}$ goes as $N_c^{-1/2}$ and $k_D = \sqrt{M_{j/\psi}^2/4 - M_D^2}$ is the modu-

lus of the three-momentum of an outgoing particle. This quantity is N_c -independent but is imaginary for $M_{j/\psi} < 2M_D$. The step function assures that in these cases the decay simply vanishes.

The j/ψ can decay into light hadrons, e.g. into pions. Formally, the same expression holds:

$$\Gamma_{j/\psi \rightarrow \pi\pi} \propto g_{j/\psi\pi\pi}^2 \cdot \frac{k_\pi^3}{M_{j/\psi}^2} \theta(M_{j/\psi} - 2M_\pi) = g_{j/\psi\pi\pi}^2 \cdot \frac{k_\pi^3}{M_{j/\psi}^2} \neq 0, \quad (89)$$

where $k_\pi = \sqrt{M_{j/\psi}^2/4 - M_\pi^2} \sim N_c^0$. How does $g_{j/\psi\pi\pi}$ scale with N_c ? A simple diagrammatic analysis, see Fig. 13, shows that

$$g_{j/\psi\pi\pi} \propto N_c^{-3/2}, \quad (90)$$

thus $\Gamma_{j/\psi \rightarrow \pi\pi} \propto N_c^{-3}$. This result applies to any similar mesonic channel. We thus find:

$$\Gamma_{j/\psi \rightarrow \text{mesons}} \propto N_c^{-3}. \quad (91)$$

This explains why these decays are so small. This result holds for any mesons whose (would be large- N_c) dominant decays are kinematically forbidden. Indeed, it is a realization of the so-called OZI (Okubo, Zweig, and Iizuka) rule, e.g. [58], according to which diagrams in which the quark lines are disconnected are suppressed. In this respect, the OZI rule can be understood as a consequence of the large- N_c results.

2) Pion decay constant and $\pi^0 \rightarrow \gamma\gamma$.

The pion decay constant f_π refers to the quark-antiquark pair forming the state π^+ . It enters as a part of the amplitude of the weak decay of π^+ , for which the chain $\pi^+ \rightarrow W^+ \rightarrow \mu^+ \nu_\mu$ takes place, see Fig. 14. It turns out that

$$f_\pi \propto N_c^{1/2}. \quad (92)$$

Indeed, this is the same scaling of the quark-antiquark condensate, see below. The correct scaling can be also seen by writing the formula for f_π as

$$f_\pi \sim g_{\pi^+ u\bar{d}} \Sigma_\pi(s = M_\pi^2) = \frac{\bar{g}_{\pi^+ u\bar{d}}}{\sqrt{N_c}} N_c \bar{\Sigma}_\pi(s = M_\pi^2) \sim \sqrt{N_c}. \quad (93)$$

This result is indeed independent on the chosen quark-antiquark meson: the weak decay constant of a generic conventional meson scales as $\sqrt{N_c}$. [Note, while the scaling is correct, the expression $g_{\pi^+ u\bar{d}} \Sigma_\pi(s = M_\pi^2)$ has dimension Energy², but f_π has dimension energy. This is due to the fact that the expression $g_{\pi^+ u\bar{d}} \Sigma_\pi(s = M_\pi^2)$ is indeed sufficient to determine the large- N_c

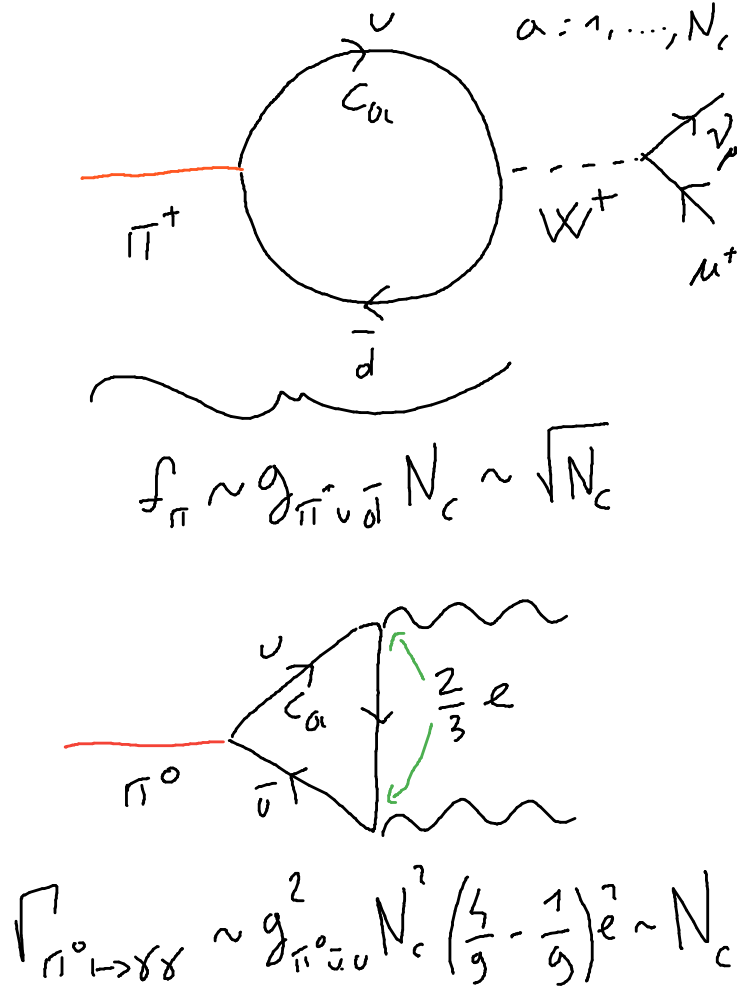


Fig. 14. Schematic diagrams leading to the large- N_c scaling of the weak decay constant f_π and $\pi^0 \rightarrow \gamma\gamma$.

scaling, but is not enough for an actual calculation of the decay constant. A closer inspection shows that $g_{\pi^+ u \bar{d}} \Sigma_\pi(s = M_\pi^2) \propto M_\pi f_\pi$. For a detailed calculation that includes the large- N_c discussion within a qualitatively similar approach, see Ref. [59]. We also refer to point 3 below for a connection of this quantity to chiral models.

For what concerns the decay of π^0 into $\gamma\gamma$, one obtains the amplitude:

$$A_{\pi^0\gamma\gamma} \propto \left[g_{\pi^0\bar{u}u} \left(\frac{2e}{3} \right)^2 + g_{\pi^0\bar{d}d} \left(-\frac{e}{3} \right)^2 \right] N_c \simeq g_{\pi^0\bar{u}u} N_c \left(\frac{4}{9} - \frac{1}{9} \right) \quad (94)$$

where $g_{\pi^0\bar{d}d} \simeq -g_{\pi^0\bar{u}u}$ has been used (this comes from $|\pi^0\rangle = \frac{1}{\sqrt{2}} |\bar{u}u - \bar{d}d\rangle$). Since $g_{\pi^0\bar{u}u}$ scales as $N_c^{-1/2}$, one finds:

$$\Gamma_{\pi^0 \rightarrow \gamma\gamma} \propto g_{\pi^0\bar{u}u}^2 N_c^2 \propto N_c. \quad (95)$$

(If one would neglect the scaling of the coupling, a N_c^2 dependence would emerge, but that is not the correct scaling).

3) Three-body decay: direct process vs decay chain.

We intend to study the three-body decay process

$$Q \rightarrow Q_1 Q_2 Q_3. \quad (96)$$

Let us consider two possible models for this decay, see Fig. 15. For the direct decay, a Lagrangian of the type (we call it ‘model A’) reads

$$\mathcal{L}_A = \lambda Q Q_1 Q_2 Q_3, \quad (97)$$

where $\lambda = \bar{\lambda}/N_c$, for which the three-body decay goes as:

$$\Gamma_{Q \rightarrow Q_1 Q_2 Q_3} \propto |A_{Q \rightarrow Q_1 Q_2 Q_3}|^2 \propto \lambda^2 \propto \frac{1}{N_c^2}. \quad (98)$$

Next, let us consider the possibility that the decay takes place via an additional intermediate quark-antiquark state S via the Lagrangian (that we shall denote as ‘model B’, see again Fig. 15):

$$\mathcal{L}_B = g_{QQ_1S} Q Q_1 S + g_{SQ_2Q_3} S Q_2 Q_3 \quad (99)$$

where both constants g_{QQ_1S} and $g_{SQ_2Q_3}$ scale as $1/\sqrt{N_c}$. Thus, one has the decay chain

$$Q \rightarrow Q_1 S \rightarrow Q_1 Q_2 Q_3 \quad (100)$$

where in the second step $S \rightarrow Q_2 Q_3$ has taken place. We assume, for simplicity, that $S \rightarrow Q_2 Q_3$ is the only available decay channel for S (the main results hold also when this is not the case).

In scenario B, the decay amplitude takes the form:

$$A_{Q \rightarrow Q_1 Q_2 Q_3} \propto g_{QQ_1S} \frac{1}{p_S^2 - M_S^2 + i\Gamma_S M_S} g_{SQ_2Q_3} \quad (101)$$

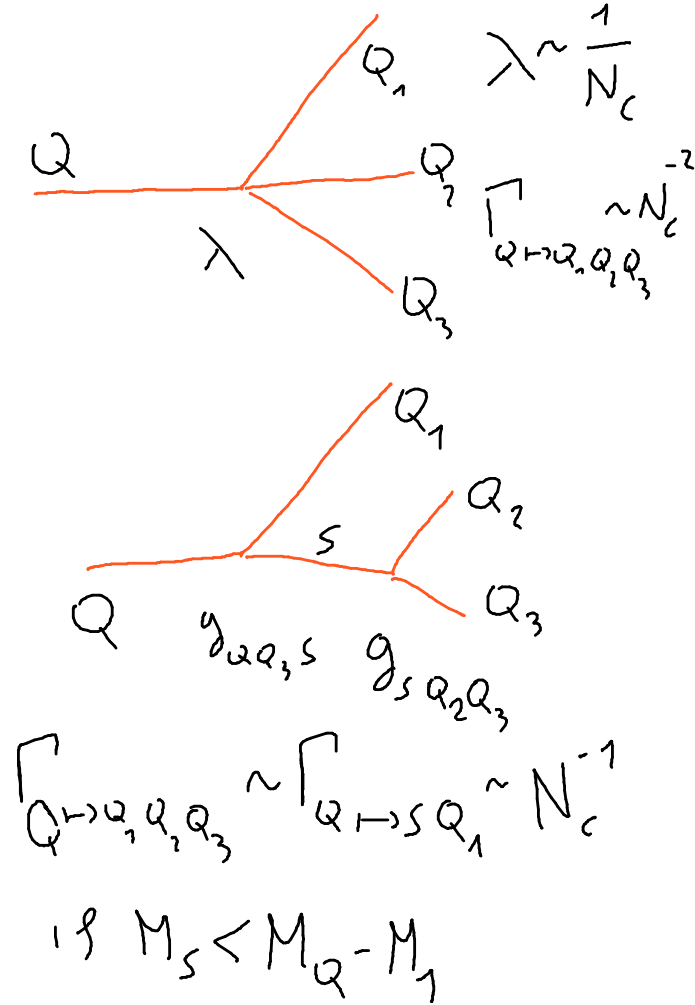


Fig. 15. Direct three-body decay vs decay chain leading to it (with an intermediate S meson). Under appropriate conditions, the latter dominates in the large- N_c limit.

Since M_S is not dependent on N_c and Γ_S is suppressed as $1/N_c$, at first sight $A_{Q \rightarrow Q_1 Q_2 Q_3}$ scales also as $1/N_c$, thus leading to the same result of model ‘A’ (direct decay). Yet, a more careful analysis leads to a different result. Following Ref. [60, 61], the decay chain leads to the integration over final

momenta leading to

$$\Gamma_{Q \rightarrow Q_1 Q_2 Q_3} = \int_0^{M_Q - M_1} dx \Gamma_{Q \rightarrow Q_1 S}(x) d_S(x) \quad (102)$$

where $\Gamma_{Q \rightarrow Q_1 S}(x)$ is the decay width for $Q \rightarrow Q_1 S$. The quantity $d_S(x)$ is the mass distribution of the S state with

$$d_S(x) = \frac{\Gamma_S}{2\pi} \frac{1}{(x - M_S)^2 + \Gamma_S^2/4} \quad (103)$$

where x is the running mass of the intermediate state S , that must be smaller than $M_Q - M_1$. Above, the nonrelativistic Breit-Wigner approximation has been used. This approximation is surely valid for narrow states. Anyway, the result is more general then that (one could use for instance the relativistic Sill distribution of Ref. [61] that takes into account threshold effects, getting the same outcome). In the large- N_c limit one obtains:

$$d_S(x) = \delta(x - M_S) , \quad (104)$$

thus

$$\Gamma_{Q \rightarrow Q_1 Q_2 Q_3} = \Gamma_{Q \rightarrow Q_1 S}(x = M_S) \propto \frac{1}{N_c} , \quad (105)$$

instead of N_c^{-2} . It is then evident that the decay chain dominates. Yet, this term is nonzero only if $M_S \leq M_Q - M_1$. If this is not the case, one should consider the next to leading term for $d_S(x)$ that scales as $1/N_c$ which again would lead to an overall $1/N_c^2$ decay of Q . This can be easily seen in the case in which M_S is much larger than M_Q , thus (for x in the range $(0, M_Q - M_1)$)

$$d_S(x) = \frac{\Gamma_S}{2\pi} \frac{1}{M_S^2} + \dots \propto \frac{1}{N_c} , \quad (106)$$

out of which

$$\begin{aligned} \Gamma_{Q \rightarrow Q_1 Q_2 Q_3} &= \int_0^{M_Q - M_1} dx \Gamma_{Q \rightarrow Q_1 S}(x) d_S(x) \\ &= \frac{\Gamma_S}{2\pi} \frac{1}{M_S^2} \int_0^{M_Q - M_1} dx \Gamma_{Q \rightarrow Q_1 S}(x) \propto \frac{1}{N_c^2} . \end{aligned} \quad (107)$$

(Note, this decay is also suppressed by the assumed large mass M_S).

As anticipated, the outcome is unchanged if S has more than a single decay channel. Namely, in this case the spectral function refers to the specific decay channel [62] with:

$$d_S(x) = \frac{\Gamma_{S \rightarrow Q_2 Q_3}}{2\pi} \frac{1}{(x - M_S)^2 + \Gamma_S^2/4} \quad (108)$$

which reduces to

$$d_S(x) = \frac{\Gamma_{S \rightarrow Q_2 Q_3}}{\Gamma_S} \delta(x - M_S) \quad (109)$$

in the large- N_c limit. Then

$$\Gamma_{Q \rightarrow Q_1 Q_2 Q_3} = \frac{\Gamma_{S \rightarrow Q_2 Q_3}}{\Gamma_S} \Gamma_{Q \rightarrow Q_1 S}(x = M_S) \propto \frac{1}{N_c} \quad (110)$$

if, of course, $M_S \leq M_Q - M_1$.

In conclusion, the decay chain is dominant, if appropriate kinematic conditions are met.

3) Chiral models.

Let us study the large- N_c scaling in a chiral model. For simplicity, we consider one scalar σ particle and one pseudoscalar π corresponding to the case of a single flavor ($N_f = 1$). (Note, we neglect at first the chiral anomaly, thus π emerges as a Goldstone boson: in this respect, it is more pion-like than η' -like).

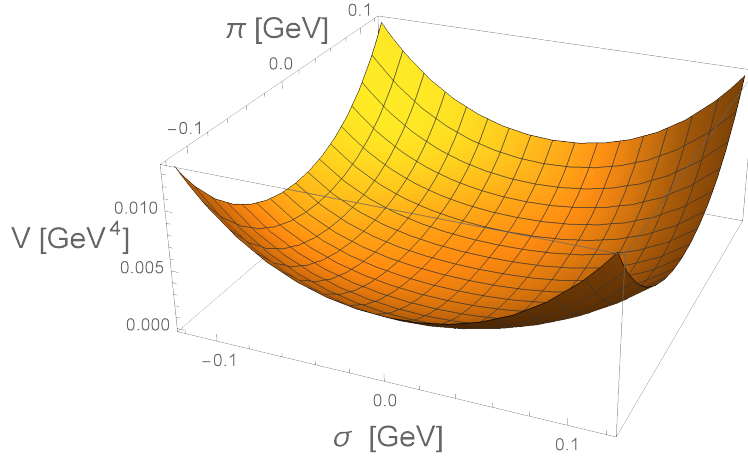


Fig. 16. Form of the chiral potential of Eq. (114) for $m_0^2 > 0$. The minimum sits at the origin.

The basic chiral ‘multiplet’ reads

$$\Phi = \sigma + i\pi . \quad (111)$$

A chiral transformation amounts to $\Phi \rightarrow e^{i\alpha} \Phi$ (it is an $O(2)$ rotation in the space spanned by (σ, π)), thus the quantity

$$\Phi^\dagger \Phi = \Phi^* \Phi = \sigma^2 + \pi^2 \quad (112)$$

is a chiral invariant object. For a generic N_f the quantity Φ is a $N_f \times N_f$ matrix, e.g. [23, 63, 64, 65, 66], but for $N_f = 1$ it is a scalar, thus $\Phi^\dagger = \Phi^*$. Interestingly, the main large- N_c outcomes that we shall discuss are independent on N_f .

For $N_f = 1$ the chirally invariant potential takes the simple form:

$$V(\sigma, \pi) = \frac{m_0^2}{2} \Phi^* \Phi + \frac{\lambda}{4} (\Phi^* \Phi)^2 = \frac{m_0^2}{2} (\pi^2 + \sigma^2) + \frac{\lambda}{4} (\pi^2 + \sigma^2)^2 . \quad (113)$$

The large- N_c scaling is an immediate consequence of our previous discussion:

$$m_0 \sim N_c^0, \lambda \sim N_c^{-1} . \quad (114)$$

For $m_0^2 > 0$ the potential is plotted in Fig. 16 for $m_0^2 = 0.6^2 \text{ GeV}^2$ and $\lambda = 40$: it has a single minimum for $P_{\min} = (\sigma = \pi = 0)$. The masses of the particles correspond to the second derivatives evaluated at the minimum:

$$M_\pi^2 = \left. \frac{\partial^2 V}{\partial \pi^2} \right|_{P=P_{\min}} = m_0^2 \sim N_c^0 , \quad (115)$$

$$M_\sigma^2 = \left. \frac{\partial^2 V}{\partial \sigma^2} \right|_{P=P_{\min}} = m_0^2 \sim N_c^0 . \quad (116)$$

Both particles have the same mass m_0 . This is a manifest realization of chiral symmetry. Yet, this is not how Nature works. Chiral partners do not have the same mass.

The splitting of masses is possible without explicit breaking of chiral symmetry by considering $m_0^2 < 0$. The corresponding potential, plotted in Fig. 17 for $m_0^2 = -0.6^2 \text{ GeV}^2$ and $\lambda = 40$, can be rewritten as:

$$V(\sigma, \pi) = \frac{\lambda}{4} (\pi^2 + \sigma^2 - F^2)^2 - \frac{m_0^4}{4\lambda} \text{ with } F = \sqrt{\frac{-m_0^2}{\lambda}} \sim N_c^{1/2} > 0 . \quad (117)$$

It has the typical shape of a Mexican hat, in which the origin (for $\sigma = \pi = 0$) is not a minimum but a maximum. In fact, upon calculating the masses around the origin, they would turn out to be imaginary. There is however a circle of equivalent minima for:

$$\pi^2 + \sigma^2 = F^2 = -\frac{m_0^2}{\lambda} \sim N_c > 0 . \quad (118)$$

Moreover, the radius of this circle goes as $N_c^{1/2}$. SSB is realized when a specific minimum is picked up. Following the usual convention we choose:

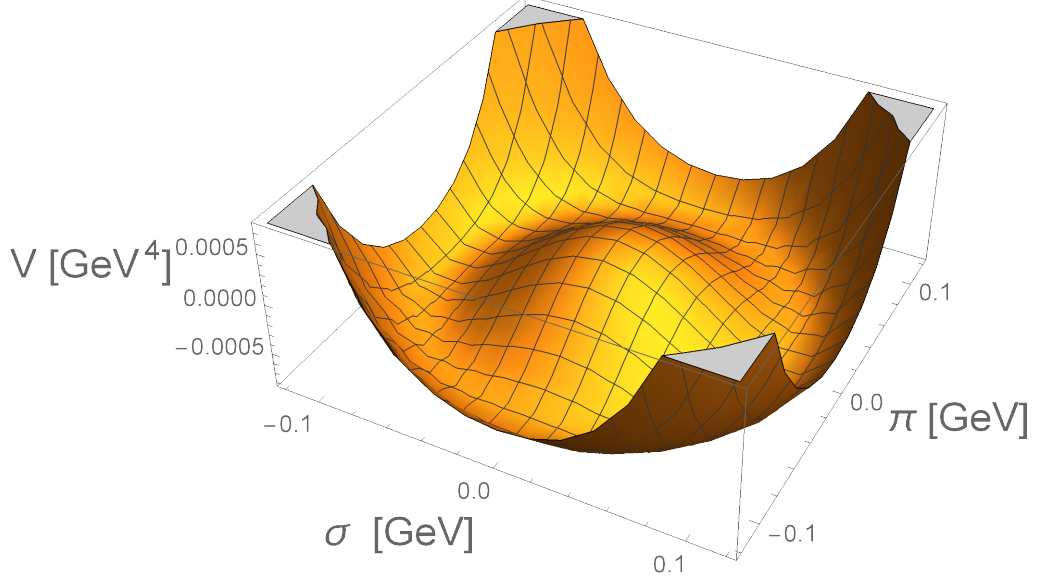


Fig. 17. Form of the chiral potential of Eq. (114) for $m_0^2 < 0$. There is a circle of minima for $\sigma^2 + \pi^2 = F^2 = -m_0^2/\lambda$.

$$P_{\min} = \left(\sigma_{\min} = \phi_N = \sqrt{-\frac{m_0^2}{\lambda}} = F, 0 \right). \quad (119)$$

The quantity $\phi_N = F$ is also denoted as the chiral condensate. Quite remarkably, a closer inspection of chiral models show that the previously studied pion decay constant is proportional to ϕ_N

$$\phi_N \sim f_\pi \sim N_c^{1/2}. \quad (120)$$

Namely, the coupling to the weak boson W^\pm emerges from an interaction term term of the type

$$g_{\text{weak}} W_\mu^\pm \sigma \partial^\mu \pi^\mp, \quad (121)$$

hence when σ condenses to $\phi_N \sim f_\pi$, the direct W - π mixing

$$W_\mu^\pm \longleftrightarrow \pi^\pm \quad (122)$$

arises.

Within this model, the masses are:

$$M_\pi^2 = \left. \frac{\partial^2 V}{\partial \pi^2} \right|_{P=P_{\min}} = 0 \sim N_c^0, \quad (123)$$

$$M_\sigma^2 = \left. \frac{\partial^2 V}{\partial \sigma^2} \right|_{P=P_{\min}} = m_0^2 + 3\lambda\phi_N^2 = -2m_0^2 = 2\lambda\phi_N^2 \sim N_c^0 > 0, \quad (124)$$

which are not degenerate: the pion has a vanishing mass (it is a Goldstone boson), while the σ is massive. One then realizes how spontaneous chiral symmetry breaking generates different masses for chiral partners. Note, M_σ is proportional to the chiral condensate ϕ_N . Both masses are still $\sim N_c^0$. Yet, as shown in [51], SSB is expected to occur for large N_c , just as it does for $N_c = 3$.

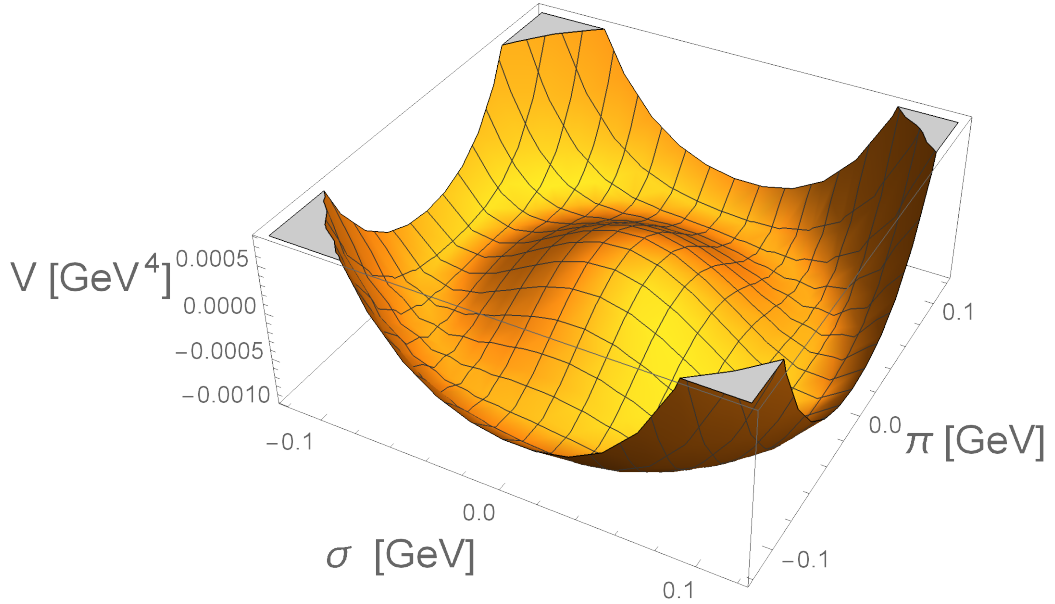


Fig. 18. Same as in Fig. 17 but with the explicit symmetry breaking of Eq. (125). There is now a unique minimum for $\sigma = \phi_N > 0$ and $\pi = 0$.

In Nature, the pion has a small but nonzero mass. In order to take this fact into account, the potential is modified as:

$$V(\sigma, \pi) = \frac{m_0^2}{2} (\pi^2 + \sigma^2) + \frac{\lambda}{4} (\pi^2 + \sigma^2)^2 - h\sigma, \quad (125)$$

where $-h\sigma$ breaks chiral symmetry explicitly. This term follows directly from the mass term $-m\bar{q}q$ in the QCD Lagrangian. We thus expect that

$h \propto m_n$, where m_n is the bare quark mass (e.g. the average $(m_u + m_d)/2$). The potential, plotted in Fig. 18 (same parameters as before and $h = m_\pi^2 f_\pi$ with $f_\pi = 92$ MeV and $m_\pi = 135$ MeV) has now a unique minimum for

$$P_{\min} = (\sigma_{\min} = \phi_N, 0) \quad (126)$$

with

$$\left. \frac{\partial V(\sigma, 0)}{\partial \sigma} \right|_{\sigma=\sigma_{\min}=\phi_N} = m_0^2 \phi_N + \lambda \phi_N^3 - h = 0 ,$$

which is of third order. (Only one of the three solutions corresponds to an absolute minimum). The pion mass is now nonzero:

$$M_\pi^2 = \left. \frac{\partial^2 V}{\partial \pi^2} \right|_{P=P_{\min}} = m_0^2 + \lambda \phi_N^2 = \frac{h}{\phi_N} > 0 . \quad (127)$$

We realize that the pion mass scale as $M_\pi \propto \sqrt{h} \propto \sqrt{m_n}$. This is indeed a nontrivial dependence, since one would naively expect that $M_\pi \propto h$, i.e. to the mass of its constituents. This is not the case, signaling that the tilted Mexican hat form of the potential is actually realized in Nature. This peculiar feature is also confirmed by lattice QCD studies, e.g. [67].

In order to fulfill the large- N_c expectation, one must require that:

$$h \sim N_c^{1/2} \rightarrow M_\pi^2 \sim N_c^0 . \quad (128)$$

This is indeed in agreement with the result for $f_\pi \propto N_c^{1/2}$. The term $h\sigma$ acts as a source term for σ , thus h scales as $N_c^{1/2}$. Yet, a closer look reveals a kind of problem: h has dimension energy³ and is proportional to m_n , then one would naively write $h \sim m_n \Lambda_{QCD}^2$, but Λ_{QCD} is N_c independent. How to reconcile that with the required scaling $h \sim N_c^{1/2}$? This point will be clarified in Sec. 3.2 after discussing the dilaton at large N_c .

The mass of the σ -particle is:

$$M_\sigma^2 = \left. \frac{\partial^2 V}{\partial \sigma^2} \right|_{P=P_{\min}} = m_0^2 + 3\lambda \phi_N^2 = M_\pi^2 + 2\lambda \phi_N^2 \sim N_c^0 . \quad (129)$$

The mass difference $m_\sigma^2 - m_\pi^2 = 2\lambda \phi_N^2 \sim N_c^0 > 0$ does not depend on h . The plot of the potential along the σ -direction is shown in Fig. 19 for two values of N_c .

The chiral condensate ϕ_N can be related to the quark condensate

$$\langle 0_{QCD} | \bar{q}q | 0_{QCD} \rangle < 0 \quad (130)$$

via the GOR relation(e.g. [68]):

$$M_\pi^2 f_\pi^2 = -2m_n \langle 0_{QCD} | \bar{q}q | 0_{QCD} \rangle , \quad (131)$$

where both members of this equation scale with N_c^2 . Note, this equation is also in agreement with $M_\pi^2 \propto m_n$.

The chiral condensate ϕ_N enters also in decays, such as $\sigma \rightarrow \pi\pi$. This is determined by performing the shift $\sigma \rightarrow \sigma + \phi_N$ and then isolating the term $\lambda\phi_N\sigma\pi^2$, out of which:

$$\Gamma_{\sigma \rightarrow \pi\pi} = 2 \frac{k_\pi}{8\pi M_\sigma^2} [\lambda\phi_N]^2 \sim N_c^{-1} , \quad (132)$$

where $k_\pi = \sqrt{\frac{M_\sigma^2}{4} - M_\pi^2} \propto N_c^0$ is the modulus of the three-momentum of one of the outgoing particle. Also in this case, the expected scaling is recovered.

In the full $N_f = 3$ version of the model, see e.g. Refs. [23, 28], the masses and decays are calculated by following the very same steps. Obviously, there are many more fields and decay channels, but the principle and the basic ideas are exactly the same as those discussed here.

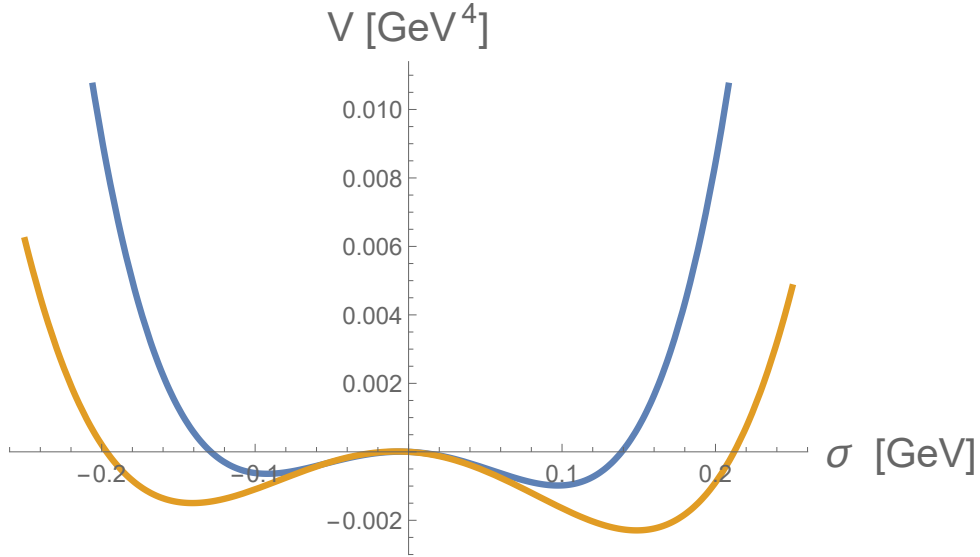


Fig. 19. Potential of Eq. (125) along the σ direction for $N_c = 3$ (upper blue curve) and for $N_c = 7$ (lower yellow curve). The minimum gets deeper on the vertical axis ($V_{min} \sim -N_c$) and its location on the horizontal axis moves to the right ($\phi_N \sim N_c^{1/2}$).

As stated above, in this $N_f = 1$ example, the anomaly has been disregarded. There are however some interesting large- N_c considerations that

can be done. The Lagrangian describing the anomaly for any N_f takes the form [69]:

$$\begin{aligned}\mathcal{L}_A &= -c_1(\det \Phi + \det \Phi^\dagger) - c_2(\det \Phi - \det \Phi^\dagger)^2 - c_3(\det \Phi + \det \Phi^\dagger)^2 \\ &= -2c_1\sigma + 4c_2\pi^2 - 4c_3\sigma^2 .\end{aligned}\quad (133)$$

The mass arising from the anomaly scales as $M_\pi^2 \sim N_c^{-1}$. (Actually, the name $M_{\eta_0}^2 \sim N_c^{-1}$ [52] with η_0 being the flavor singlet would be more appropriate, but for simplicity we stick to π).

For $N_f = 1$, the first terms is analogous to $h\sigma$ seen before, but the scaling is different, $c_1 \sim N_c^{-1/2}$ so that $M_\pi^2 \sim N_c^{-1}$ follows. For the same reason $c_2 \sim N_c^{-1}$, $c_3 \sim N_c^{-1}$. The former is evident, for the latter one needs to calculate the pion mass that turns out to be (for $h = c_1 = c_2 = 0$) $M_\pi^2 = 8c_3$. Thus:

$$c_1 \sim N_c^{-1/2}, \quad c_2 \sim N_c^{-1}, \quad c_3 \sim N_c^{-1} . \quad (134)$$

When changing N_f , these scaling behaviors are modified in such a way to preserve $M_{\eta_0}^2 \sim N_c^{-1}$. By properly counting the condensates that scale as $N_c^{1/2}$, one finds:

$$c_1 \sim N_c^{-N_f/2}, \quad c_2 \sim N_c^{-N_f}, \quad c_3 \sim N_c^{-N_f} . \quad (135)$$

For recent applications and extensions of the axial anomaly, see Refs. [70, 71].

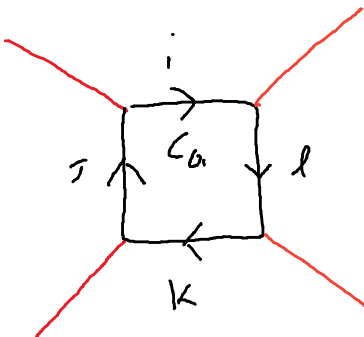
4) Different interaction types: a single trace ‘wins’.

The study of the full $N_f = 3$ chiral model is not within the scope of this lecture, but there is indeed an interesting point related to large- N_c that is worth to be discussed. To this end, let us introduce the nonet of pseudoscalar states [23, 72]

$$P = \begin{pmatrix} \frac{\eta_N + \pi^0}{\sqrt{2}} & \pi^+ & K^+ \\ \pi^- & \frac{\eta_N - \pi^0}{\sqrt{2}} & K^0 \\ K^- & \bar{K}^0 & \eta_S \end{pmatrix} \equiv \begin{pmatrix} u\bar{u} & u\bar{d} & u\bar{s} \\ d\bar{u} & d\bar{d} & d\bar{s} \\ s\bar{u} & s\bar{d} & s\bar{s} \end{pmatrix} \quad (136)$$

with $\pi^0 = \sqrt{1/2}(u\bar{u} - d\bar{d})$, and where $\eta(547)$ and $\eta'(958)$ emerge as a mixing of $\eta_N = \sqrt{1/2}(u\bar{u} + d\bar{d})$ and $\eta_S = s\bar{s}$. In chiral models such as [23, 66], there are typically two types of quartic interactions that emerge:

$$\mathcal{L}_P = -\lambda_2 \text{Tr}[P^4] - \lambda_1 (\text{Tr}[P^2])^2 . \quad (137)$$

$$\lambda_2 \text{Tr}[PPPP] = \lambda_2 P_{i\bar{j}} P_{\bar{j}k} P_{kl} P_{li}$$


$a = 1, \dots, N_c$
color

$$\lambda_2 \sim g_{Q\bar{q}q}^4 N_c \sim \frac{1}{N_c}$$

$i, \bar{j}, k, l : u, d, s$
flavor

Fig. 20. Large- N_c scaling of the term proportional to λ_2 in the Lagrangian of Eq. (137).

Their scaling is depicted in Figs. 20 and 21 respectively showing that $\lambda_2 \sim N_c^{-1}$ and $\lambda_1 \sim N_c^{-2}$.

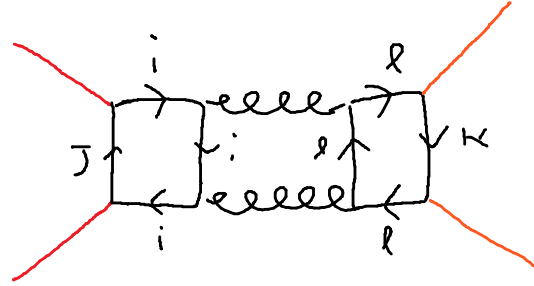
Note, other terms are possible, as:

$$\mathcal{L}'_P = -\lambda_3 \text{Tr}[P] \text{Tr}[P^3] - \lambda_4 (\text{Tr}[P])^4. \quad (138)$$

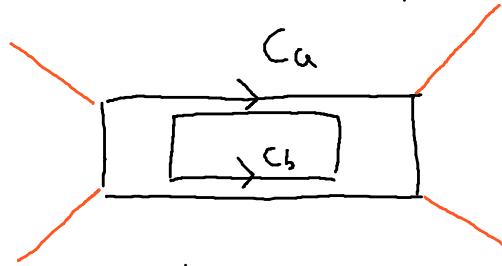
The scaling for λ_4 can be determined by drawing the corresponding diagrams of Fig. 22, leading to $\lambda_4 \sim N_c^{-4}$. A similar study for λ_3 leads to $\lambda_3 \sim N_c^{-2}$.

In conclusion, even if all the terms proportional to $\lambda_{1,2,3,4}$ are quartic terms in the mesonic fields, the large- N_c results show that only one domi-

$$\lambda_1 (\text{Tr}[PP])^2 : \lambda_1 P_{ij} P_{ji} \cdot P_{kl} P_{lk}$$



$$i, j, k, l = u, d, s$$



$$a, b = 1, \dots, N_c$$

$$\lambda_1 \sim g_{Q\bar{q}q}^2 N_c^2 \sim N_c^{-2}$$

Fig. 21. Large- N_c scaling of the four-leg term proportional to λ_1 in the Lagrangian of Eq. (137).

nates, the one that contains a single trace (the λ_2 -term). Interestingly, this result deals with an interplay of flavor and color d.o.f.. It is also relevant for models, since it makes clear which terms should be at first kept and which can be disregarded, see e.g. [73, 74].

5) Connection to correlations.

$$\lambda_4 \text{Tr}[P]^4 = \lambda_4 P_{ii} P_{jj} P_{kk} P_{ll}$$

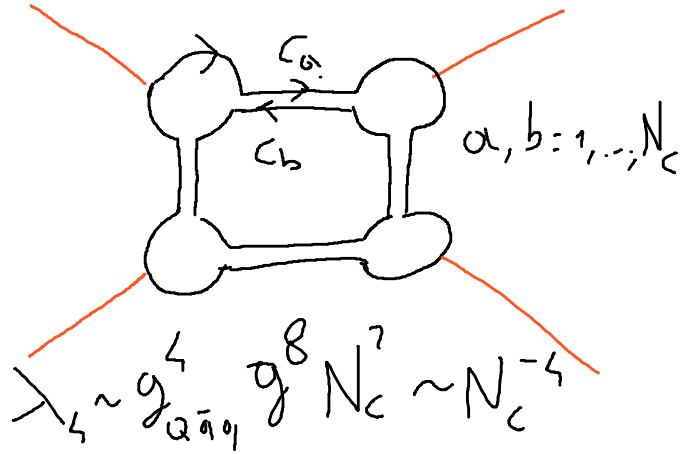
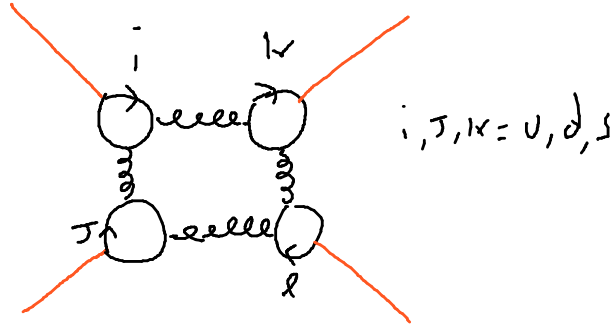


Fig. 22. Large- N_c scaling of the four-leg term proportional to λ_4 in the Lagrangian of Eq. (138).

In [6, 30] as well as other works on large- N_c , the starting point is the correlation function

$$\langle J_Q(x_2) J_Q(x_1) \rangle = -i \int \frac{d^4 p}{(2\pi)^2} F_Q(p) e^{ip(x_1 - x_2)}, \quad (139)$$

where the quantity $F_Q(p)$ is the loop contribution with total momentum

p . Within our framework, at lowest order this is just the loop function $-\Sigma_Q(s = p^2)$. Expanding $F_Q(p)$ we get (see Fig. 23 for an illustration of these processes):

$$F_Q(p) = -\Sigma_Q(s = p^2) (1 + \Sigma_Q(s)K_Q + \dots) = -\frac{\Sigma_Q(s)}{1 - \Sigma_Q(s)K_Q} = -\frac{\Sigma_Q(s)}{K_Q} \frac{1}{K_Q^{-1} - \Sigma_Q(s)}. \quad (140)$$

The pole is realized for the quarkonium mass M_Q^2 with the already encountered equation $K_Q^{-1} - \Sigma_Q(s = M_Q^2) = 0$. Upon expanding close to the pole, we find:

$$F_Q(p) = \frac{\Sigma_Q(s)\Sigma_Q(M_Q^2)}{\Sigma'_Q(M_Q^2)(s - M_Q^2)} \simeq \frac{\Sigma_Q^2(M_Q^2)g_{Q\bar{q}q}^2}{s - M_Q^2} \simeq \frac{f_Q^2}{s - M_Q^2} \quad (141)$$

where

$$f_Q = \Sigma_Q(M_Q^2)g_{Q\bar{q}q} = \frac{\Sigma_Q(M_Q^2)}{\sqrt{\Sigma'_Q(s = M_Q^2)}} \sim N_c^{1/2} \quad (142)$$

is the amplitude for the vacuum creation of the meson Q . Indeed, this expression has the same large- N_c behavior of the weak decay constant of this meson, see the previous discussion about f_π . (This equivalence does not hold for glueballs or hybrids).

Since for any given set of quantum numbers an infinity of conventional mesons exists [6], the previous equation may be generalized as:

$$F_Q(p) \simeq \sum_{n=1}^{\infty} \frac{f_{Q,n}^2}{s - M_{Q,n}^2} \sim N_c \quad (143)$$

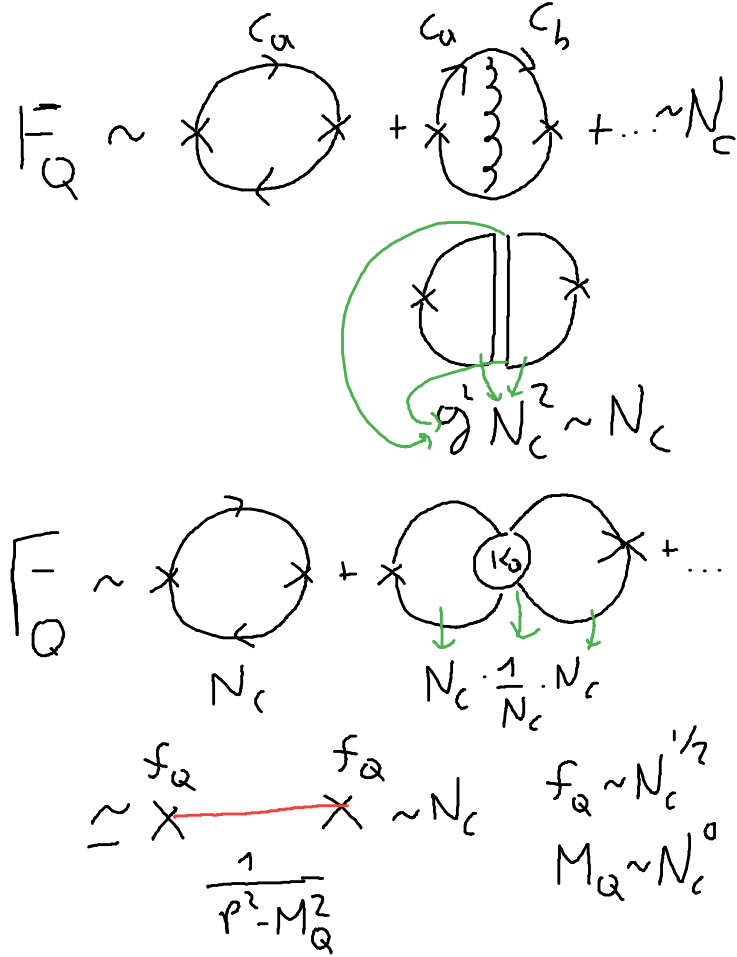
since $f_{Q,n}^2 \sim N_c$ and $M_{Q,n}^2 \sim N_c^0$. This equation can be found in Ref. [6].

6) Connection to Weinberg compositeness condition.

Finally, we study the Weinberg compositeness condition [16, 17] along the large- N_c direction. The starting point is the Lagrangian

$$\mathcal{L}_{Qq} = \mathcal{L}_q + g_{Q\bar{q}q}Q(x)J_Q(x) - \frac{\alpha}{2}Q^2, \quad (144)$$

where Q has no kinetic term and \mathcal{L}_q contains the kinetic part for the quark field as well as eventual other interactions not relevant here. Note, the parameter α is *not* the physical mass squared, see below. The basic assumption is that $g_{Q\bar{q}q} \sim N_c^{-1/2}$.

Fig. 23. Large- N_c scaling of the correlator $F_Q(s)$.

Upon using the e.o.m. for the field Q one has

$$\frac{\partial \mathcal{L}_{Qq}}{\partial Q} = g_{Q\bar{q}q} J_Q(x) - \alpha Q(x) = 0 \rightarrow Q(x) = \frac{g_{Q\bar{q}q}}{\alpha} J_Q(x). \quad (145)$$

Plugging it back into Eq. 144 one obtains a Lagrangian that depends on the quark field q only:

$$\mathcal{L}_{Qq} \equiv \mathcal{L}_q + \frac{g_{Q\bar{q}q}^2}{2\alpha} J_Q^2. \quad (146)$$

This is not a surprise, since Q had no kinetic term from the very beginning. One then gets the correspondence

$$K_Q = \frac{g_{Q\bar{q}q}^2}{\alpha} = \frac{1}{\Sigma_Q(M_Q^2)}, \quad (147)$$

where Eq. (77) has been used. Then:

$$\alpha = \frac{\Sigma_Q(M_Q^2)}{\Sigma'_Q(M_Q^2)} \sim N_c^0, \quad (148)$$

out of which:

$$J_Q(x) = \frac{\alpha}{g_{Q\bar{q}q}} Q(x) = \Sigma_Q(M_Q^2) g_{Q\bar{q}q} Q(x) = f_Q Q(x), \quad (149)$$

which shows that the microscopic quark current $J_Q(x)$ is proportional to the composite meson field $Q(x)$, and the constant of proportionality is the amplitude for production of this field in the QCD vacuum. In this way, the correlator $\langle J_Q(x_2) J_Q(x_1) \rangle$ takes the form

$$\langle J_Q(x_2) J_Q(x_1) \rangle = f_Q^2 \langle Q(x_2) Q(x_1) \rangle = -i f_Q^2 \int \frac{d^4 p}{(2\pi)^2} \frac{1}{p^2 - M_Q^2} e^{ip(x_1 - x_2)} \quad (150)$$

hence

$$F_Q(p) = \frac{f_Q^2}{p^2 - M_Q^2} \quad (151)$$

follows consistently.

The formal way to show the result above (especially Eq. (149)) starts from the Lagrangian containing the bare mesonic coupling, mass and field:

$$\mathcal{L}_{Qq} = \mathcal{L}_q + g_{Q_0\bar{q}q} Q_0(x) J_Q(x) - \frac{M_{Q_0}^2}{2} Q_0^2 + \frac{1}{2} (\partial_\mu Q_0)^2, \quad (152)$$

with

$$g_{Q_0\bar{q}q} \sim N_c^{-1/2} \text{ and } M_0 \sim N_c^0. \quad (153)$$

The propagator of the bare field Q_0 reads:

$$\frac{1}{p^2 - M_{Q_0}^2 + g_{Q_0\bar{q}q}^2 \Sigma_Q(p^2)} \sim N_c^0. \quad (154)$$

The first natural condition is to impose that the pole is realized for the physical mass M_Q^2 :

$$M_Q^2 - M_{Q_0}^2 + g_{Q_0\bar{q}q}^2 \Sigma_Q(M_Q^2) = 0. \quad (155)$$

Upon expanding the denominator of the propagator of Q_0 reads:

$$\begin{aligned} & \frac{1}{(p^2 - M_Q^2) \left(1 + g_{Q_0 \bar{q}q}^2 \Sigma'_Q(M_Q^2) \right) + g_{Q_0 \bar{q}q}^2 \tilde{\Sigma}_Q(p^2)} \\ & \simeq \frac{1}{(p^2 - M_Q^2) \left(1 + g_{Q_0 \bar{q}q}^2 \Sigma'_Q(M_Q^2) \right)} = \frac{Z_2}{p^2 - M_Q^2}, \end{aligned} \quad (156)$$

where $\tilde{\Sigma}_Q(p^2)$ contains terms of the type $(p^2 - M_Q^2)^2$ and higher powers, which are negligible close to the pole.

In order to obtain a correctly normalized propagator, the field

$$Q = \frac{1}{\sqrt{Z_2}} Q_0 \Leftrightarrow Q_0 = \sqrt{Z_2} Q \quad (157)$$

with the renormalization constant

$$Z_2 = \frac{1}{1 + g_{Q_0 \bar{q}q}^2 \Sigma'_Q(M_Q^2)} \sim N_c^0 \quad (158)$$

is introduced.

We impose here $g_{Q_0 \bar{q}q} \rightarrow \infty$, out of which $Z_2 \rightarrow 0$. Intuitively, it means that the dressed field Q is not fundamental, realizing the main idea behind the compositeness condition. The Lagrangian takes the form:

$$\begin{aligned} \mathcal{L}_{Qq} &= \mathcal{L}_q + g_{Q_0 \bar{q}q} \sqrt{Z_2} Q(x) J_Q(x) - \frac{M_{Q_0}^2}{2} Z_2 Q_0^2 + \frac{1}{2} Z_2 (\partial_\mu Q)^2 \\ &= \mathcal{L}_q + g_{Q_0 \bar{q}q} \sqrt{Z_2} Q(x) J_Q(x) - \frac{M_{Q_0}^2}{2} Z_2 Q^2, \end{aligned} \quad (159)$$

where the dynamical term for the field $Q(x)$ has disappeared. Next:

$$g_{Q\bar{q}q} = g_{Q_0 \bar{q}q} \sqrt{Z_2} = \frac{g_{Q_0 \bar{q}q}}{\sqrt{1 + g_{Q_0 \bar{q}q}^2 \Sigma'_Q(M_Q^2)}} \stackrel{g_{Q_0 \bar{q}q} \rightarrow \infty}{\sim} \frac{1}{\sqrt{\Sigma'_Q(M_Q^2)}} \sim N_c^{-1/2} \quad (160)$$

and

$$\alpha = M_{Q_0}^2 Z_2 = \frac{g_{Q_0 \bar{q}q}^2 \Sigma_Q(M_Q^2)}{1 + g_{Q_0 \bar{q}q}^2 \Sigma'_Q(M_Q^2)} \stackrel{g_{Q_0 \bar{q}q} \rightarrow \infty}{\sim} \frac{\Sigma_Q(M_Q^2)}{\Sigma'_Q(M_Q^2)} \sim N_c^0, \quad (161)$$

which coincide with the previous derivation.

3.2. Glueballs

According to lattice QCD many glueballs with various quantum numbers should exist, see e.g. the original predictions within the bag model [45], the review of Ref. [46] and the lattice works of e.g. [44, 75] (for a recent compilation and comparison of lattice results, see Ref. [76]). The glueball wave function must be colorless. Considering for definiteness the case of the scalar glueball, the corresponding (local and gauge invariant) current reads

$$J_G = \sum_{a=1}^{N_c^2-1} G_{\mu\nu}^a G^{\mu\nu,a} . \quad (162)$$

(For other currents, see e.g. [45, 77]). Using the double-line index notation, we may rewrite it as:

$$J_G \simeq \sum_{a=1}^{N_c} \sum_{b=1}^{N_c} G_{\mu\nu}^{(a,b)} G^{\mu\nu,(b,a)} . \quad (163)$$

Then, the color wave function of this glueball can be written as

$$|G\text{-color}\rangle \simeq \frac{1}{\sqrt{N_c^2-1}} J_G |0\rangle . \quad (164)$$

Explicitly:

$$|G\text{-color}\rangle \simeq \frac{1}{N_c} |\bar{C}_1 C_1 \bar{C}_2 C_2 + \bar{C}_1 C_1 \bar{C}_3 C_3 + \dots\rangle \simeq \frac{1}{N_c} \sum_{a=1}^{N_c} \sum_{b=1}^{N_c} |\bar{C}_a C_a \bar{C}_b C_b\rangle , \quad (165)$$

where, for simplicity, on the r.h.s. all the combinations are taken into account. Again, there is one combination (the colorless one) that should be subtracted, but this is unimportant for large N_c . Besides that, the previous equation is fully general, and applies to any two-gluon glueball.

Following the same procedure as for quark-antiquark states, let us consider the processes leading to the illustrative transition:

$$\bar{C}_1 C_1 \bar{C}_2 C_2 \rightarrow \bar{C}_3 C_3 \bar{C}_4 C_4 \quad (166)$$

in which all the colors have been changed. It is easy to see that the dominant processes leading to this type of transitions scales as N_c^{-2} , see Fig. 24. In fact, a single gluon exchange or the quartic interaction, proportional to g^2 , are not sufficient for a switch of all colors, see Fig. 25.

We write down an effective Lagrangian

$$\mathcal{L}_G = K_G J_G^2 \quad (167)$$

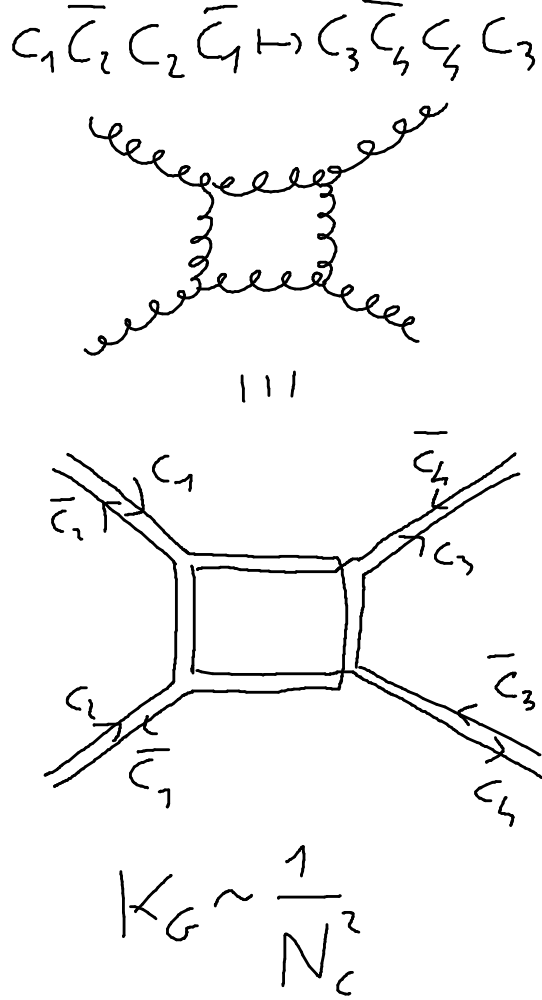


Fig. 24. Example of a leading diagram for the gluon-gluon scattering of the type $C_1 \bar{C}_2 C_2 \bar{C}_1 \rightarrow C_3 \bar{C}_4 C_4 \bar{C}_3$. Note, all colors are changed. The amplitude scales as N_c^{-2} and models the coupling in Eq. (167).

where

$$K_G \sim g^4 \sim N_c^{-4}, \text{ thus } K_G = \frac{\bar{K}_G}{N_c^2}, \quad (168)$$

with \bar{K}_G being N_c independent. Note, a (nonlocal version of this) Lagrangian was implemented in Ref. [18] to study the mixing of glueballs

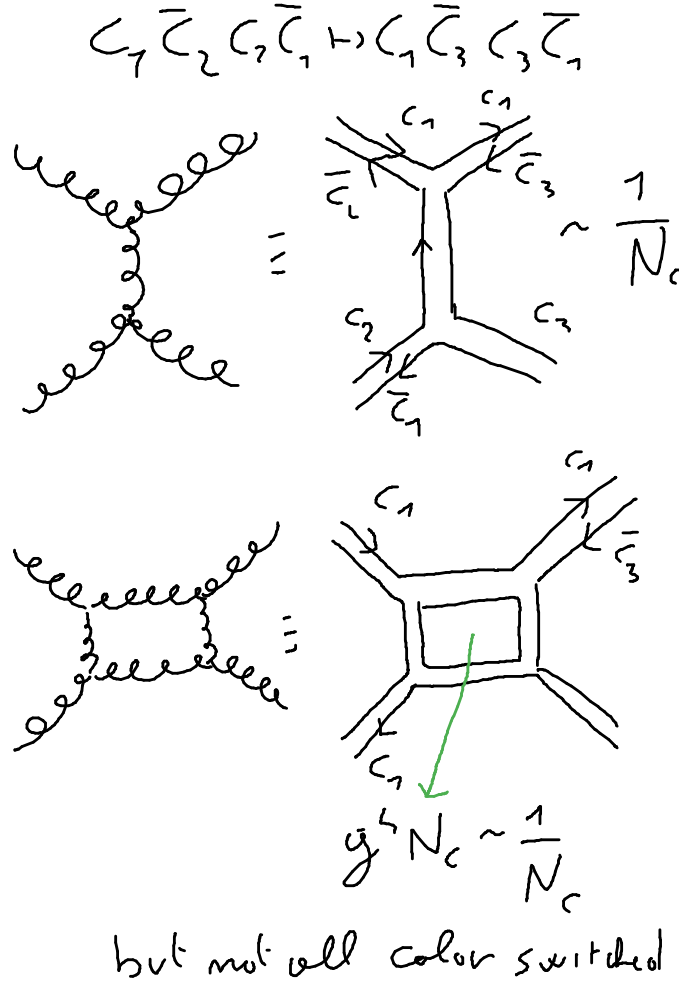


Fig. 25. Example of a leading diagram for the gluon-gluon scattering of the type $C_1 \bar{C}_2 C_2 \bar{C}_1 \rightarrow C_1 \bar{C}_4 C_4 \bar{C}_3$. Note, not all colors are switched (C_1 is in the beginning and in the end). This term, whose amplitude goes as N_c^{-1} , does **not** model the constant K_G in Eq. (167).

with quarkonia.

The gluon-gluon scattering matrix for a given selected process such as $\bar{C}_1 C_1 \bar{C}_2 C_2 \rightarrow \bar{C}_3 C_3 \bar{C}_4 C_4$ is given by

$$T_G(s) = \frac{1}{K_G^{-1} - \Sigma_G(s)} \quad (169)$$

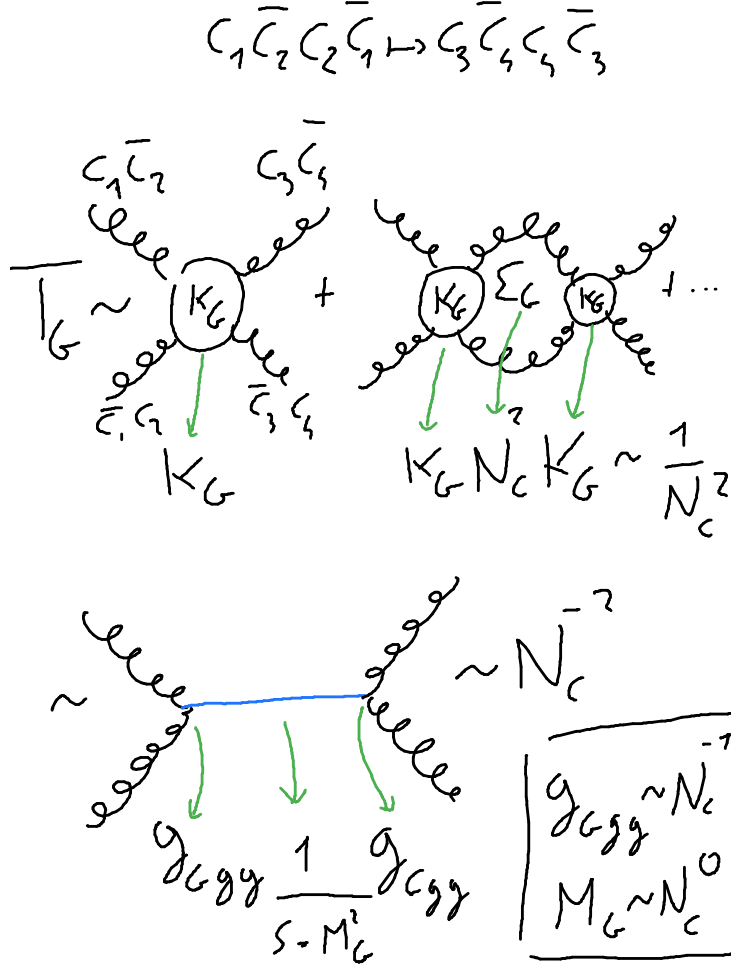


Fig.26. Resummation of diagrams for the gluon-gluon scattering of the type $C_1 \bar{C}_2 C_2 \bar{C}_1 \rightarrow C_3 \bar{C}_4 C_4 \bar{C}_3$ with consequent formation of an intermediate glueball state (blue line).

see Fig. 26 for its pictorial representation. Now, the loop $\Sigma_G(s)$ scales as [18, 78]:

$$\Sigma_G(s) = N_c^2 \bar{\Sigma}_G(s) . \quad (170)$$

Then:

$$T_G = \frac{1}{\frac{N_c^2}{K_G} - N_c^2 \bar{\Sigma}_G(s)} . \quad (171)$$

Just as for the quarkonium, the glueball mass is N_c -independent and solves the equation

$$\frac{1}{\bar{K}_G} - \bar{\Sigma}_G(s = M_G^2) = 0 \rightarrow M_G \sim N_c^0 . \quad (172)$$

Following the same steps, the amplitude can be written as

$$T_G \simeq \frac{(ig_{Ggg})^2}{s - M_G^2} \quad (173)$$

where the coupling of the glueball to its gluonic constituents is

$$g_{Ggg} = \frac{1}{\sqrt{N_c^2 \left(\frac{\partial \bar{\Sigma}_G(s)}{\partial s} \right)_{s=M_G^2}}} = \frac{\bar{g}_{Ggg}}{N_c} . \quad (174)$$

From the results above, we can easily derive the phenomenology of glueballs at large- N_c .

First, we describe the four- and six-leg purely glueball couplings, which scale as N_c^{-2} and N_c^{-3} , respectively, see Fig. 27. This is in agreement with the general amplitude for n_G glueballs being $A_{n_G G} \propto \frac{N_c^2}{N_c^{n_G}}$, see Sec. 2.6.

Next, we calculate the interaction of a glueball with mesons. The basic mixing goes as $A_{GQ} \sim N_c^{-1/2}$, while the decay amplitude scales as $A_{GQQ} \sim N_c^{-1}$ (see Fig. 28). It then follows that the glueball decay into two standard mesons is suppressed as

$$\Gamma_{G \rightarrow QQ} \sim N_c^{-2} , \quad (175)$$

thus even more suppressed than the quarkonium decay.

As additional examples, in Fig. 30 we present the scattering $GG \rightarrow QQ$ (two glueballs into two quarkonia), that behaves as N_c^{-2} , and in Fig. 27 the scattering $GGG \rightarrow QQ$ scaling with N_c^{-3} .

The general amplitude for n_Q quarkonia and n_G glueballs as $A_{(n_Q Q)(n_G G)} \propto \frac{N_c}{N_c^{n_Q/2} N_c^{n_G}}$. In this way we confirm the previously quoted results (Sec. 2.6).

An important remark is in order: glueballs with three gluons work just as above. The scaling laws are left unchanged.

Next, we describe additional consequences concerning glueballs.

1) The dilaton Lagrangian in the large- N_c limit.

The scalar glueball G can be described as a dilaton field, which is an important element of many chiral models (among which the extended linear sigma model [23]).

The dilaton Lagrangian reads [25, 26, 27, 28]

$$\mathcal{L}_{dil} = \frac{1}{2}(\partial_\mu G)^2 - V_{dil}(G) , \quad (176)$$

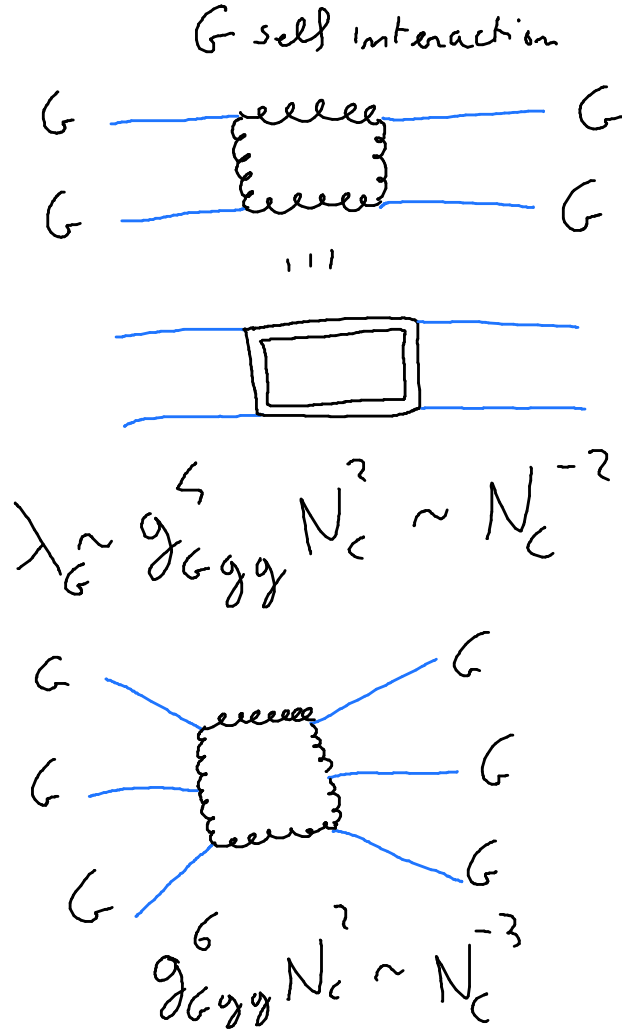


Fig. 27. Examples of processes involving only glueballs as initial and final states. Up: the amplitude $GG \rightarrow GG$ goes as N_c^{-2} . Down: the amplitude $GGG \rightarrow GGG$ goes as N_c^{-3} .

with

$$V_{dil}(G) = \frac{1}{4} \lambda_G \left[G^4 \ln \left(\frac{G}{\Lambda_G} \right) - \frac{G^4}{4} \right], \quad (177)$$

which contain the dimensionless constant λ_G and the dimensionful constant

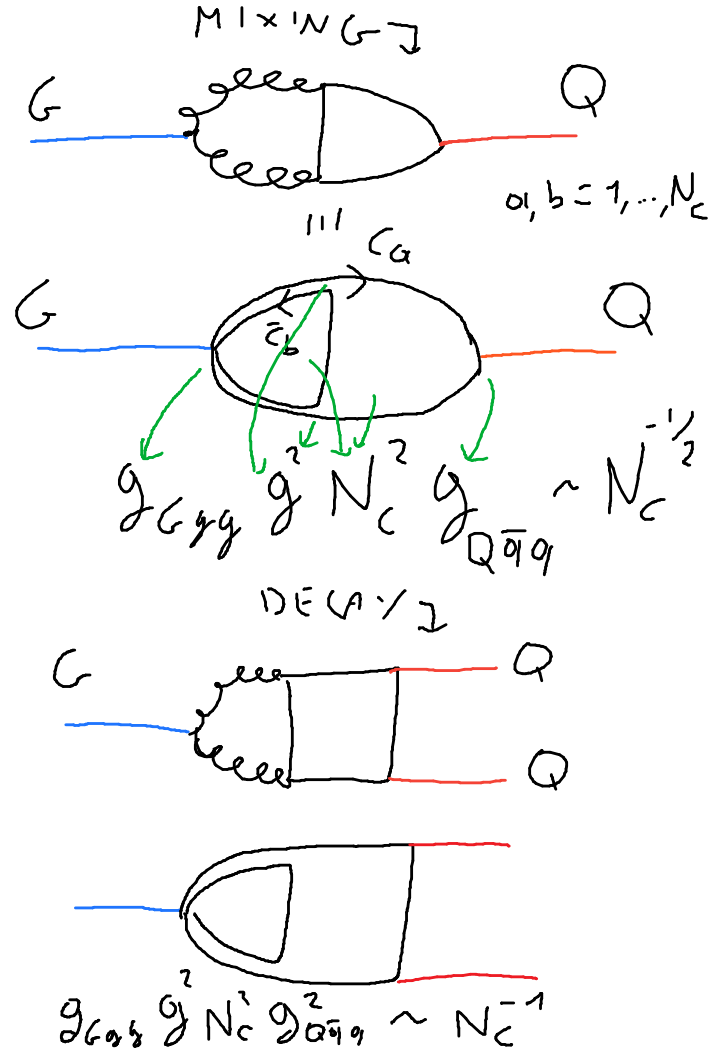


Fig. 28. Up: Mixing of a glueball (blue) and a quarkonium (red) via quarks and gluons (black straight and springy lines). The amplitude scales as $N_c^{-1/2}$. Down: Decay of a glueball (blue) into two quarkonia (red) via quarks and gluons (black). This diagram scales as N_c^{-1} , thus the glueball decay width goes as N_c^{-2} .

Λ_G . The scaling laws, to be explained below, are given by:

$$\lambda_G \sim N_c^{-2}, \Lambda_G \sim N_c. \quad (178)$$

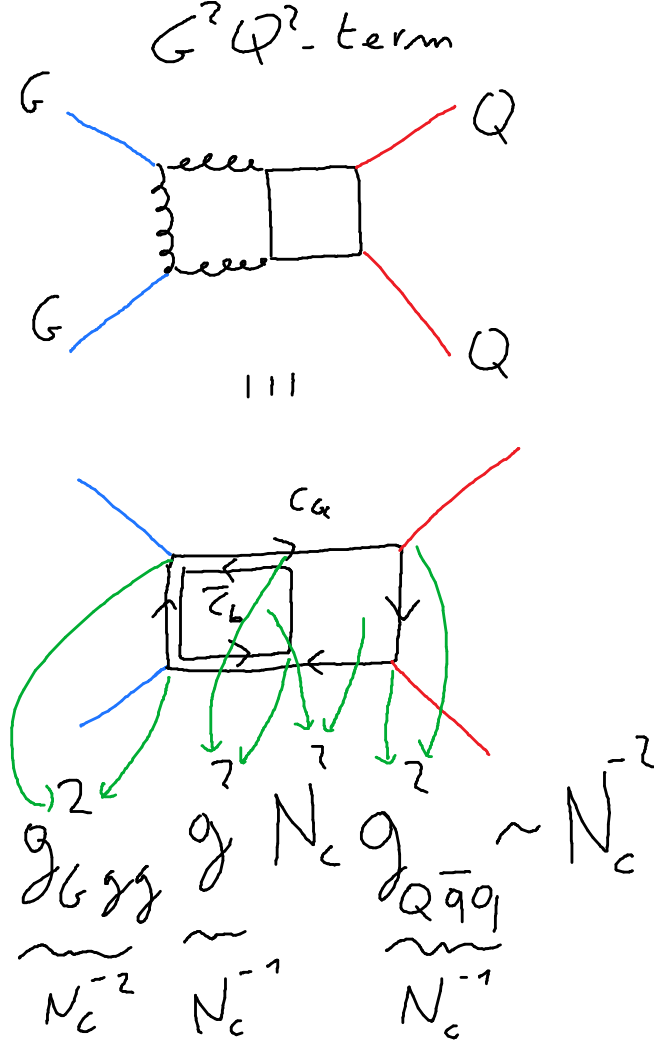


Fig.29. Leading amplitude for the process $GG \rightarrow QQ$, that scales as N_c^{-2} . As usual, glueballs are blue, quarkonia red, quarks and gluons black.

The potential is shown in Fig. 31 for two different values of N_c (3 and 7, respectively). For $N_c = 3$, the numerical values are given by $\lambda_G = 1.7^2/0.5^2$ and $\Lambda_G = 0.5^2 \text{ GeV}^2$, corresponding to a glueball mass of 1.7 GeV, in agreement with lattice estimates [44, 75].

The logarithm and the dimensional parameter Λ_G are required for de-

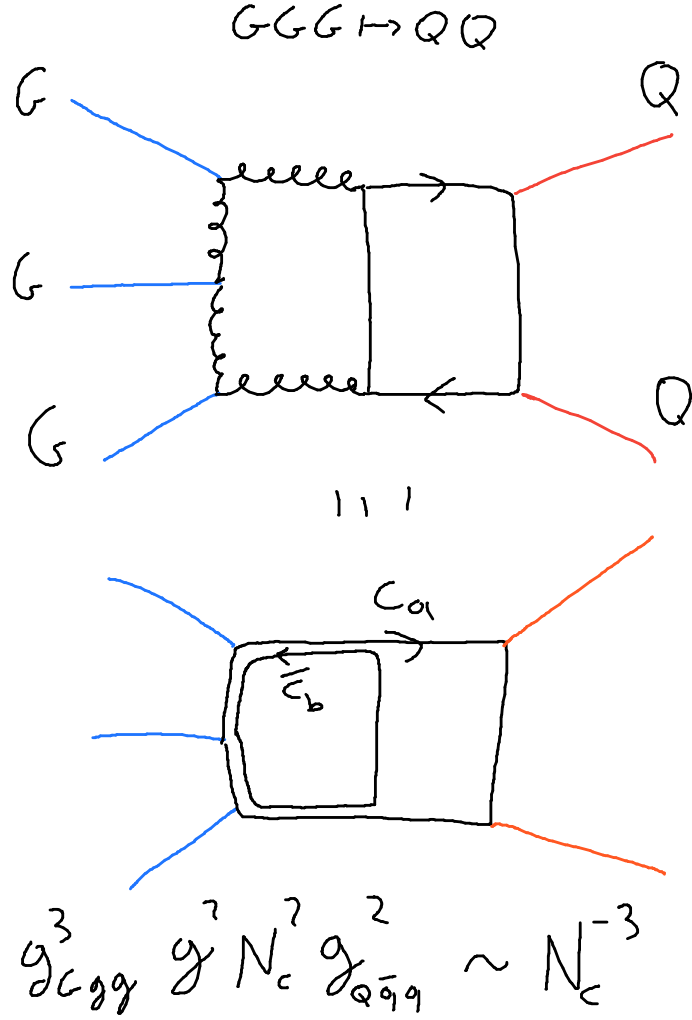


Fig. 30. Leading amplitude for the process $GGG \rightarrow QQ$, that scales as N_c^{-3} .

scribing the breaking of dilatation symmetry

$$x^\mu \rightarrow \lambda^{-1} x^\mu \text{ and } G(x) \rightarrow G'(x') = \lambda G(x)$$

in the following way:

$$\partial_\mu J^\mu = T_\mu^\mu = G \partial_G V_{dil}(G) - 4G = -\frac{1}{4} \lambda_G G^4. \quad (179)$$

This equation resembles the QCD result [2, 27]

$$(T_\mu^\mu)_{QCD} = -\frac{\alpha_s}{16\pi} \left(\frac{11}{3}N_c - \frac{2}{3}N_f \right) G_{\mu\nu}^a G^{a,\mu\nu} . \quad (180)$$

Taking the expectation value of the former equation we get:

$$\langle (T_\mu^\mu)_{QCD} \rangle = -\frac{\alpha_s}{16\pi} \left(\frac{11}{3}N_c - \frac{2}{3}N_f \right) \langle G_{\mu\nu}^a G^{a,\mu\nu} \rangle , \quad (181)$$

which scales as N_c^2 because the gluon condensate $\langle G_{\mu\nu}^a G^{a,\mu\nu} \rangle \sim N_c^2$ and $\alpha_s \sim N_c^{-1}$ (for a numerical estimate of the gluon condensate for $N_c = 3$, see Ref. [79]). Does the dilaton potential reproduce this scaling? In order to see that, let us expand the dilaton potential around the minimum, which is realized for $G_0 = \Lambda_G$. Upon performing the shift $G \rightarrow G_0 + \Lambda_G$, we obtain [80]:

$$V_{dil}(G) = -\lambda_G \Lambda_G^4 + \frac{1}{2} \lambda_G \Lambda_G^2 G^2 + \frac{5\lambda_G \Lambda_G}{3!} G^3 + \frac{11\lambda_G}{4!} G^4 + \dots \quad (182)$$

where $V_{dil}(G = \Lambda_G) = -\lambda_G \Lambda_G^4 \sim N_c^2$ has been used. From the term proportional to G^4 it follows that

$$\lambda_G \sim N_c^{-2} . \quad (183)$$

The glueball mass reads

$$M_G^2 = \lambda_G \Lambda_G^2 \sim N_c^0 \rightarrow \Lambda_G \sim N_c . \quad (184)$$

Note, the G^3 terms scales as $\lambda_G \Lambda_G \sim N_c^{-1}$, which is in agreement with the previous general rules. Going to higher order in the expansions would also generate terms in agreement with those rules (for instance, G^5 goes as $\lambda_G/\Lambda_G \sim N_c^{-3}$ as expected, etc.).

The fact that the scale Λ_G scales as N_c implies that it can be intuitively expressed as

$$\Lambda_G \sim N_c \Lambda_{QCD} . \quad (185)$$

Finally, let us have a look at the condensate of the dilaton field:

$$\langle T_\mu^\mu \rangle = -\frac{1}{4} \lambda_G \langle G^4 \rangle = -\frac{1}{4} \lambda_G \Lambda_G^4 \sim -N_c^2 \quad (186)$$

in agreement with the QCD scaling of Eq. (181).

The scalar glueball is the lightest gluonic state predicted by lattice QCD and is a natural element of the chiral models with dilatation invariance

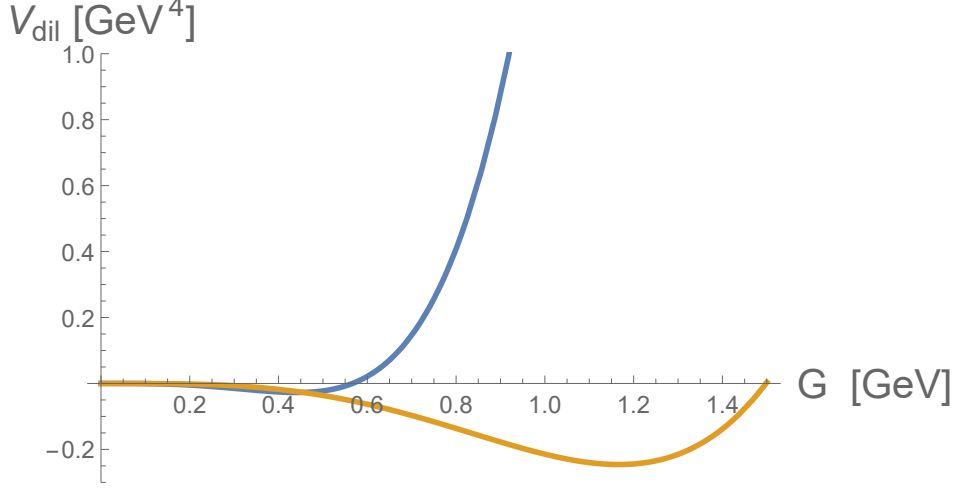


Fig. 31. Function $V_{dil}(G)$ expressed in Eq. (177) for $N_c = 3$ (blue line) and for $N_c = 7$ (yellow line). The value of the minimum G_0 increases with N_c , while its depth scales with $-N_c^2$. The numerical value for $N_c = 3$ are: $\Lambda_G = 0.5$ GeV, and $\lambda_G = 1.7^2/\Lambda_G^2$, corresponding to a scalar glueball mass of $M_G = 1.7$ GeV.

[23, 28]. Presently, the resonance $f_0(1710)$ is a good candidate for being predominantly the scalar glueball, see e.g. [28, 81, 82, 83, 84, 85] and refs. therein.

2) Coupling the dilaton to other glueballs.

The lightest scalar glueball is special since it is related to dilatation symmetry and its breaking, but other fields can be easily introduced. For illustrative purposes, let us couple the dilaton to the pseudoscalar glueball \tilde{G} and the tensor glueball $T_{\mu\nu}$:

$$\mathcal{L} = \mathcal{L}_{dil} + \mathcal{L}_{kin} - \frac{\lambda_{\tilde{G}G}}{2} \tilde{G}^2 G^2 - \lambda_{\tilde{G}} \tilde{G}^4 + \frac{\lambda_{TG}}{2} T_{\mu\nu} T^{\mu\nu} G^2 + \frac{\lambda_T}{2} (T_{\mu\nu} T^{\mu\nu})^2 + \dots \quad (187)$$

where the only dimensionful parameter is Λ_G entering in \mathcal{L}_{dil} . All the λ parameters scale as N_c^{-2} , since each of them describes a four-leg interaction among glueballs.

When considering the shift $G \rightarrow \Lambda_G + G$, the other glueballs get a mass: $m_{\tilde{G}}^2 = \lambda_{\tilde{G}G} \Lambda_G^2 \sim N_c^0$ and $m_T^2 = \lambda_{TG} \Lambda_G^2 \sim N_c^0$. For an explicit study of the scattering of tensor glueballs using the Lagrangian above see Ref. [76].

3) Coupling the dilaton to the LSM.

We consider, again for simplicity, the case $N_f = 1$. The potential for the chiral model containing both the dilaton as well as the chiral multiplet

$\Phi = \sigma + i\pi$ is given by:

$$V(G, \sigma, \pi) = V_{dil}(G) + \frac{a}{2}G^2\Phi^*\Phi + \frac{\lambda}{4}(\Phi^*\Phi)^2 . \quad (188)$$

Above, the only dimensionful parameter is Λ_G entering in $V_{dil}(G)$. Above, the constant a scales as

$$a \sim N_c^{-2} , \quad (189)$$

since it parameterizes a vertex with 2 glueballs and two quarkonia. The realistic $N_f = 3$ treatment of this model can be found in Ref. [28].

The search for the minimum of the model is more complicated than in the LSM case, since now two scalar fields are present and can condense. Namely, setting the pion field to zero ($\pi = 0$), one has:

$$V(G, \sigma, 0) = \frac{1}{4}\lambda_G \left[G^4 \ln \left(\frac{G}{\Lambda_G} \right) - \frac{G^4}{4} \right] + \frac{a}{2}G^2\sigma^2 + \frac{\lambda}{4}\sigma^4 , \quad (190)$$

with

$$\lambda_G \sim N_c^{-2} , \Lambda_G \sim N_c , a \sim N_c^{-2} , \lambda \sim N_c^{-1} . \quad (191)$$

The minimum is searched for:

$$\partial_G V(G, \sigma, 0) = \lambda_G G^3 \ln \left(\frac{G}{\Lambda_G} \right) + aG\sigma^2 = 0 , \quad (192)$$

$$\partial_\sigma V(G, \sigma, 0) = aG^2\sigma + \lambda\sigma^3 = 0. \quad (193)$$

For $a > 0$, the minimum is realized for $G_0 = \Lambda_G \neq 0$, $\sigma_0 = 0$, but as explained above this is not what we have in Nature.

For $a < 0$, the minimum is realized for $G_0 \neq 0$, $\sigma_0 \neq 0$: spontaneous breaking of chiral symmetry is realized. In particular, one has

$$\sigma_0^2 = -\frac{aG_0^2}{\lambda} \rightarrow \sigma_0 = \sqrt{\frac{-m_0^2}{\lambda}} \sim N_c^{1/2} \text{ with } m_0^2 = aG_0^2 < 0 . \quad (194)$$

The equation for G_0 reads:

$$\lambda_G G_0^3 \ln \left(\frac{G_0}{\Lambda_G} \right) = -aG_0\sigma_0^2 = \frac{a^2 G_0^3}{\lambda} , \quad (195)$$

or

$$\ln \left(\frac{G_0}{\Lambda_G} \right) = \frac{a^2}{\lambda \lambda_G} , \quad (196)$$

hence:

$$G_0 = \Lambda_G e^{\frac{a^2}{\lambda \lambda_G}} \geq \Lambda_G . \quad (197)$$

In terms of large- N_c , we have:

$$G_0 \sim N_c e^{1/N_c} \sim N_c \left(1 + \frac{1}{N_c} + \dots \right) . \quad (198)$$

Thus in the large- N_c limit

$$G_0 = \Lambda_G \quad (199)$$

How far is G_0 from Λ_G ? For $N_c = 3$ that depends on the numerical values, but typically $G_0 \simeq \Lambda_G$ is well fulfilled [80].

Finally, let us briefly discuss the explicit symmetry breaking. That can be achieved by a term of the type

$$\lambda_n m_n G^2 \sigma \quad (200)$$

where the coupling constant λ_n scales as

$$\lambda_n \sim N_c^{-3/2} \quad (201)$$

since it represents the coupling to two glueballs to an ordinary meson.

Then, the parameter h in Eq. (125) turns out to be (upon dilaton condensation ($G = G_0$)):

$$h = \lambda_n m_n G_0^2 \simeq \lambda_n m_n \Lambda_G^2 \sim N_c^{1/2} , \quad (202)$$

as required for getting a pion mass that does not depend on N_c .

Another interesting consequence of this toy model is the decay of G into pions [80]:

$$\Gamma_{G \rightarrow \pi\pi} = 2 \frac{k_\pi}{8\pi M_\sigma^2} [aG_0]^2 = 2 \frac{k_\pi}{8\pi M_\sigma^2} \left[\frac{-m_0^2}{G_0} \right]^2 \quad (203)$$

$$\simeq 2 \frac{k_\pi}{8\pi M_\sigma^2} \left[\frac{M_\sigma^2}{2\Lambda_G} \right]^2 \sim N_c^{-2} , \quad (204)$$

where $k_\pi = \sqrt{\frac{M_G^2}{4} - M_\pi^2}$. The scaling, that follows from $\Lambda_G \sim N_c$, is in agreement with the expected results.

All in all, a fully consistent picture, that is correctly embedded in chiral models with the dilaton, is obtained in the large- N_c limit.

4) Decays of other glueballs.

Other glueballs also decays into conventional quark-antiquark mesons. A special case is given by the pseudoscalar glueball, whose coupling to mesons may be written down as [86]

$$\mathcal{L}_{\tilde{G}} = ic_{\tilde{G}}\tilde{G}(\det \Phi - \det \Phi^\dagger) \quad (205)$$

where

$$c_{\tilde{G}} \propto N_c^{-1/2-N_f/2} . \quad (206)$$

A numerical evaluation of $c_{\tilde{G}}$ via instantons can be found in Ref. [71]. The recently discovered resonance $X(2600)$ by the BES III collaboration is a promising candidate for being the pseudoscalar glueball [87].

For the study of various glueball decays we refer to chiral models of Refs. [86, 88, 89] and to the Witten-Sakai-Sugimoto approach (which also makes use of large- N_c arguments) of Refs. [84, 90, 91].

5) Connection to correlations

When considering the correlation involving glueball currents

$$\langle J_G(x_2)J_G(x_1) \rangle = -i \int d^4p F_G(p) e^{ip(x_1-x_2)} , \quad (207)$$

$F_G(p)$ is the loop contribution with total momentum p . At lowest order this is just the loop function $-\Sigma_G(s=p^2)$. Evaluating $F_G(p)$ according to Fig. 32 we get:

$$\begin{aligned} F_G(p) &= -\Sigma_G(s=p^2) (1 + \Sigma_G(s)K_G + \dots) = \\ &= -\frac{\Sigma_G(s)}{1 - \Sigma_G(s)K_G} = -\frac{\Sigma_G(s)}{K_G} \frac{1}{K_G^{-1} - \Sigma_G(s)} . \end{aligned} \quad (208)$$

The pole takes place (just as previously) for $K_G^{-1} - \Sigma_G(s=M_G^2) = 0$. Upon expanding close to the pole, we find:

$$F_G(p) = \frac{\Sigma_G(s)\Sigma_G(M_G^2)}{\Sigma'_G(M_G^2)(s-M_G^2)} \simeq \frac{\Sigma_G^2(M_G^2)g_{Ggg}^2}{s-M_G^2} \simeq \frac{f_G^2}{s-M_G^2} \quad (209)$$

where

$$f_G = g_{Ggg}\Sigma_G(M_G^2) \sim N_c^{-1} \cdot N_c^2 \sim N_c \quad (210)$$

is the vacuum production/annihilation amplitude of the glueball G . In some cases, f_G may also be referred as a ‘decay constant’, yet it should be stressed that this is not the weak decay constant. This is so because W^\pm and Z^0 couple directly to quarks and not to gluons. In order to obtain the weak

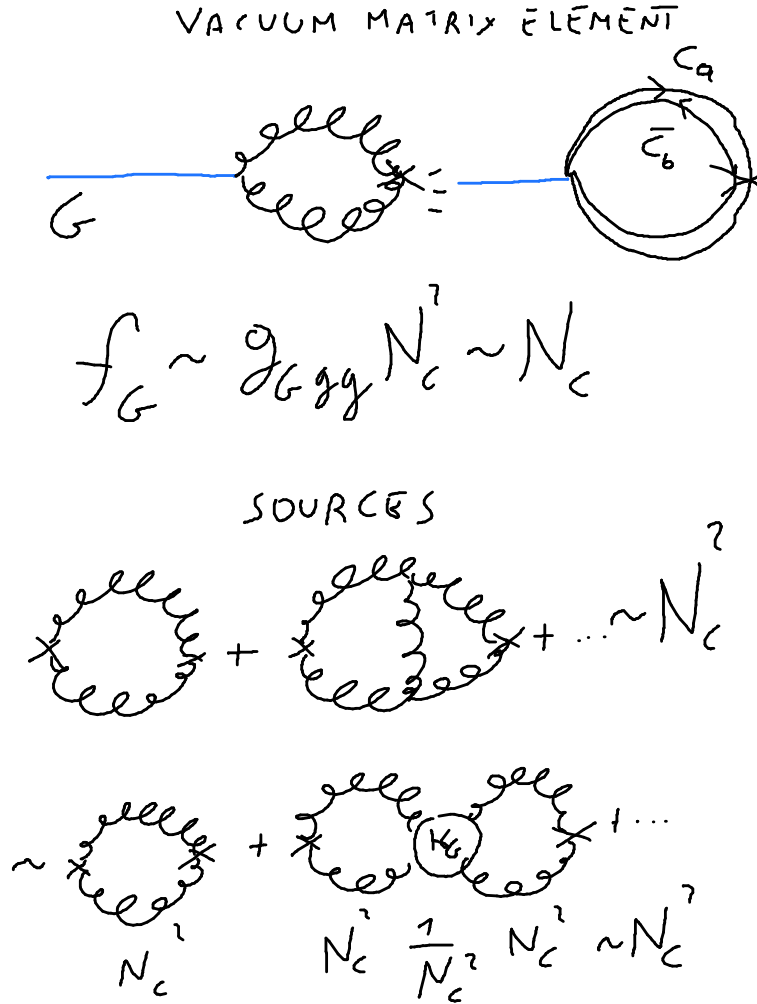


Fig. 32. Up: Amplitude for the production of the glueball, denoted as f_G , scales with N_c . Down: Correlator due to colorless sources of gluon-gluon states (glueballs): the bubbles scale as N_c^2 . One may understand this process with a (tower of) glueball(s) as intermediate states, see Eq. (3.2).

decay constant of glueballs, an additional suppression of N_c enters, leading to

$$f_G^{weak} \sim N_c^0. \quad (211)$$

Indeed, the same result can be obtained starting with an external glueball

G , which transforms to a Q (mixing proportional $N_c^{-1/2}$), which then annihilates weakly (process proportional to $f_Q \sim N_c^{1/2}$). The scaling goes as $f_G^{weak} \sim N_c^{-1/2} \cdot f_Q \sim N_c^0$.

3.3. Hybrids

Hybrids are bound states containing a quark-antiquark pair and a gluon, see the review of Ref. [92] and the lattice results in Ref. [93]. As an example of an hybrid current, we consider the lightest 1^{-+} hybrid case:

$$J_H^\mu = \sum_{a=1}^{N_c^2-1} \bar{q} G^{a,\mu\nu} t^a \gamma^5 \gamma_\nu q . \quad (212)$$

The quantity $\bar{q} G^{a,\mu\nu} t^a \gamma^5 \gamma_\nu q$ is a scalar in color space. Schematically (and neglecting Lorentz indices and Dirac matrices), the hybrid current in the double-line notation reads

$$J_H = \sum_{a=1}^{N_c} \sum_{b=1}^{N_c} \bar{q}^{(a)} A^{(a,b)} q^{(b)} = C_1 (\bar{C}_1 C_2) \bar{C}_2 + C_3 (\bar{C}_3 C_4) \bar{C}_4 + \dots \quad (213)$$

The corresponding interaction Lagrangian for the hybrid formation is expressed as:

$$\mathcal{L}_H = K_H J_H^2 \quad (214)$$

In line with the previous cases, let us consider a specific transition (see Fig. 33):

$$C_1 (\bar{C}_1 C_2) \bar{C}_2 \rightarrow C_3 (\bar{C}_3 C_4) \bar{C}_4 \quad (215)$$

in which all colors have been switched.

The basic (connected) interaction turns out to be of the order of (see Fig. 33):

$$K_H \propto g^4 \propto N_c^{-2} \rightarrow K_H = \frac{\bar{K}_H}{N_c^2} . \quad (216)$$

We then proceed as before by resumming over loop diagrams, see Fig. 34, finding:

$$T_H(s) = \frac{1}{K_H^{-1} - \Sigma_H(s)} . \quad (217)$$

Now, the loop $\Sigma_H(s)$ scales as:

$$\Sigma_H(s) = N_c^2 \bar{\Sigma}_H(s) . \quad (218)$$

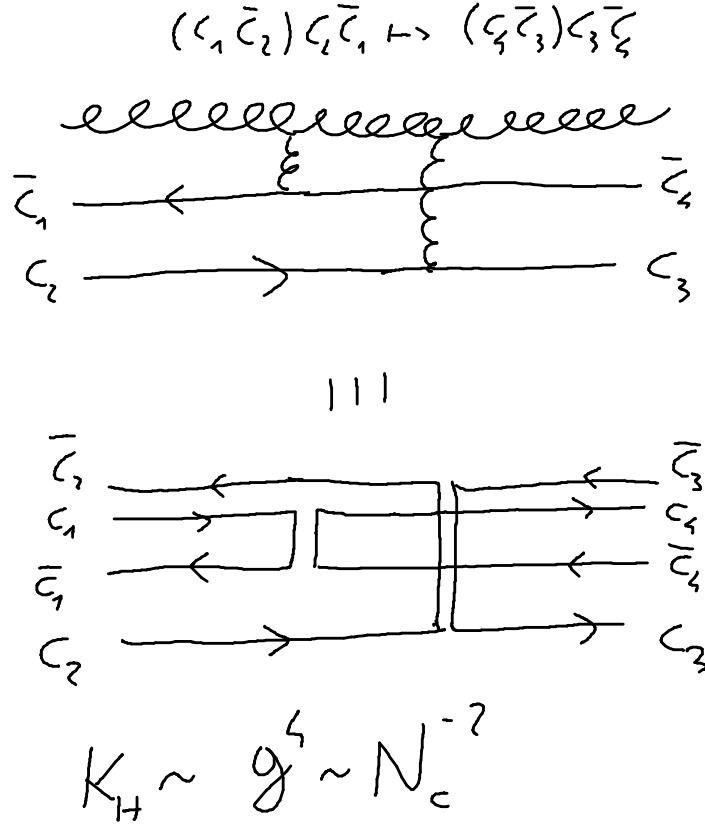


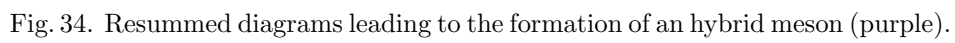
Fig.33. Amplitude for gluon-quark-antiquark (hybrid) scattering of the type $(C_1 \bar{C}_2) C_2 \bar{C}_1 \rightarrow (C_4 \bar{C}_3) C_3 \bar{C}_4$. Then initial gluon is $(C_1 \bar{C}_2)$ and the final one $(C_4 \bar{C}_3)$. Note, all colors have been switched. The corresponding amplitude scales as N_c^{-2} and models the constant K_H appearing in the interaction Lagrangian of Eq. (214).

Then:

$$T_H = \frac{1}{\frac{N_c^2}{K_H} - N_c^2 \bar{\Sigma}_H(s)} . \quad (219)$$

Just as for quarkonia and glueballs, the hybrid mass is N_c -independent:

$$\frac{1}{K_H} - \bar{\Sigma}_H(s = M_H^2) = 0 \rightarrow M_H \sim N_c^0 \quad (220)$$


$$T_H \simeq \frac{(ig_{H\bar{q}qg})^2}{s - M_H^2}, \quad (221)$$
$$g_{H\bar{q}qg} = \frac{1}{\sqrt{N_c^2 \left(\frac{\partial \bar{\Sigma}_G(s)}{\partial s} \right)_{s=M_G^2}}} = \frac{\bar{g}_{H\bar{q}qg}}{N_c} . \quad (222)$$

H-G MIXING

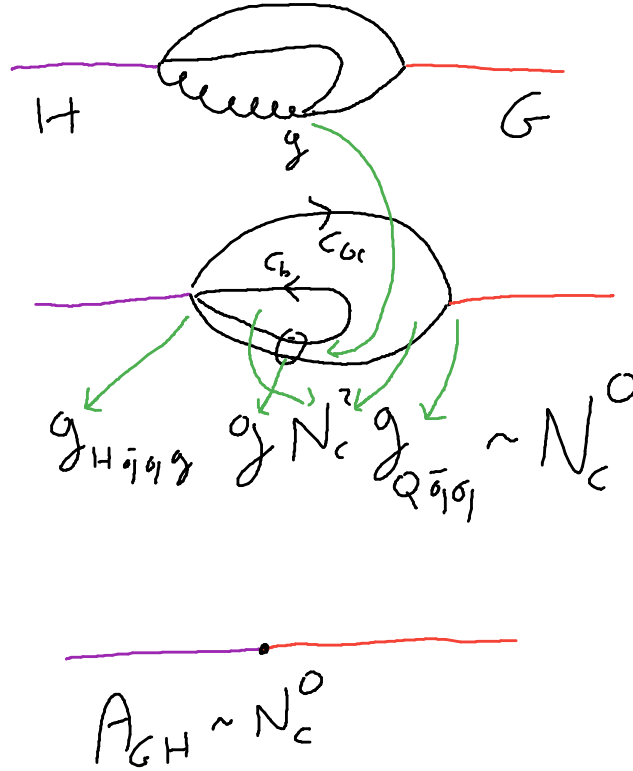


Fig. 35. The mixing of an hybrid meson H with a conventional quarkonium Q scales as N_c^0 , implying that hybrids and quarkonia can freely mix at large- N_c and therefore behave (mostly) in a similar way.

We then proceed with the phenomenological consequences at large- N_c . The most important one is that the mixing of a hybrid state H with a quarkonium state Q (with the same quantum numbers, of course) scales as:

$$A_{HQ} \sim \frac{1}{N_c} N_c^2 \frac{1}{\sqrt{N_c}} \frac{1}{\sqrt{N_c}} \sim N_c^0 \quad (223)$$

which is N_c independent! (This case is depicted in Fig. 35). This result means that hybrids behave as quarkonia in the large- N_c limit.

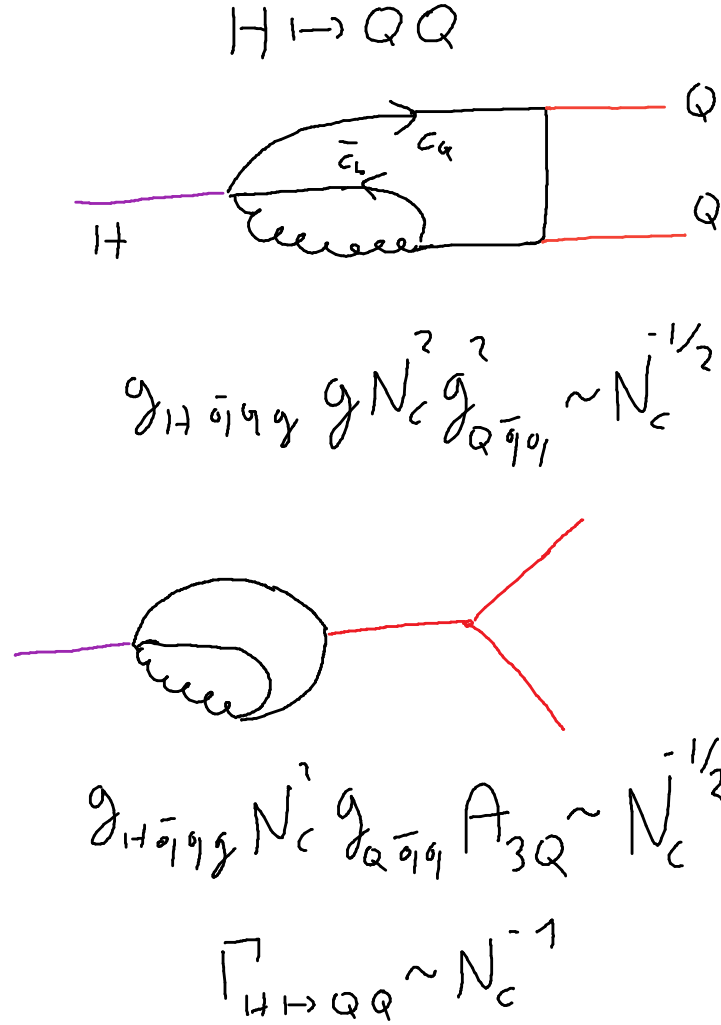


Fig. 36. Upper part: Decay of an hybrid meson (purple line) into two quarkonia mesons (red lines) via quarks and gluons (black lines). The amplitude scales as $N_c^{-1/2}$, just as for the standard decay of a quarkonium. Lower part: the same result is obtained by converting an hybrid into a quarkonium which then goes into two quarkonia. Even simpler, one could just use the previous result concerning mixing and study the chain $H \rightarrow Q \rightarrow QQ$, that goes as $N_c^{-1/2}$.

For example, the decay of a hybrid into two standard quarkonia mesons

(see Fig. 36) scales as

$$A_{HQQ} \sim \frac{1}{N_c} N_c^2 \frac{1}{\sqrt{N_c}} \left(\frac{1}{\sqrt{N_c}} \right)^2 = \frac{1}{\sqrt{N_c}} , \quad (224)$$

just as a regular quark-antiquark mesonic decay.

The same applies to interactions with an arbitrary number of hybrids, that scales as $N_c/N_c^{n_H/2}$, as well as of hybrids and quarkonia, that goes as $N_c/(N_c^{n_Q/2} N_c^{n_H/2})$. In the case of $n_Q = 0$ and $n_H = 1$, one obtains $N_c^{1/2}$, which corresponds to the weak decay constant of an hybrid meson. Namely, the hybrid production/annihilation amplitude goes as

$$f_H \sim g_{Hqq} \Sigma_H(M_H^2) \sim N_c^{-1} \cdot N_c^2 \sim N_c , \quad (225)$$

but the weak decay goes with an additional suppression of $N_c^{1/2}$ (the gluon needs to disappear):

$$f_H^{weak} \sim N_c^{1/2} . \quad (226)$$

This result is also obtained by taking an external H , which converts to Q (amplitude N_c^0), which subsequently annihilates (amplitude $N_c^{1/2}$), resulting in $N_c^{1/2}$.

Indeed, hybrids can form nonets just as regular mesons, and thus can be embedded into chiral approaches [94, 95].

The interaction of hybrids and glueballs can also be studied, see Fig. 37 for the explicit case of the decay of an hybrid meson into two glueballs, that scales as $N_c^{-3/2}$.

3.4. Summary of the scaling for an arbitrary number of Q, G, H states

Putting all the results together, we recover the general scaling law for the amplitude with n_Q quarkonia, n_G glueballs, and n_H hybrids (see Sec. 2.6) as:

$$A_{(n_Q Q)(n_G G)(n_H H)} \propto \frac{N_c \cdot N_c^{2(1-\text{sign}(n_Q+n_H))}}{N_c^{n_Q/2} N_c^{n_G} N_c^{n_H/2}} \quad (227)$$

where $\text{sign}(x)$ is the sign function with $\text{sign}(0) = 1/2$. If $n_Q + n_H > 0$, thus at least one quarkonium or an hybrid is present, $N_c \cdot N_c^{2(1-\text{sign}(n_Q+n_H))} = N_c$, while for $n_Q = n_H = 0$, the purely gluonic case is recovered: $N_c \cdot N_c^{2(1-\text{sign}(n_Q+n_H))} = N_c^2$.

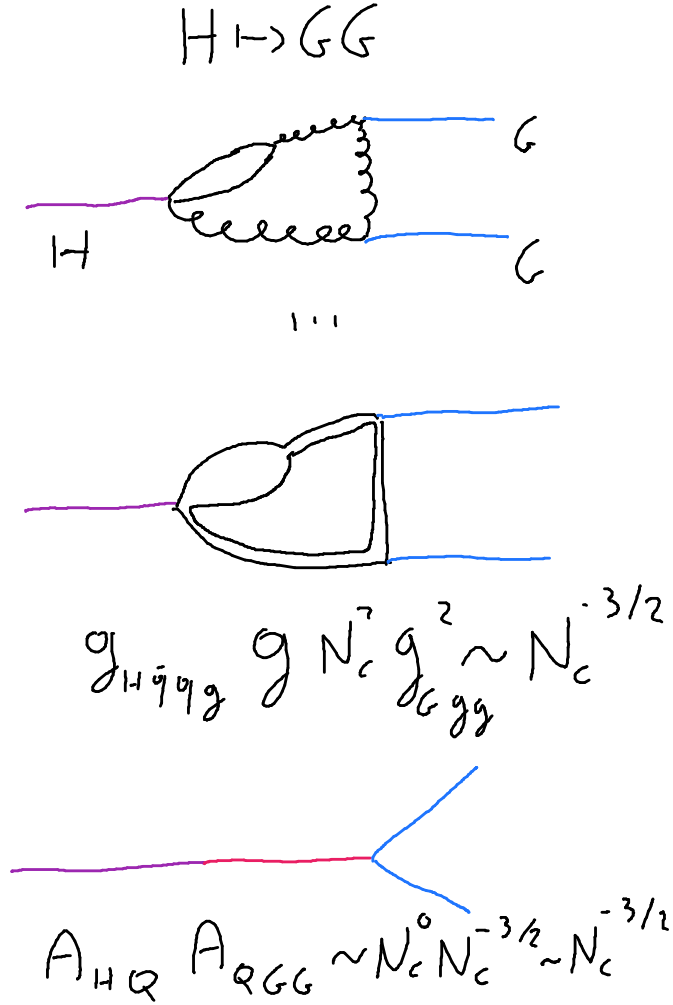


Fig. 37. Up: Decay of an hybrid meson (purple line) into two glueballs (blue lines) via quarks and gluons (black lines). The amplitude scales as $N_c^{-3/2}$. Lower part: the same result is obtained by converting an hybrid into a quarkonium which then converts into two glueballs.

3.5. Four-quark states

The treatment of four-quark states in the large N_c limit is subject to an ongoing debate, see [12] for a review. Some of the questions related to

it are unsettled yet. The first question is what one can understand under four-quark states, since different possibilities are available.

As a specific example, we shall consider the meson $a_0(980)$, for which different interpretations have been proposed in the literature, that we briefly review in the following.

(1) Molecular states, such as the binding of two colorless quark-antiquark mesons.

For the illustrative state $a_0^+(980)$, this amounts to consider a bound state of K^+ and \bar{K}^0 [96, 97] resulting into the state:

$$|a_0^+(980)\rangle = |K^+\bar{K}^0\rangle . \quad (228)$$

In general, such a molecule is of the type $|QQ\rangle$ and its current can be expressed as $J_{QQ}(x) = Q^2(x)$. The basic interaction takes the form

$$\mathcal{L}_{QQ} = K_{QQ} J_{QQ}^2(x) , \quad (229)$$

where

$$K_{QQ} \sim N_c^{-1} \rightarrow K_{QQ} \simeq \frac{\bar{K}_{QQ}}{N_c} \quad (230)$$

being a quartic interaction between conventional mesonic fields.

Upon repeating the previous steps, the resummed T -matrix for the eventual formation of a QQ bound states (see Fig. 38) reads:

$$T_{QQ}(s) = \frac{1}{K_{QQ}^{-1} - \Sigma_{QQ}(s)} \quad (231)$$

with $\Sigma_{QQ}(s) = \bar{\Sigma}_{QQ}(s)$ being large- N_c independent (it is the loop of two colorless states). The mass of the molecular states corresponds to a solution of the equation

$$\frac{N_c}{\bar{K}_{QQ}} - \bar{\Sigma}_{QQ}(s = M_{QQ}^2) = 0 . \quad (232)$$

This equation might have a solution for $N_c = 3$, but this is not the case of large N_c .

Let us first consider the case of a genuine molecular state whose mass M_{QQ} is below the threshold $2M_Q$ for $N_c = 3$. The function $\Sigma_{QQ}(s)$ is real below threshold and has a maximum (cusp) just at it. If the bound state exists for $N_c = 3$ for a value $M_{QQ} < 2M_Q$ below threshold, there is a maximal value N_c^{\max} for which the molecular state forms just at threshold, $M_{QQ} = 2M_Q$. Yet, upon increasing N_c further, the state ceases to form. Indeed, this is very intuitive: by increasing N_c , the attraction decreases and there is no N_c factor to compensate it. Molecular states of this type fade away for large N_c .

MESONIC MOLECULES

$$\begin{aligned}
 T_{qq} &\sim \cancel{\text{diagram}} + \cancel{\text{diagram}} + \dots \\
 &\sim K_{qq} + K_{qq} \sum_{qq} K_{qq} + \dots \\
 &\sim \frac{1}{N_c} + \frac{1}{N_c} \cdot N_c^0 \cdot \frac{1}{N_c} + \dots \\
 &\sim \frac{1}{K_{qq}^{-1} - \sum_{qq}} \sim \frac{1}{\frac{N_c}{\bar{K}_{qq}} - \sum_{qq}} \\
 &\text{NO MOLECULES FOR LARGE } N_c
 \end{aligned}$$

Fig. 38. Resummation of regular meson-meson scattering diagrams needed to investigate the eventual emergence of a molecular bound state. While for $N_c = 3$ these states can form, this is not the case for large- N_c . Namely, the attraction decreases as N_c^{-1} but the intermediate states in the bubble are colorless, thus the loop function cannot compensate for the decrease of attraction. See text for more details.

Indeed, the previous argumentation may be extended also to molecular resonances with mass above $2M_Q$, since $\Sigma_{QQ}(s)$ is a limited function. For N_c large enough, $T_{QQ}(s) \simeq K_{QQ} \simeq \bar{K}_{QQ}/N_c$, which is the lowest order

interaction, obviously with no bound state.

Molecular states may also emerge from glueballs or hybrids. The case of glueball molecular states, so-called glueballonia, has been recently studied in Ref. [80]. Quite remarkably, for the binding of two scalar glueball such a state may be stable in pure Yang-Mills and be a resonance in full QCD for $N_c = 3$. Yet, for large N_c it fades away even faster than QQ molecular states. In fact, one has:

$$\mathcal{L}_{GG} = K_{GG} J_{GG}^2(x) \quad (233)$$

where $J_{GG} = G^2(x)$ and

$$K_{GG} \sim N_c^{-2} \rightarrow K_{GG} \simeq \frac{\bar{K}_{GG}}{N_c^2} . \quad (234)$$

(being the quartic interaction between glueballs). Then:

$$T_{GG}(s) = \frac{1}{K_{GG}^{-1} - \Sigma_{GG}(s)} = \frac{1}{\frac{N_c}{\bar{K}_{GG}} - \bar{\Sigma}_{GG}(s)} \quad (235)$$

with $\Sigma_{GG}(s) = \bar{\Sigma}_{GG}(s)$ being N_c -independent. Again, no glueballonium can form at large- N_c . It is important to note that the same large- N_c scaling for the glueballonium formation is obtained in the more advanced approach of Ref. [80], where two unitarization methods have been used to study its formation. This fact shows again that the rather simple separable interaction considered above is fully consistent with general large- N_c results and is therefore suitable to study the large- N_c scaling. Additional bound states of regular mesons with glueballs and/or hybrids can be studied [98], but for the very same reason they shall also not survive in the large- N_c domain.

(2) Dynamically generated states: the example of companion poles.

A specific example of companion pole was presented for the case of the meson $a_0(980)$ in Refs. [99, 100]. The starting point is a Lagrangian which contains a single conventional scalar quark-antiquark bare state, roughly correspondent to $a_0 \equiv a_0(1450)$. One then writes the interaction term as:

$$\mathcal{L}_{int} = g_{a_0 K K} a_0^+ K^- K^0 + g_{a_0 \pi \eta} a_0^+ \pi^- \eta + \dots \quad (236)$$

with the standard scaling

$$g_{a_0 K K} \sim N_c^{-1/2} , g_{a_0 \pi \eta} \sim N_c^{-1/2} . \quad (237)$$

Then, one study loops and the full dressed propagator of $a_0(1450)$, arising from the decays into $\bar{K}K$, $\pi\eta$, etc. As a consequence, the propagator takes the form

$$\frac{1}{p^2 - M_{a_0}^2 + g_{a_0 KK}^2 \Sigma_{KK}(p^2) + g_{a_0 \pi\eta}^2 \Sigma_{\pi\eta}(p^2) + \dots} \quad (238)$$

with $M_{a_0} \simeq 1.4 \text{ GeV} \sim N_c^0$. The coupling constants are set to reproduce the physical results for the resonance $a_0(1450)$ for the physical case $N_c = 3$.

Then, upon solving the pole equation in the complex plane

$$p^2 - M_{a_0}^2 + g_{a_0 KK}^2 \Sigma_{KK}(p^2) + g_{a_0 \pi\eta}^2 \Sigma_{\pi\eta}(p^2) + \dots = 0 \quad (239)$$

two poles are found (in this specific case on the third and second Riemann sheets, respectively, but this aspect is not relevant for our analysis).

One pole is close to the expected bare quarkonium result and corresponds to $a_0(1450)$: when increasing N_c , this pole converges toward the real axis, that is its imaginary part decreases as N_c^{-1} , as expected.

The second pole appears close the $\bar{K}K$ threshold and corresponds to $a_0(980)$. In the large- N_c limit it behaves differently: its width increases instead of decreasing, showing that this additional state is not an ordinary quark-antiquark object. Eventually it disappears from the original (second) Riemann sheet.

These features concerning dynamical generated companion poles are quite general and apply, with minor changes, to other states as well, such as the scalar resonances $f_0(500)$ [101, 102] and $K_0^*(700)$ [103, 104], or the famous $X(3872)$ (as a virtual pole) [105].

It should be also stressed that companion poles are not the only possibility for dynamically generated states, see e.g. [102, 106] but it shows a quite general feature: these solutions fade away in the large- N_c limit¹.

(3) Genuine tetraquark state as a bound state of two diquarks.

Referring to $a_0(980)$ as our example, we may interpret it as a bound state of a good diquark and a good anti-diquark [109, 110], where a good diquark state is antisymmetric in both color and flavors, e.g.:

$$|us, \text{good}\rangle = |\text{space: } L=0\rangle |\text{spin: } S=0\rangle |\text{color: } RG - GR\rangle |\text{flavor: } us - su\rangle . \quad (240)$$

¹ A word of caution is required; in some cases, one may obtain certain mesons as solutions of bound-state equations out of effective Lagrangians. Yet, these mesons can be ordinary quark-antiquark states, but the way they have been obtained would make them look like molecular states that do not survive the large- N_c limit. We refer to Ref. [107] (see also [108]) for this subtlety and for the related notion of ‘dynamical reconstruction’.

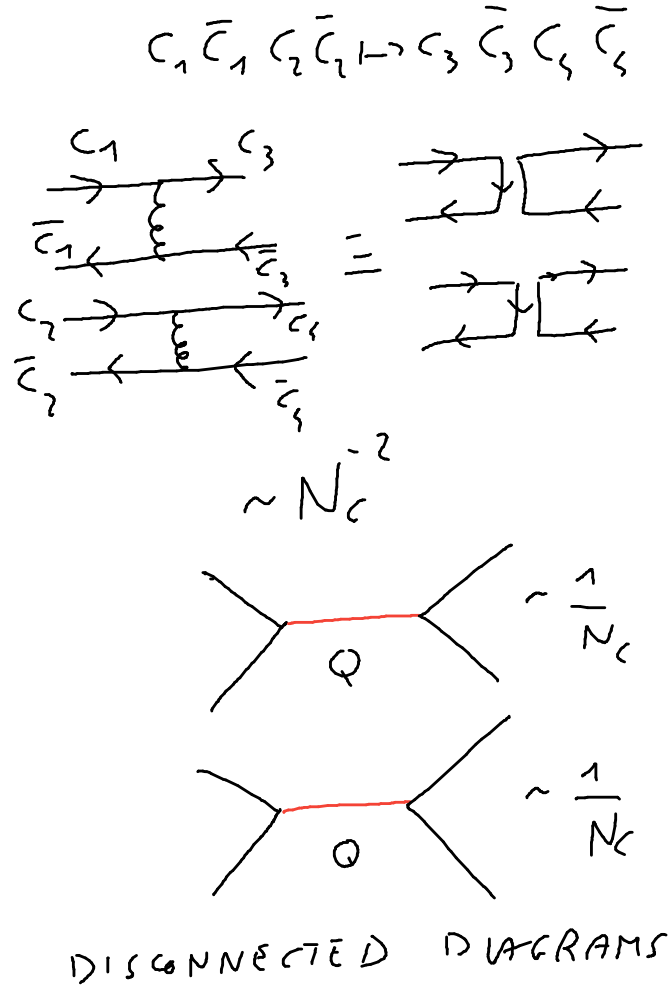


Fig. 39. Disconnected diagram for the reaction $C_1 \bar{C}_1 C_2 \bar{C}_2 \rightarrow C_3 \bar{C}_3 C_4 \bar{C}_4$. All the colors have been switched, but these diagrams (properly resummed) eventually generate two intermediate conventional Q states. Indeed, the scaling N_c^{-2} is in agreement with this interpretation.

Then

$$|a_0^+(980)\rangle = |us, \text{good}\rangle |\bar{d}\bar{s}, \text{good}\rangle . \quad (241)$$

Indeed, one can build nonets of states and describe these objects in a chiral context [66, 111, 112, 113].

What about the large- N_c scaling of these configurations? The issue is

that the straightforward generalization of the good diquark is an object that contains $N_c - 1$ quarks, e.g. [33]. This object may be used to construct baryons in the large- N_c limit (see next Section for its explicit implementation), but is not useful for building tetraquarks states (with ‘tetra’ in the sense of four).

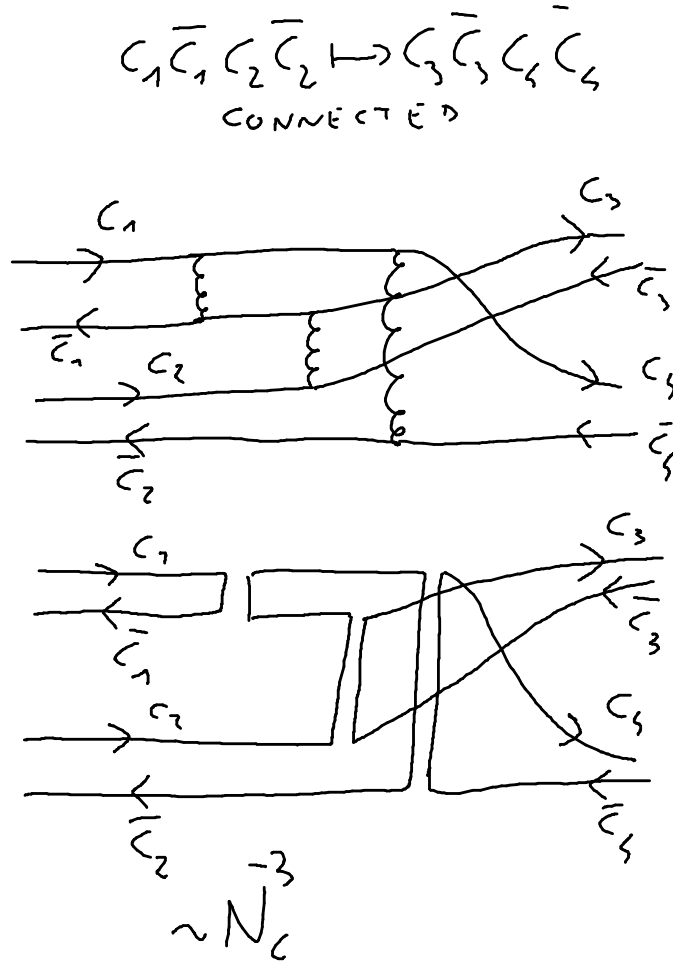


Fig.40. Connected diagram for the reaction $C_1 \bar{C}_1 C_2 \bar{C}_2 \rightarrow C_3 \bar{C}_3 C_4 \bar{C}_4$. All the colors have been switched. It scales as N_c^{-3} .

In the classic lecture of Coleman [9], it is stated that tetraquarks (of whatever type) do not exist in the large- N_c limit because four quark states rather arrange into two free mesons, see Fig. 39.

DO TETRAQUARKS BIND?

$$\begin{aligned}
 T_T &\sim \text{diagram with } K_T \text{ and } 6 \text{ external lines} \sim \frac{1}{N_c^3} \\
 + &\text{diagram with } K_T, \Sigma_T, K_T \text{ and } 6 \text{ external lines} \\
 &\sim \frac{1}{N_c^3} N_c^2 \frac{1}{N_c^3} \sim \frac{1}{N_c^4} \\
 &\sim \frac{1}{K_T^{-1} - \Sigma_T} \approx \frac{1}{\frac{N_c^3}{K_T} - N_c^2 \Sigma_T} \\
 &\Rightarrow T \text{ SEEMS NOT TO BIND}
 \end{aligned}$$

Fig. 41. Tentative resummation of connected diagrams with a colorless four-quark configuration in the initial and in the final states. The attraction seems to decrease too fast to allow for a bound-state (a genuine tetraquark state) formation.

Weinberg realized years later [29] that one should rather look at connected diagrams, hence certain tetraquarks states might exist and show scaling laws similar to regular mesons. A debate has followed [12, 30, 31, 32, 33, 34], basically confirming Weinberg point of view but always stressing

that it is not clear if such tetraquark states do form in the large- N_c limit. Indeed, in [32] it is argued that they eventually do not.

Does the bound-state approach discussed in these lectures help? Here, we limit to some basic considerations that are not conclusive yet, but may be the starting point for future investigations. To this end, let us consider the most general four-quark current [33]:

$$J_T = C_1 \delta^{ac} \delta^{bd} q^a q^b \bar{q}^c \bar{q}^d + C_2 \delta^{ad} \delta^{bc} q^a q^b \bar{q}^c \bar{q}^d . \quad (242)$$

Then, the separable interaction takes the form

$$\mathcal{L}_T = K_T J_T^2(x) , \quad (243)$$

where we need to discuss the large- N_c scaling of K_T . If one considers a connected four-quark diagram, one obtains (see Fig. 40):

$$K_T \sim N_c^{-3} \rightarrow K_T \simeq \frac{\bar{K}_T}{N_c^3} \quad (244)$$

being a quartic interaction between conventional mesonic fields. Namely, a disconnected diagram, in which the two quark-antiquark parts interact separately, would scale as N_c^{-2} , see again Fig. 39, but this is not what we search.

Then, the resummed T -matrix for the eventual formation of a tetraquark state state, see Fig. 41, reads:

$$T_T(s) = \frac{1}{K_T^{-1} - \Sigma_T(s)} \quad (245)$$

where $\Sigma_T(s)$ scales as N_c^2 . Whatever is the specific tetraquark configuration, the order is always N_c^2 . (If, for example, we consider only antisymmetric diquark color configurations, there are $N_c(N_c - 1)/2 \sim N_c^2$ choices for the diquark color.) Hence, $\Sigma_T(s) \simeq N_c^2 \bar{\Sigma}_T(s)$, leading to

$$T_T(s) = \frac{1}{\frac{N_c^3}{K_T} - N_c^2 \bar{\Sigma}_T(s)} . \quad (246)$$

This result suggests that no tetraquark bind for large- N_c , since the interaction strength decreases too fast, just as mesonic molecular states.

Note, if we would study the tetraquark correlator $\langle J_T(x_2) J_T(x_1) \rangle$, one should indeed remove the disconnected part $\Sigma_T(s) \sim N_c^2$, hence the lowest order contribution $\Sigma_T(s) K_T^{-1} \Sigma_T(s)$ scales as N_c , as expected. Future studies are needed to check if the present heuristic arguments against the emergence of tetraquarks can be made rigorous.

4. Brief study of baryons at large- N_c

The topic of baryons at large- N_c is a rich one and cannot be fully covered in these lectures. Here, our aim is to show that an approach similar to the one applied to mesons (bound state formation) is also consistent with baryonic large- N_c scaling properties. To this end, let us introduce the generalized ‘diquark’ D^{a_1} as a $N_c - 1$ quark object with the structure

$$D^{a_1} = \frac{1}{\sqrt{(N_c - 1)!}} \sum_{a_2, a_3, \dots, a_{N_c}=1}^{N_c} \varepsilon_{a_1 a_2 \dots a_{N_c}} q^{a_2} q^{a_3} \dots q^{a_{N_c}} . \quad (247)$$

There are N_c generalized diquarks, just as there are N_c antiquarks. Indeed, under color transformations D^{a_1} transforms as an antiquark. Then, one may interpret the baryon as a bound state of such a generalized diquark and a quark. The current is given by:

$$J_B = \sum_{a_1=1}^{N_c} D^{a_1} q^{a_1} . \quad (248)$$

Following the mesonic case, we write down the interaction Lagrangian as

$$\mathcal{L}_B = K_B J_B^2 . \quad (249)$$

The determination of the scaling of K_B can be deduced from Fig. 42. Since at lowest order no gluon is involved and a simple switch suffices to change the color of both D and q (this is due to the fact that D contains already $N_c - 1$ colors). It then follows that:

$$K_B \sim N_c^0 , \quad (250)$$

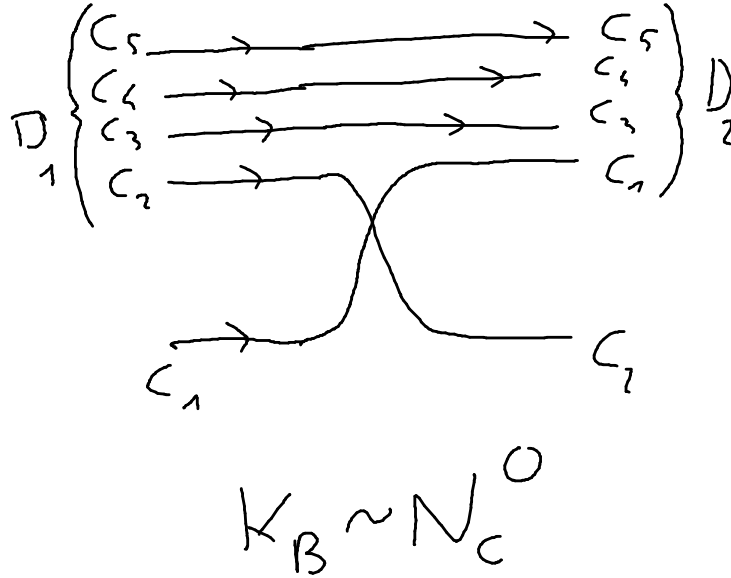
hence $K_B \simeq \bar{K}_B$. On the other hand, the loop $\Sigma_B(E)$ involving D - q goes with N_c for what concerns the color circulating in it, but contains also a dependence on the mass of the generalized diquark D with $m_D \propto N_c - 1$. Since m_D is very large, we resort to non-relativistic propagators and use the energy E (and not $s = E^2$) as an argument of the loop $\Sigma_B(E)$. This function can be expanded in E finding:

$$\Sigma_B(E) \simeq N_c \bar{\Sigma}_B(E) \simeq N_c \left(\frac{c_1}{m_D} + c_2 \frac{E}{m_D^2} + \dots \right) , \quad (251)$$

which scales as $N_c^0 + N_c^{-1} + \dots$. It then follows that the T -matrix for the illustrative scattering process $D^1 q^1 \rightarrow D^2 q^2$ reads (Fig. 43):

$$T_B = \frac{1}{K_B^{-1} - \Sigma_B(E)} \simeq \frac{1}{\bar{K}_B^{-1} - N_c \bar{\Sigma}_B(E)} . \quad (252)$$

Barion as Diquark state



D as $(N_c - 1)$ multiquark

Fig. 42. Scattering of a generalized diquark D_1 and a quark with color C_1 into D_2 and C_2 (thus color 'changed'). A simple switch of quarks does the job, thus at leading order no gluon is present and the amplitude goes with N_c^0 .

The pole equation reads

$$\bar{K}_B^{-1} - N_c \left(\frac{c_1}{m_D} + c_2 \frac{E}{m_D^2} + \dots \right) = 0, \quad (253)$$

leading to

$$\frac{N_c}{m_D} c_1 + c_2 \frac{N_c}{m_D} \frac{E}{m_D} + \dots = \bar{K}_B^{-1}, \quad (254)$$

thus

$$c_2 \frac{N_c}{m_D} \frac{E}{m_D} = \bar{K}_B^{-1} - \frac{N_c}{m_D} c_1 \sim N_c^0. \quad (255)$$

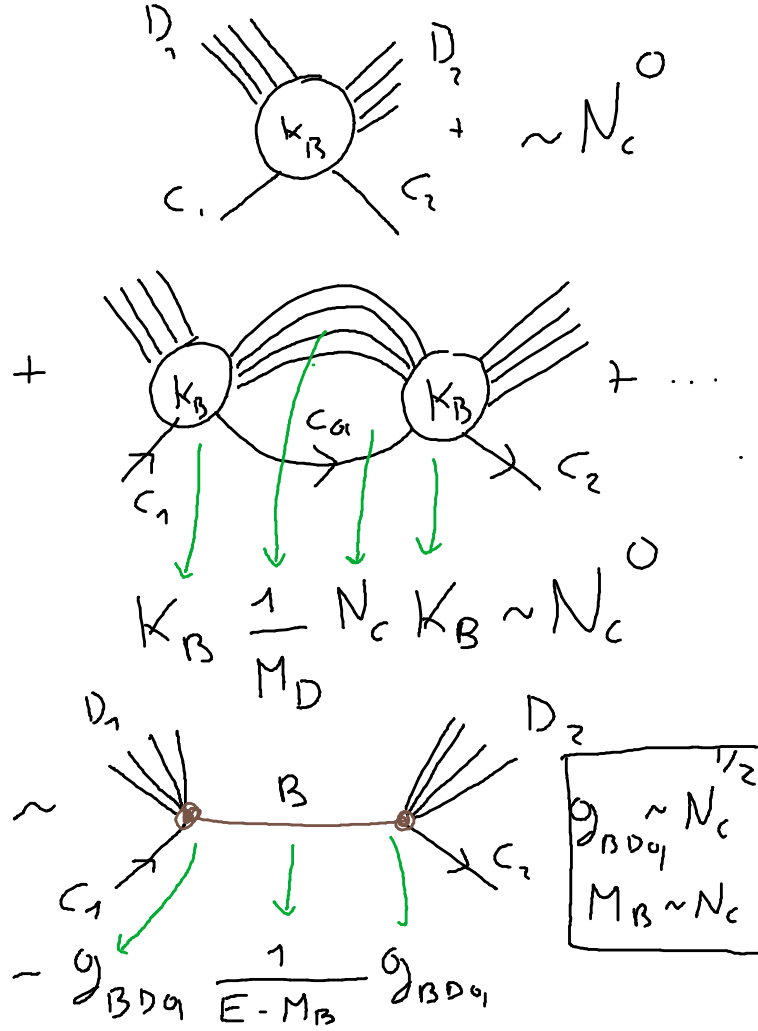


Fig. 43. Resummation of the scattering $D_1 C_1 \rightarrow D_2 C_2$ with consequent formation of one baryon (as brown line) as intermediate state.

It then follows that

$$E \equiv M_B \sim m_D \frac{m_D}{N_c} \sim m_D \sim N_c. \quad (256)$$

In other words, we find that, if $m_D \sim N_c$, then $M_B \sim m_D \sim N_c$ as well, being a consistent (and expected) result.

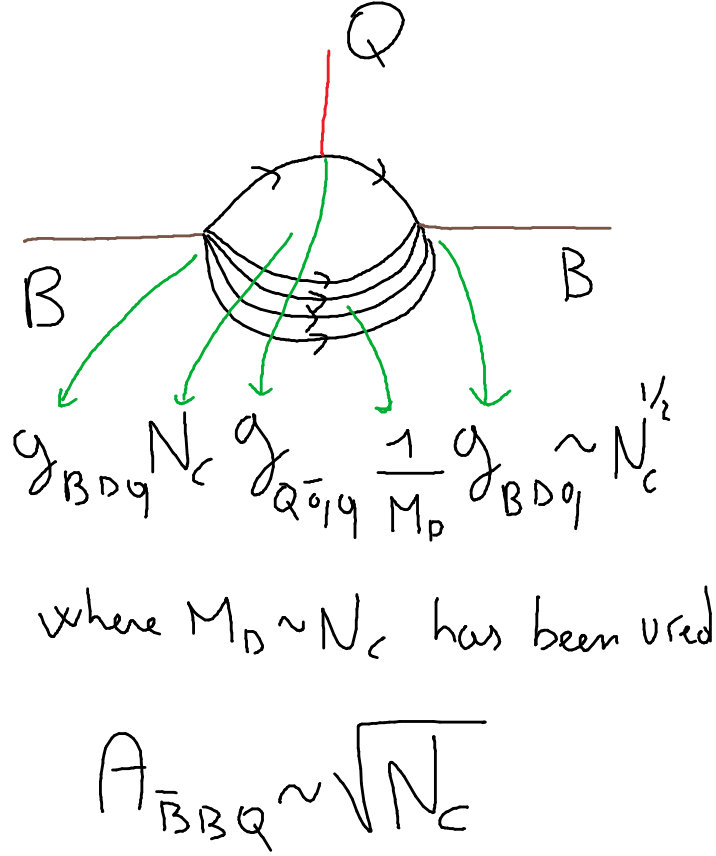


Fig. 44. Vertex of two baryons B (brown lines) and one conventional meson Q (red line). The amplitude, that corresponds to the generic meson-baryon-baryon coupling scales with $N_c^{1/2}$.

Upon expanding around the pole, we find:

$$T_B \simeq \frac{(ig_{BDq})^2}{E - M_B} \quad (257)$$

with

$$g_{BDq} \simeq \sqrt{\frac{1}{\Sigma'_B(E = M_B)}} \simeq \sqrt{\frac{1}{\frac{N_c c_2}{m_D^2} + \dots}} \sim \sqrt{\frac{1}{\frac{1}{N_c}}} \sim N_c^{1/2}, \quad (258)$$

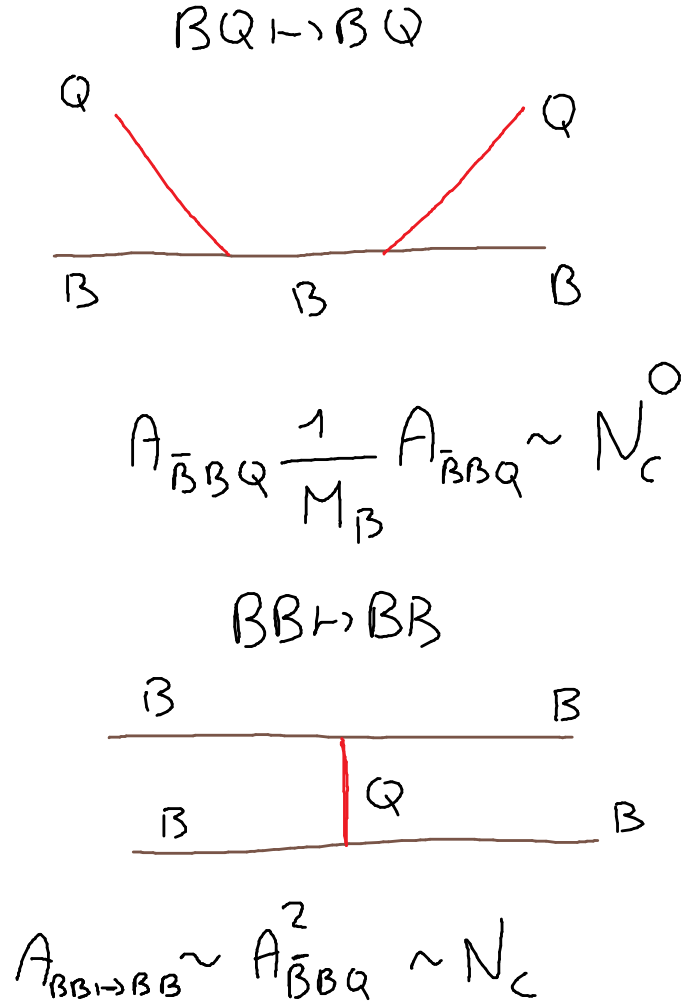


Fig. 45. Up: baryon-meson scattering, which goes with N_c^0 (note, the intermediate baryon gives a N_c^{-1} contribution. Down: baryon-baryon scattering that scales as N_c .

thus the baryon coupling to its generalized diquark D and quark q increases as $N_c^{1/2}$.

From these scaling laws, one can determine all the others. The quarkonium-baryon coupling goes as (see Fig. 44 as well as Ref. [114]):

$$g_{\bar{B}BQ} \sim N_c^{1/2} . — \quad (259)$$

The scaling is the same for any number of $\bar{B}B$ pairs.

By increasing the number of quarkonia to n_Q , we find (see Fig. 45, upper part, for an example) that the generic amplitude

$$A_{(\bar{B}B\bar{B}B\cdots)(n_Q Q)} \sim \frac{N_c}{N_c^{n_Q/2}} . \quad (260)$$

The coupling to a single glueball goes as (see Fig. 46):

$$g_{\bar{B}BG} \sim N_c^0 \quad (261)$$

and then the one to n_G glueballs as

$$A_{(\bar{B}B\bar{B}B\cdots)(n_G G)} \sim \frac{N_c}{N_c^{n_G}} . \quad (262)$$

The coupling to hybrid meson is identical to quark-antiquark ones:

$$g_{\bar{B}BH} \sim N_c^{1/2} , \quad (263)$$

$$A_{(\bar{B}B\bar{B}B\cdots)(n_H H)} \sim \frac{N_c}{N_c^{n_H/2}} . \quad (264)$$

The final coupling of an arbitrary number of baryon-antibaryon pairs to n_Q quarkonia, n_G glueballs, and n_H hybrid mesons is:

$$A_{(\bar{B}B\bar{B}B\cdots)(n_Q Q)(n_G G)(n_H H)} \sim \frac{N_c}{N_c^{n_Q/2} N_c^{n_G} N_c^{n_H/2}} . \quad (265)$$

What about the scattering of baryons? Following the same ‘visual’ approach (Fig. 45), the amplitude for the process $BB \rightarrow BB$ goes as

$$A_{BB \rightarrow BB} \sim N_c . \quad (266)$$

Indeed, it does not change for any arbitrary number of baryons, provided that the initial number of baryons is equal to the final one (baryon number conservation). In turn, it is equal to the amplitude with n_B baryons and n_B antibaryons, and can be formally recovered from the previous case of Eq. (265) upon setting $n_Q = n_G = n_H = 0$.

How to implement baryons in a chiral model? In line with previous simplified treatments, we consider a single flavor (and disregard the chiral anomaly). We introduce a nucleon field Ψ_1 , which is as usual split into right-handed and left-handed parts as:

$$\Psi_{1,R} = \frac{1 + \gamma^5}{2} \Psi_1 , \quad \Psi_{1,L} = \frac{1 - \gamma^5}{2} \Psi_1 . \quad (267)$$

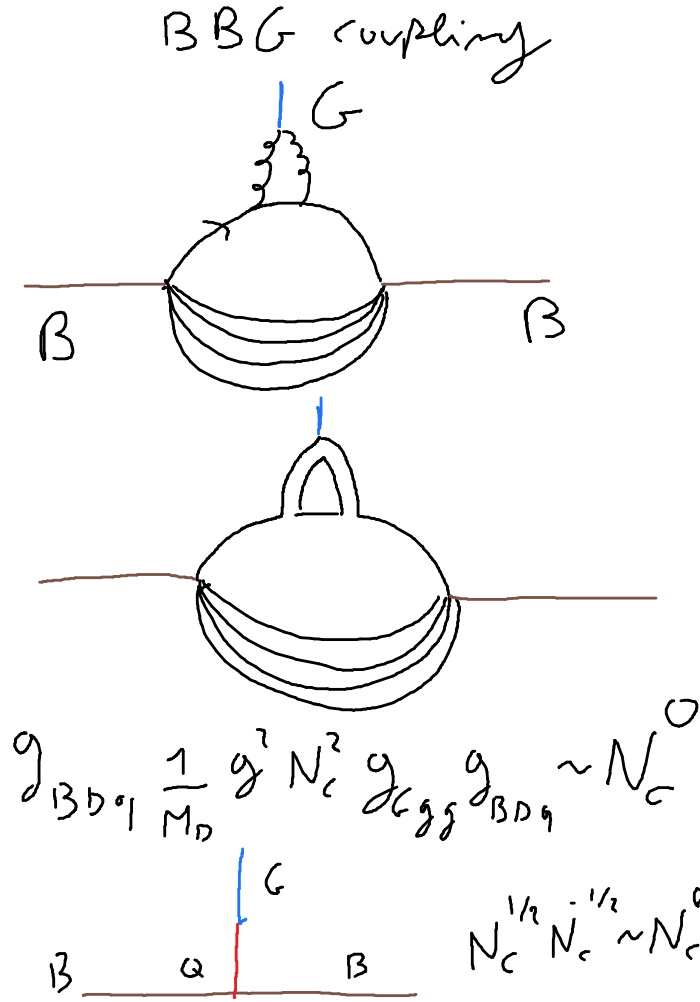


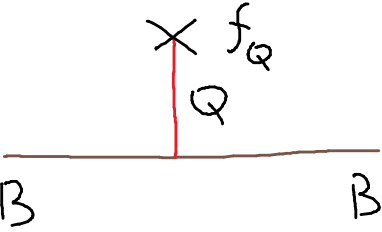
Fig. 46. Coupling of a baryon (brown lines) to a glueball (blue line). This is shown both at the level of intermediate quarks and gluons (upper part) and color double-line notation (in the middle). This interaction scales with N_c^0 . At the bottom, the very same result can be obtained by coupling the baryon to a quarkonium Q and Q to G , and then by using previous results.

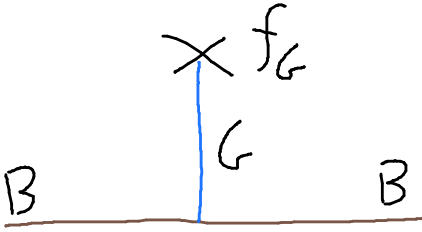
A chiral transformation at the level of the nucleon amounts to:

$$\Psi_{1,R} \rightarrow e^{i\alpha/2} \Psi_{1,R}, \quad \Psi_{1,L} \rightarrow e^{-i\alpha/2} \Psi_{1,L}, \quad (268)$$

where the the right and left pieces transform with different sign of the phase

B-mass terms



$$A_{\bar{B}BQ} f_Q \sim N_c^{1/2} N_c^{1/2} \sim N_c$$


$$A_{\bar{B}BG} f_G \sim N_c^0 N_c \sim N_c$$

Fig. 47. Contribution to the mass of the baryon emerging from its interaction to a scalar quarkonium field Q and to a scalar glueball G . One obtains that, in both cases, when the quarkonium field condenses or the glueball field condenses, the mass of the baryon scales with N_c , as expected. These results are implemented in the context of chiral models for the nucleon: the upper one corresponds to the standard LSM, the second one to the so-called mirror assignment (see text).

(for equal sign, one has a simple $U(1)$ baryon transformation). Because of this chiral transformation, a mass term of the type

$$\bar{\Psi}_1 \Psi_1 = \bar{\Psi}_{1,R} \Psi_{1,L} + \bar{\Psi}_{1,L} \Psi_{1,R} \quad (269)$$

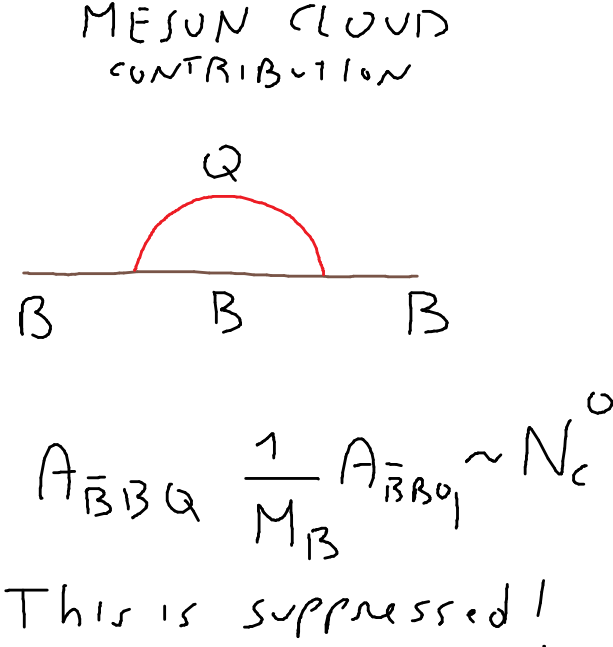


Fig. 48. The contribution of a meson emission and absorption is suppressed in the large- N_c limit.

is *not* chirally invariant! Thus, it seems that the nucleon needs to be -at first- massless.

As indeed well known, one can generate a massive nucleon by fulfilling chiral symmetry upon coupling the nucleon field to the mesonic field Φ , which transforms as $\Phi \rightarrow e^{i\alpha}\Phi$. Then, an invariant term that generates a mass (via SSB) is obtained as (e.g. [115]):

$$\mathcal{L}_{\Psi_1\Phi} = -g_{\Psi_1\Phi} \left(\bar{\Psi}_{1,R}\Phi\Psi_{1,L} + \bar{\Psi}_{1,L}\Phi^\dagger\Psi_{1,R} \right) \quad (270)$$

where

$$g_{\Psi_1\Phi} \sim N_c^{1/2} . \quad (271)$$

When Φ condenses via SSB to $\phi_N \sim N_c^{1/2}$, a nucleon mass proportional to the chiral condensate ϕ_N is generated as:

$$M_N \sim g_{\Psi_1\Phi}\phi_N \sim N_c^{1/2} \cdot N_c^{1/2} \sim N_c \quad (272)$$

with the expected large- N_c behavior, see Fig. 47 for a pictorial representation of this result.

Note, the mesonic loop mass correction contributes with N_c^0 to the nucleon mass and is thus suppressed, as shown in Fig. 48. The ‘bulk’ mass dominates the formation of the nucleon mass.

If the only mass term is the only one of Eq. (272), it means that the nucleon mass disappears when the chiral condensate vanishes (as e.g. in a confined but chirally restored phase of matter, see next Section).

Interestingly, there is a second chiral way to give mass to the nucleon. To this end, a second nucleon field (the chiral partner of the nucleon, with opposite parity w.r.t. the bare nucleon field Ψ_1) is considered, see for example [116, 117, 118, 119, 120, 121, 122] and refs. therein. We consider its chiral transformation as being mirror-like

$$\Psi_{2,R} \rightarrow e^{-i\alpha/2} \Psi_{2,R}, \quad \Psi_{2,L} \rightarrow e^{i\alpha/2} \Psi_{2,L}. \quad (273)$$

Besides a standard interaction

$$\mathcal{L}_{\Psi_2\Phi} = g_{\Psi_2\Phi} \left(\bar{\Psi}_{2,R} \Phi^\dagger \Psi_{2,L} + \bar{\Psi}_{2,L} \Phi \Psi_{2,R} \right) \quad (274)$$

an invariant mass term is obtained as [119, 121]:

$$\begin{aligned} \mathcal{L}_{mirror,mass} &= -c_N G (\bar{\Psi}_{1,L} \Psi_{2,R} - \bar{\Psi}_{1,R} \Psi_{2,L} - \bar{\Psi}_{2,L} \Psi_{1,R} - \bar{\Psi}_{2,R} \Psi_{1,L}) \\ &= -c_N G (\bar{\Psi}_1 \gamma^5 \Psi_2 - \bar{\Psi}_2 \gamma^5 \Psi_1), \end{aligned} \quad (275)$$

where $c_N \sim N_c^0$ is a dimensionless constant independent on N_c and G is, as usual, the dilaton/glueball field. Hence, a chirally invariant mass terms

$$m_{N,0} = c_N G_0 \simeq c \Lambda_{QCD} \sim N_c \quad (276)$$

emerges with the correct scaling, see Fig. 47 (lower part).

The mass of the nucleon and its chiral partners are obtained by properly diagonalizing the system, finding:

$$\begin{pmatrix} N \\ N^* \end{pmatrix} = \frac{1}{\sqrt{2 \cosh \delta}} \begin{pmatrix} e^{\delta/2} & \gamma^5 e^{-\delta/2} \\ \gamma^5 e^{-\delta/2} & e^{\delta/2} \end{pmatrix} \begin{pmatrix} \Psi_1 \\ \Psi_2 \end{pmatrix} \quad (277)$$

with

$$M_{N,N^*} = \sqrt{m_{N,0}^2 + \frac{1}{4} (g_{\Psi_1\Phi} + g_{\Psi_2\Phi})^2 \phi_N^2} \pm \frac{1}{2} (g_{\Psi_1\Phi} - g_{\Psi_2\Phi}) \phi_N \sim N_c \quad (278)$$

and

$$\cosh \delta = \frac{M_N + M_{N^*}}{2m_{N,0}} \sim N_c^0 . \quad (279)$$

Note, for $m_{N,0} = 0$, one has $M_N = g_{\Psi_1 \Phi} \phi_N$ and $M_{N^*} = g_{\Psi_2 \Phi} \phi_N$, as expected. On the other hand, if $\phi_N = 0$, the chiral partners are degenerate with $M_N = M_{N^*} = m_{N,0}$.

There is another interesting aspect of chiral models, that regards the axial coupling constant of the nucleon. In the model above, for $m_{N,0} = 0$ the axial coupling constant turns out to be one, $g_A^N = 1$. If $m_{N,0}$ is nonzero, the mixing sets in with

$$g_A^N = \frac{1}{2 \cosh \delta} \left(e^{\delta/2} - e^{-\delta/2} \right) \sim N_c^0 . \quad (280)$$

Yet, the Skyrme model predicts $g_A^N \sim N_c$ [38]. How to reconcile these different results?

The key is to consider vector and axial-vector mesons. We introduce

$$R^\mu = \rho^\mu - a_1^\mu , \quad L^\mu = \rho^\mu + a_1^\mu \quad (281)$$

(recall that we are in the one-flavor case, so we could have as well used ω^μ and f_1^μ instead), which under a chiral transformation are separately invariant: $R^\mu \rightarrow R^\mu$, $L^\mu \rightarrow L^\mu$. However, under parity: $R^\mu \leftrightarrow L^\mu$. Hence, the chirally and parity invariant coupling to (axial-)vector states is:

$$\begin{aligned} \mathcal{L}_{(axial-)\text{vector}} = & c_{\Psi_1} R_\mu \bar{\Psi}_{1,R} \gamma^\mu \Psi_{1,R} + c_{\Psi_1} L_\mu \bar{\Psi}_{1,L} \gamma^\mu \Psi_{1,L} \\ & + c_{\Psi_2} R_\mu \bar{\Psi}_{2,R} \gamma^\mu \Psi_{2,R} + c_{\Psi_2} L_\mu \bar{\Psi}_{2,L} \gamma^\mu \Psi_{2,L} \end{aligned} \quad (282)$$

where

$$c_{\Psi_1} \sim N_c^{1/2} , \quad c_{\Psi_2} \sim N_c^{1/2} . \quad (283)$$

The exact calculation of the axial coupling constants goes beyond the scope of these lectures, since it involves subtle issues, such as the mixing of the a_1 and π occurring in chiral models with (axial-)vector mesons [23, 28, 63, 64, 65]. Yet, we can provide the final results of this calculation. The previous expression for the axial coupling g_A is modified into:

$$g_A^N = \frac{1}{2 \cosh \delta} \left(g_A^{(1)} e^{\delta/2} + g_A^{(2)} e^{-\delta/2} \right) \quad (284)$$

with

$$g_A^{(1)} = 1 - \frac{c_{\Psi_1}}{g_1} \left(1 - \frac{1}{Z^2} \right) , \quad g_A^{(2)} = -1 + \frac{c_{\Psi_2}}{g_1} \left(1 - \frac{1}{Z^2} \right) \quad (285)$$

where $g_1 \sim N_c^{-1/2}$ is the coupling of one vector meson to two pseudoscalar ones (hence a standard QQQ vertex that scales as $N_c^{-1/2}$), and

$$Z = \left(1 - \frac{g_1^2 \phi_N^2}{M_{a_1}^2}\right)^{-1/2} \sim N_c^0 \quad (286)$$

is a constant that appears when dealing with the mixing between the pion and the a_1 meson [23, 28, 63, 64, 65]. It then follows that

$$g_A^{(1)} \sim N_c \text{ and } g_A^{(2)} \sim N_c \quad (287)$$

thus

$$g_A^N \sim N_c, \quad (288)$$

in agreement with the Skyrme approach. This result implies that one cannot neglect axial-vector mesons, otherwise basic large- N_c properties might be lost.

5. Brief description of QCD at nonzero temperature and densities at large- N_c

The QCD phase diagram at large- N_c is a rich topic that would deserve a series of lectures on its own. Here, we limit ourselves to a summary of some basic facts and to some interesting recent developments.

As shown in [35], when N_c is large, gluons dominate: a first order phase transition between the deconfined and confined phases at $T_c \simeq 300 \propto N_c^0$ MeV (see [76] for a compilation of results) is expected for any value of the chemical potential. This is utterly different from the QCD phase diagram for $N_c = 3$ [3], which is cross-over along the T direction and first order along the μ one.

In the following, we first concentrate on the main expected properties of confinement/deconfinement phase transition for varying N_c and then on four snapshots concerning large- N_c properties in the medium.

Since relevant for our purposes, we write down the vacuum contribution of the dilaton-LSM confined matter, see Sec. 3.1 (consequence 3) and Sec. 3.2 (consequence 1):

$$V_{vac} = V(G = G_0, \sigma = \sigma_0, 0) = \frac{1}{4} \lambda_G G_0^4 \left[\ln \left(\frac{G_0}{\Lambda_G} \right) - \frac{1}{4} \right] + \frac{a}{2} G_0^2 \sigma_0^2 + \frac{\lambda}{4} \sigma_0^4. \quad (289)$$

with

$$G_0 = \Lambda_G e^{\frac{a^2}{\lambda \lambda_G}} \sim N_c, \quad \sigma_0^2 = -\frac{a G_0^2}{\lambda} \sim N_c. \quad (290)$$

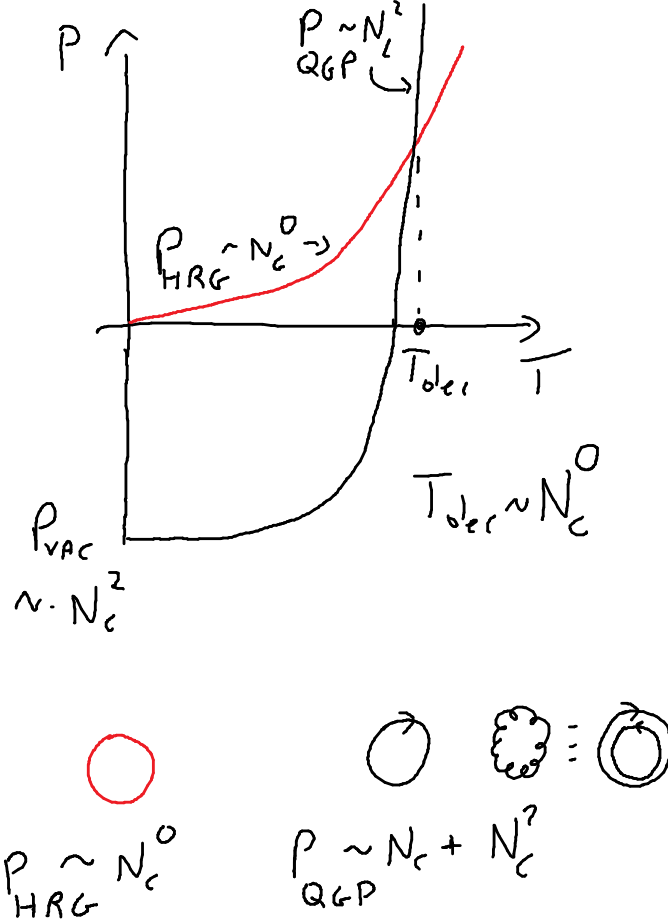


Fig. 49. Schematic representation of the pressure in the confined and the deconfined phases. In the confined one, the pressure of the hadron resonance gas scales as N_c^0 (red loop down left) and vanishes (by convention) at $T = 0$. Then, the quark-gluon pressure contains the free parts of quarks and gluons, that scale as N_c and N_c^2 respectively (quark and gluon loops down right), as well a vacuum part that has two similar terms, but with opposite sign. Thus, in order the QGP to be realized, the pressure needs first to become positive: this occurs for a temperature of the order of N_c^0 . Shortly after, the QGP pressure overcomes the HRG one, realizing deconfinement.

Hence,

$$V_{vac} = V_{G,vac} + V_{\sigma,vac} , \quad (291)$$

with

$$V_{G,vac} = \frac{1}{4} \lambda_G \Lambda_G^4 e^{\frac{4a^2}{\lambda \lambda_G}} \left[\frac{a^2}{\lambda \lambda_G} - \frac{1}{4} \right] \sim N_c \left[N_c^{-1} - \frac{1}{4} \right] \sim -N_c^2 < 0 , \quad (292)$$

and

$$V_{\sigma,vac} = \frac{a}{2} G_0^2 \sigma_0^2 + \frac{\lambda}{4} \sigma_0^4 = -\frac{a^2}{4\lambda} G_0^4 \sim -N_c < 0 . \quad (293)$$

We may then express the QCD vacuum pressure as function of N_c , by two terms (see Fig. 49 for a sketch of the situation):

$$P_{QCD,vac} = P_{G,vac} + P_{\sigma,vac} \quad (294)$$

with

$$P_{G,vac} \simeq B_G N_c^2 > 0 , P_{\sigma,vac} \simeq B_G N_c > 0 \quad (295)$$

Now, strictly speaking this pressure should be added (as a positive term) to the confined phase, as it is derived from a confined model of QCD. We will however follow the usual convention and subtract this term from the QCD vacuum, thus at zero temperature and density the pressure of the confined phase vanishes. One has then to subtract this term from the corresponding quark-gluon-plasma (QGP) phase.

Hence, the pressure of the QGP can be expressed as [123]

$$\begin{aligned} P_{QGP}(T) &= 2N_c^2 \frac{\pi^2}{90} T^4 + 2N_c N_f \frac{\pi^2}{90} T^4 - P_{G,vac} \\ &= 2N_c^2 \frac{\pi^2}{90} T^4 + 2N_c N_f \frac{\pi^2}{90} T^4 - B_G N_c^2 - B_G N_c , \end{aligned} \quad (296)$$

where it is visible that gluons dominate for N_c large enough. The pressure for the confined phase (referred to as Hadron Resonance Gas (HRG) [3]) reads

$$P_{HRG}(T) = \sum_n P_n(T) , \quad (297)$$

with

$$P_n(T) = -T \zeta_n \int_k \ln \left[1 - \frac{\sqrt{k^2 + M_n^2}}{T} \right] \text{ if } n \text{ is a meson} , \quad (298)$$

$$P_n(T) = T \zeta_n \int_k \ln \left[1 + \frac{\sqrt{k^2 + M_n^2}}{T} \right] \text{ if } n \text{ is a baryon} , \quad (299)$$

where ς_n is the appropriate degeneracy factor and M_n is the mass of the n -th hadron. Clearly, mesons dominate at large- N_c , since baryons are very heavy in this limit. Hence:

$$P_{HRG}(T) \simeq P_{HRG}^{\text{mesons}}(T) \sim N_c^0. \quad (300)$$

Note,

$$P_{HRG}(T = 0) = 0 \quad (301)$$

in agreement with the adopted normalization.

The confinement/deconfinement phase transition takes place for $T = T_{dec}$ given by (see Fig. 49):

$$P_{HRG}(T_{dec}) = P_{QGP}(T_{dec}). \quad (302)$$

It is easy to understand that this is the case for

$$T_{dec} \sim N_c^0. \quad (303)$$

Namely, at large N_c the gluons dominate and the transition take place basically just after the QGP pressure comes positive:

$$T_{dec} \gtrsim \frac{B_G}{2\frac{\pi^2}{90}} \sim N_c^0. \quad (304)$$

Note, the present simple treatment is not able to correctly guess the order of the transition, which by construction is a first-order, but in reality it is known to be a cross-over [3].

Moreover, it is also expected that the phase transition for chiral restoration takes place for a similar temperature as the deconfined one, as supported by models, e.g. [3, 56, 124].

Next, let us consider zero temperature and finite density. To this end, we introduce the quark chemical potential μ_q and the baryon chemical potential $\mu_B = N_c \mu_q$. In the confined phase, one has only baryons. We follow here one possible choice described in Ref. [42], that corresponds to a confined stiff matter with speed of sound equal to the speed of light. Intuitively, it corresponds to an interaction dominated gas. In this case, the pressure in the baryonic phase is (for large values of the baryonic chemical potential)

$$P_B = a_B \mu_B^2 \quad (305)$$

where a_B is a constant with dimension Energy², whose N_c dependence must be established².

² In a more realistic treatment, one may consider at high density $P_B = a_B \mu_B^\alpha - K$ (with α a free parameter) which needs to be matched to known equation of state of nuclear matter at about $2n_0$ [42]. The large- N_c behavior is not affected.

The baryon density follows as

$$n_B = dP_B/d\mu_B = 2a_B\mu_B \quad (306)$$

and the energy density as $\varepsilon_B = P_B$, hence the speed of sound is $v_B = \sqrt{dP_B/d\varepsilon_B} = 1$. This result is indeed in agreement with the high density limit of nuclear matter described in Ref. [125], which takes place when vector meson driven interaction dominates. Hence, since a_B has energy² and since the appropriate dimension is constructed by m_V^2/g_{BBV}^2 with $g_{BBV} \sim N_c^{1/2}$ being the baryon-baryon-vector coupling, one gets

$$a_B \sim N_c^{-1} \rightarrow a_B = \frac{\bar{a}_B}{N_c} . \quad (307)$$

In fact, the pressure as function of the density can be written as

$$P_B = \frac{n_B^2}{4a_B} \simeq \frac{1}{2} \frac{g_{BBV}^2}{m_V^2} n_B^2 \quad (308)$$

where the right hand side follows for Sec. 4.11 of Ref. [125] (high-density limit). It thus shows the direct proportionality of a_B to m_V^2/g_{BBV}^2 .

Finally, in terms of the quark chemical potential, we may write the baryonic pressure

$$P_B(\mu_q) = N_c \bar{a}_B \mu_q^2 \quad (309)$$

implying that we have a confined phase whose pressure scales with N_c . This is in agreement with the quarkyonic phase discussed in Refs. [35, 36, 40], and also with the result of the Walecka-type model at large N_c and for high densities, see Ref. [4].

Next, let us consider the QGP phase, which contains only quarks as d.o.f. (gluons are not present at $T = 0$) as well as the already discussed vacuum contribution:

$$P_{QGP}(\mu_q) = P_q(\mu_q) = \frac{N_c N_f}{12\pi^2} \mu_q^4 + P_{QCD,vac} = \frac{N_c N_f}{12\pi^2} \mu_q^4 - B_G N_c^2 - B_G N_c. \quad (310)$$

The deconfinement phase transition takes place for $P_B(\mu_{q,dec}) = P_q(\mu_{q,dec})$, leading to

$$\mu_{q,dec} \sim N_c^{1/4} , \quad (311)$$

thus the deconfinement phase transition takes place at higher and higher densities when N_c increases. Here, one expects a different behavior of the chiral phase transition, which should take place for $\mu_{q,c} \sim N_c^0$.

Additional topics related to large- N_c in the medium are briefly discussed below.

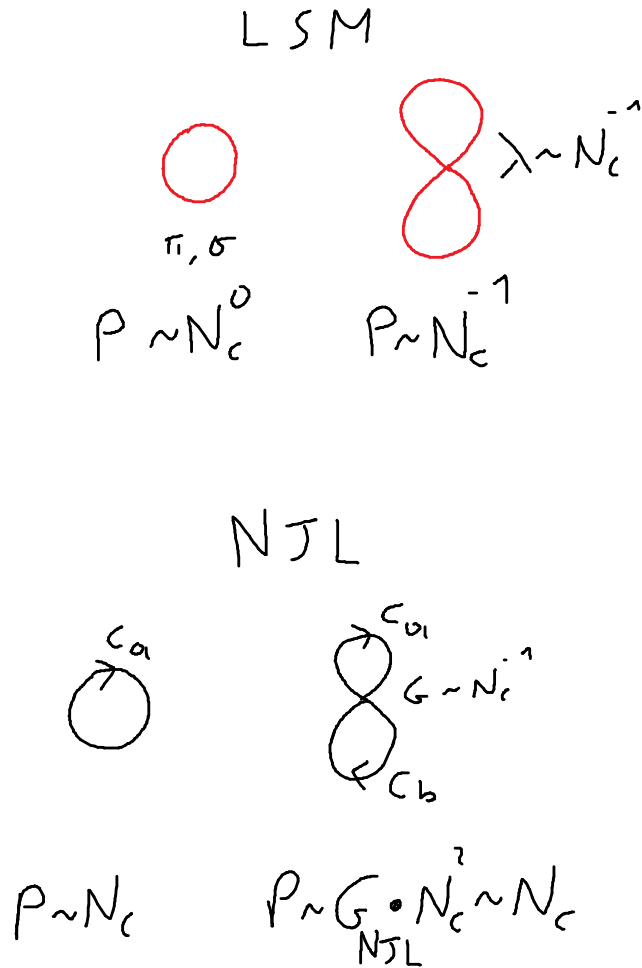


Fig. 50. Vacuum diagrams can be used to establish the scaling of the contribution to the pressure. Upper part: the LSM case; the pressure of free mesons goes with N_c^0 , while the interaction contribution goes as N_c^{-1} . This is why in the large- N_c limit chiral restoration takes place at higher and higher T . Lower part: the NJL case; the free quarks give rise to a pressure proportional to N_c , just as the interaction terms. Accordingly, the critical temperature for chiral restoration is N_c -independent.

1) **Chiral mesonic models at nonzero T : a problem and how to cure it.**

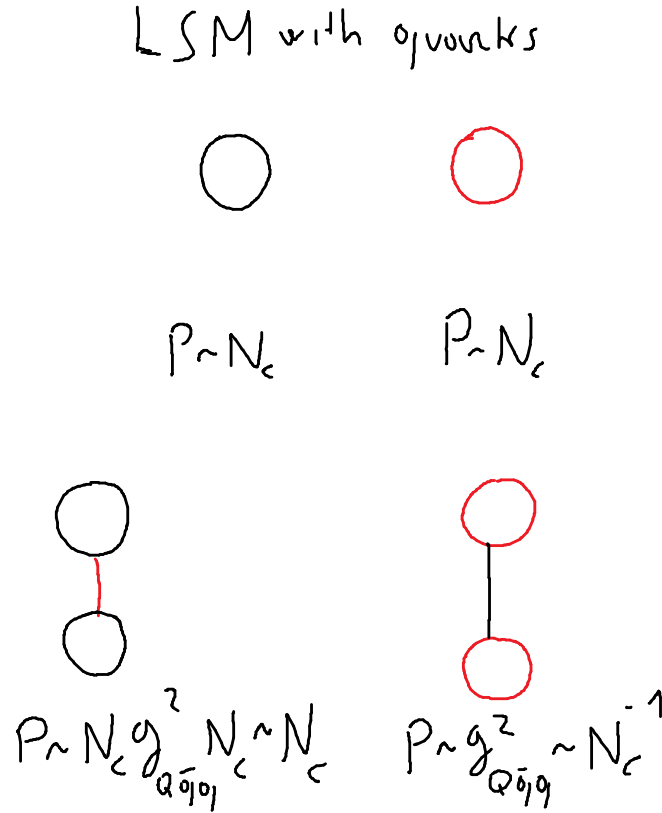


Fig. 51. Quark-level LSM. The free part contains two contributions for the pressure, the meson one (N_c^0) and the quark one (N_c). Two interaction terms are outlined: one with quark loops, whose pressure contribution goes as N_c (just as the free quark part) and one with mesonic loops, whose pressure contribution goes as N_c^{-1} . Quarks dominate in both cases, and the final outcome is similar to the NJL model: the critical temperature for chiral restoration scales as N_c^0 .

If a purely mesonic model as the one of Eq. (125) is considered, chiral restoration can be studied by evaluating the chiral condensate as function of the temperature, $\phi_N \rightarrow \phi_N(T)$. For large T , $\phi_N(T)$ tends to zero and the way it does also specifies the order of the chiral phase transition. For $N_c = 3$ one expects a smooth cross-over [3, 124, 126].

What about the behavior of the chiral phase transition at large N_c ? One indeed expects that the critical temperature for chiral restoration, denoted

as T_c , should be N_c -independent:

$$T_c \sim T_{dec} \sim \Lambda_{QCD} \sim N_c^0 . \quad (312)$$

Yet, in purely mesonic models, the contribution of the interaction to the effective potential (or equivalently to the pressure) scales as $1/N_c$ and is therefore suppressed. Correspondingly, one finds:

$$T_c \sim f_\pi \sim N_c^{1/2} , \quad (313)$$

hence the chiral restoration takes at larger and larger N_c [39]. This result is depicted as in Fig. 50 (upper part), in which the vacuum diagrams give rise to the contribution for the pressure, see Ref. [124] and refs. therein. It seems therefore that such models cannot correctly describe the expected large- N_c results.

How to reconcile chiral models with the expected large- N_c scaling? In Ref. [39] some recipes were put forward. An intuitive heuristic approach consists in considering the following potential with an explicit dependence on the temperature T :

$$\begin{aligned} V(\sigma, \pi) &= \frac{m_0^2}{2} \left(1 - \frac{T^2}{T_0^2} \right) \Phi^* \Phi + \frac{\lambda}{4} (\Phi^* \Phi)^2 \\ &= \frac{m_0^2}{2} \left(1 - \frac{T^2}{T_0^2} \right) (\sigma^2 + \pi^2) + \frac{\lambda}{4} (\sigma^2 + \pi^2)^2 , \end{aligned} \quad (314)$$

where $T_0 \sim \Lambda_{QCD} \sim N_c^0$. In this way, the chiral restoration is enforced by this modification. At $T = T_0$ the bare potential is such that only the quartic interaction is present. With this ‘ad hoc’ modification, $T_c \sim N_c^0$ is obtained.

A more formal way of achieving this result is realized by coupling the chiral multiplet Φ to the expectation value of the Polyakov loop (see e.g. [3, 48]). This quantity, denoted as $l(T)$, describes effectively the gluonic sector, more specifically the restoration of the symmetry under $Z(N_c)$ transformations in the vacuum. In particular, $|l(T)| = 1$ at large temperature (in the deconfined phase) while it vanishes at small T . One can couple the Polyakov loop to the LSM in the following way:

$$V(\sigma, \pi, l) = \frac{m_0^2}{2} \left(1 - c_l T^2 |l(T)|^2 \right) \Phi^* \Phi + \frac{\lambda}{4} (\Phi^* \Phi)^2 , \quad (315)$$

where $c_l \sim N_c^0$ is a dimensionless constant. Indeed, the proper description of the Polyakov loop at large N_c is not an easy task, but certain relatively simple choices are possible [24, 48]. Within LSMs with Polyakov loop, the critical temperature for chiral restoration scales as $T_c \propto N_c^0$, as expected.

The already mentioned famous NJL model [13, 14] contains only quarks with a chiral interaction of the type

$$V_{NJL}(\sigma, \pi, l) = G_{NJL}[(\bar{\psi}\psi)^2 + (\bar{\psi}i\gamma^5\psi)^2] \quad (316)$$

where the chiral transformation (in this one-flavor case) is $\psi \rightarrow e^{i\alpha\gamma^5/2}\psi$, and where $G_{NJL} \sim N_c^{-1}$ (this is just as the constant K_Q studied in the case of the quarkonium formation; indeed, the NJL model has been widely used to study $\bar{q}q$ bound states [14, 15]). Here, the interaction type is of the same order of the free quark ones. The SSB takes place if G_{NJL} is large enough and chiral restoration takes place at nonzero T , with $T_c \sim N_c^0$, see Fig. 50.

The last case that we examine is the one that involves quark-meson type model [24, 56, 57], in which both mesons and quarks are present:

$$V_{LSM,quarks}(\sigma, \pi, l) = g_\sigma \sigma (\bar{\psi}\psi) + g_\pi \pi (\bar{\psi}i\gamma^5\psi) . \quad (317)$$

In this case, the interaction contribution to the pressure is also of the order N_c just as the quarks, thus $T_c \sim N_c^0$, see Fig. 51.

2) Critical endpoint CEP at large- N_c

It is well known that the confinement/deconfinement as well as the chiral phase transition(s) are of cross-over type along the T direction, and first order along the μ_q one. At least one critical point is therefore expected, whose search is important for both theoretical and experimental investigations, e.g. [3, 56, 128, 129].

Yet, at large N_c , as shown in details in [24] using an extended linear sigma model with quarks and Polyakov loop, the phase diagram turns out to be utterly different: one has a first-order along T and a cross-over along μ_q . A critical point is present at about $(T_{CEP}, \mu_{q,CEP})$ where $T_{CEP} \propto \Lambda_{QCD} \sim N_c^0$ while $\mu_{q,CEP}$ increases for increasing N_c . Quite remarkably, for intermediate N_c (from 4 up to about 50), only cross-over phases are present in the whole phase diagram [24].

The pressure at very large N_c resembles the expected behavior, in particular we have the following areas, see Fig. 52 as well as the detailed explanations in ref. [24]

(i) $P \sim N_c^0$ for low- T and low- μ_q within the confined and chirally broken phase.

(ii) $P \sim N_c$ for low- T and high- μ_q within the confined and chirally restored (quarkyonic) phase. Note, in this phase the nucleons do not need to be massless, see the discussion in Sec. 4.

(iii) $P \sim N_c^2$ for high T and high- μ_q within the deconfined QGP phase.

Finally, along the T line and for small μ_q the chiral and the deconfinement phase transition coincide, while along the μ_q line and for small T

the chiral transition occurs for $\mu_{q,c} \sim N_c^0$ and the deconfinement one for increasing N_c .

In the recent work of Ref. [127] the effect of the chiral anomaly on the phase diagram is discussed. Yet, anomaly terms decrease fast for increasing N_c , thus they shall not modify the overall large- N_c picture outlined above.

3) Nuclear matter at large- N_c

Does nuclear matter bind at large N_c ? This question was already posed in the introduction, and at first put aside since quite (too?) philosophical. Yet, is $N_c = 3$ somewhat special?

Indeed, the issue is quite subtle. In the easiest scenario, one considers a standard σ - ω model coupled to the nucleon

$$V = g_{\sigma N} \bar{\Psi}_1 \Psi_1 + g_{\omega N} \omega_\mu \bar{\Psi}_1 \gamma^\mu \Psi_1 , \quad (318)$$

with

$$g_{\sigma N} \sim N_c^{1/2} \text{ and } g_{\omega N} \sim N_c^{1/2} , \quad (319)$$

where σ corresponds to $f_0(500)$ and ω to $\omega(782)$. If the masses of these fields are N_c^0 (as quark-antiquark regular states), then the mean field equations show that nuclear matter forms for any N_c (and becomes more and more bound).

Yet, it is well known that $f_0(500)$ is *not* predominantly a $\bar{q}q$ [102]. Considering this fact, changes the picture completely: no nuclear matter exist, already for $N_c \geq 4$.

Indeed, for very large N_c the pion cannot be neglected and being ‘de facto’ massless should generate a kind of loosely bound nuclear matter similar to atomic matter (basically an attractive almost Coulomb force would act among nucleons in this limit). The detailed study of this hypothetical state of matter is a task for the future.

4) Neutron stars at large- N_c

One may apply the previous discussion about baryonic and quark matter to neutron stars, see Ref. [42] for details.

Using the baryonic equation of state of Eq. (309) that corresponds to stiff matter (speed of sound equal 1), for $N_c = 3$ the maximal mass of a neutron star is about

$$M_{NS}^{\max} \simeq 2.2 M_\odot . \quad (320)$$

Namely, for higher masses a phase transition to deconfined quark phase takes place, which is however unstable [130]. (The maximal value quoted above can be increased if the vacuum pressure is increased).

When increasing N_c , the phase transition to quark matter takes place for higher and higher density. Already for $N_c \gtrsim 5.5$, quark matter plays no role, and the maximum mass is about $3M_\odot$.

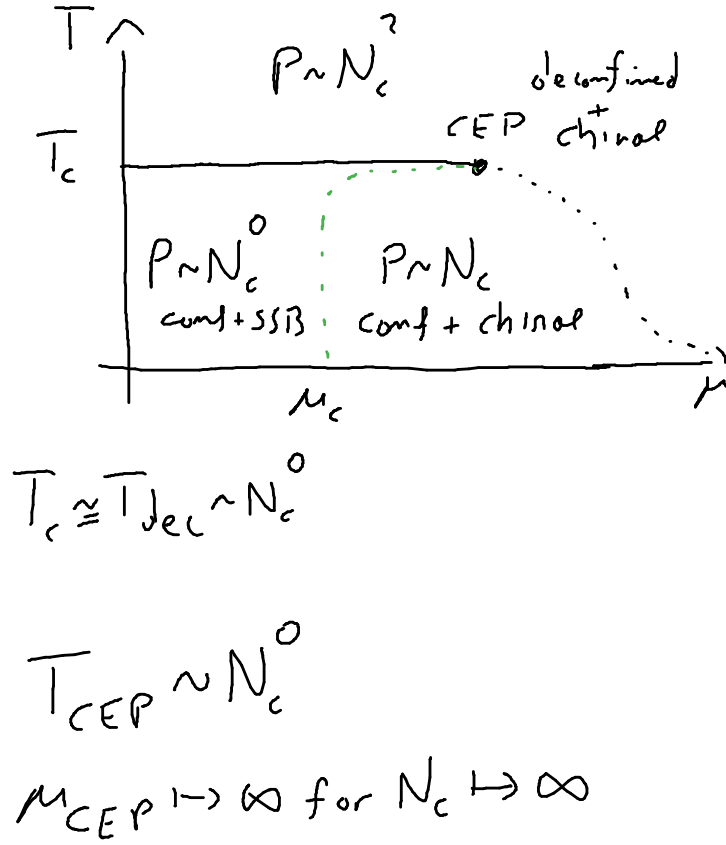


Fig. 52. Schematic and simplified representation of the QCD phase diagram for large- N_c . For low T and μ , a confined and chirally broken (SSB) phase with pressure proportional to N_c^0 is present. If the temperature is above T_c , for any chemical potential μ , a deconfined phase with pressure proportional to N_c^2 is realized. Here, chiral symmetry is also restored. For large μ but $T < T_{dec} = T_c$, the system is still confined but chiral symmetry is restored: the pressure is proportional to N_c (as a gas of quarks would have). Important aspects: the type of the phase transition is a first-order one along T and a cross-over along μ . Along T , the chiral and the deconfinement transitions coincide. Along μ , they do not: the chiral one (green dashed) is of the order N_c^0 , the deconfinement one (black dashed) moves toward infinity. The critical end point also tends to infinity along the μ direction. For details, see Ref. [24].

6. Conclusions

In these lectures we have revisited the main features of QCD at large- N_c for both mesons and baryons. To this end, we have used a bound-state approach in which a simple separable Ansatz has been applied. This is indeed similar to certain approaches of QCD, such as the NJL model. Yet, the large- N_c scaling that can be derived are fully general and do not depend on this specific Ansatz. In this way, we could recover all the large- N_c scaling behavior for regular mesons, for glueballs, and for hybrid mesons. Also their mutual interactions, decays and mixing, could be properly described.

Many consequences of these results have been investigated, among which the reason why certain mesons are narrow, how dominant and subdominant interaction terms arise, and most importantly, how chiral models behave in the large- N_c limit. Also the behavior of the dilaton/glueball field and its coupling to chiral models has been reviewed in some detail. An overall nice and consistent picture of large- N_c QCD has emerged.

Four-quark states were briefly discussed. Molecular states and dynamically generated states do not form in the large- N_c limit, as our bound-state approach easily shows. Yet, the case of tetraquark objects is more complicated. Our present results suggest that all of them share the same fate: they do not form in the large- N_c limit, but this last statement is not yet conclusive.

Baryons were presented following the same line applied to mesons, upon interpreting them as bound states of a generalized diquark built with $N_c - 1$ quarks, and a quark. Upon taking the mass of the generalized diquark as increasing with N_c , it was possible to recover the known large- N_c results for baryons. Chiral models have been studied for baryons as well: the chirally invariant mass generation via the quark condensate and via the dilaton condensate (the latter in the so-called mirror assignment) fulfill the expected large- N_c properties.

Finally, we have discussed the main features of the phase diagram of QCD in the large- N_c domain. Simple scaling laws show that at large N_c gluons dominate if the temperature is high enough. The temperature for confinement/deconfinement transition is N_c independent, but the chemical potential increases for increasing N_c . This means that in the large- N_c limit matter is confined below a certain T_{dec} and deconfined above, for any chemical potential. Yet, for high density, one may have a confined and chirally restored matter whose pressure is proportional to N_c , which well fits with the concept of a quarkyonic phase. These results also imply that the phase diagram at large N_c looks quite different than the one for the real $N_c = 3$ world.

Moreover, we have also discussed some related issue, such as the failure

of certain chiral models at large N_c and how to improve them, the formation (or non-formation) of nuclear matter, and implications for neutron stars.

In conclusion, large- N_c QCD is an interesting theoretical framework, often the only one available to arrive at certain conclusion. It offers a consistent picture, somewhat simplified from our physical one, but definitely not trivial.

Coming back to our original question: is $N_c=3$ large? We have shown that in most cases it is, but not in all of them. There is therefore not a simple and always valid answer to that seemingly naive question but one needs, case by case, to study the consequences of increasing N_c and see how much the outcomes depart from the real world. Yet, in many cases the lesson gained from large N_c is very useful for understanding our world with $N_c = 3$.

Acknowledgments: The author thanks A. Pilloni, G. Pagliara, Gy. Kovacs, P. Kovacs, C. Fischer, R. Pisarski, S. Jafarzade, E. Trotti, J. Pelaez, D. Rischke, A. Koenigstein, and V. Shastri for very useful discussions. Financial support from the Polish National Science Centre (NCN) via the OPUS project 2019/33/B/ST2/00613 is acknowledged.

REFERENCES

- [1] R.L. Workman et al. (Particle Data Group), Prog. Theor. Exp. Phys. 2022, 083C01 (2022) and 2023 update.
- [2] A. W. Thomas and W. Weise, The Structure of the Nucleon, Berlin, Germany: Wiley-VCH (2001) 389 p.
- [3] C. Ratti and R. Bellwied, The Deconfinement Transition of QCD: Theory Meets Experiment, Lect. Notes Phys. **981** (2021), 1-216 2021, ISBN 978-3-030-67234-8, 978-3-030-67235-5 doi:10.1007/978-3-030-67235-5
- [4] L. Bonanno and F. Giacosa, Does nuclear matter bind at large N_c ?, Nucl. Phys. A **859** (2011), 49-62 [arXiv:1102.3367 [hep-ph]].
- [5] G. 't Hooft, 'A PLANAR DIAGRAM THEORY FOR STRONG INTERACTIONS, Nucl. Phys. B **72** (1974) 461.
- [6] E. Witten, Nucl. Phys. B **160** (1979) 57.
- [7] G. 't Hooft, "Large N ," doi:10.1142/9789812776914_0001 [arXiv:hep-th/0204069 [hep-th]].
- [8] R. F. Lebed, Phenomenology of large $N(c)$ QCD, Czech. J. Phys. **49** (1999), 1273-1306 doi:10.1023/A:1022820227262 [arXiv:nucl-th/9810080 [nucl-th]].
- [9] S. R. Coleman, "1/ N ," 17th International School of Subnuclear Physics: Pointlike Structures Inside and Outside Hadrons 31 July-10 August 1979. Erice, Italy (C79-07-31) SLAC-PUB-2484.
- [10] B. Lucini and M. Panero, Introductory lectures to large- N QCD phenomenology and lattice results, Prog. Part. Nucl. Phys. **75** (2014), 1-40 doi:10.1016/j.ppnp.2014.01.001 [arXiv:1309.3638 [hep-th]].
- [11] C. Bonanno, M. D'Elia, B. Lucini and D. Vadacchino, Towards glueball masses of large- N $SU(N)$ pure-gauge theories without topological freezing, Phys. Lett. B **833** (2022), 137281 doi:10.1016/j.physletb.2022.137281 [arXiv:2205.06190 [hep-lat]].
- [12] W. Lucha, D. Melikhov and H. Sazdjian, Tetraquarks in large- N_c QCD, Prog. Part. Nucl. Phys. **120** (2021), 103867 doi:10.1016/j.ppnp.2021.103867 [arXiv:2102.02542 [hep-ph]].
- [13] Y. Nambu and G. Jona-Lasinio, Dynamical Model of Elementary Particles Based on an Analogy with Superconductivity. 1., Phys. Rev. **122** (1961), 345-358 doi:10.1103/PhysRev.122.345
- [14] T. Hatsuda and T. Kunihiro, QCD phenomenology based on a chiral effective Lagrangian, Phys. Rept. **247** (1994), 221-367 doi:10.1016/0370-1573(94)90022-1 [arXiv:hep-ph/9401310 [hep-ph]]; S. P. Klevansky, The Nambu-Jona-Lasinio model of quantum chromodynamics, Rev. Mod. Phys. **64** (1992), 649-708 doi:10.1103/RevModPhys.64.649
U. Vogl and W. Weise, The Nambu and Jona Lasinio model: Its implications for hadrons and nuclei, Prog. Part. Nucl. Phys. **27** (1991), 195-272 doi:10.1016/0146-6410(91)90005-9

- [15] M. K. Volkov and A. E. Radzhabov, The Nambu-Jona-Lasinio model and its development, *Phys. Usp.* **49** (2006), 551-561 doi:10.1070/PU2006v049n06ABEH005905 [arXiv:hep-ph/0508263 [hep-ph]].
- [16] S. Weinberg, Evidence That the Deuteron Is Not an Elementary Particle, *Phys. Rev.* **137** (1965), B672-B678 doi:10.1103/PhysRev.137.B672
- [17] K. Hayashi, M. Hirayama, T. Muta, N. Seto and T. Shirafuji, Compositeness criteria of particles in quantum field theory and S-matrix theory,” *Fortsch. Phys.* **15** (1967) no.10, 625-660 doi:10.1002/prop.19670151002
- [18] F. Giacosa, T. Gutsche and A. Faessler, A Covariant constituent quark/gluon model for the glueball-quarkonia content of scalar - isoscalar mesons, *Phys. Rev. C* **71** (2005), 025202 doi:10.1103/PhysRevC.71.025202 [arXiv:hep-ph/0408085 [hep-ph]].
- [19] A. Faessler, T. Gutsche, M. A. Ivanov, V. E. Lyubovitskij and P. Wang, Pion and sigma meson properties in a relativistic quark model, *Phys. Rev. D* **68** (2003), 014011 doi:10.1103/PhysRevD.68.014011 [arXiv:hep-ph/0304031 [hep-ph]].
- [20] R. Alkofer and L. von Smekal, The Infrared behavior of QCD Green’s functions: Confinement dynamical symmetry breaking, and hadrons as relativistic bound states, *Phys. Rept.* **353** (2001), 281 doi:10.1016/S0370-1573(01)00010-2 [arXiv:hep-ph/0007355 [hep-ph]].
- [21] C. S. Fischer, Infrared properties of QCD from Dyson-Schwinger equations, *J. Phys. G* **32** (2006), R253-R291 doi:10.1088/0954-3899/32/8/R02 [arXiv:hep-ph/0605173 [hep-ph]].
- [22] G. Eichmann, H. Sanchis-Alepuz, R. Williams, R. Alkofer and C. S. Fischer, Baryons as relativistic three-quark bound states, *Prog. Part. Nucl. Phys.* **91** (2016), 1-100 doi:10.1016/j.ppnp.2016.07.001 [arXiv:1606.09602 [hep-ph]].
- [23] D. Parganlija, P. Kovacs, G. Wolf, F. Giacosa and D. H. Rischke, Meson vacuum phenomenology in a three-flavor linear sigma model with (axial-)vector mesons, *Phys. Rev. D* **87** (2013) no.1, 014011 doi:10.1103/PhysRevD.87.014011 [arXiv:1208.0585 [hep-ph]].
- [24] P. Kovács, G. Kovács and F. Giacosa, Fate of the critical endpoint at large N_c , *Phys. Rev. D* **106** (2022) no.11, 116016 doi:10.1103/PhysRevD.106.116016 [arXiv:2209.09568 [hep-ph]].
- [25] A. A. Migdal and M. A. Shifman, Dilaton Effective Lagrangian in Gluodynamics, *Phys. Lett. B* **114** (1982), 445-449 doi:10.1016/0370-2693(82)90089-2
- [26] A. Salomone, J. Schechter and T. Tudron, Properties of Scalar Gluonium, *Phys. Rev. D* **23** (1981), 1143 doi:10.1103/PhysRevD.23.1143
- [27] J. R. Ellis and J. Lanik, IS SCALAR GLUONIUM OBSERVABLE?, *Phys. Lett. B* **150** (1985), 289-294 doi:10.1016/0370-2693(85)91013-5
- [28] S. Janowski, F. Giacosa and D. H. Rischke, Is $f_0(1710)$ a glueball?, *Phys. Rev. D* **90** (2014) no.11, 114005 doi:10.1103/PhysRevD.90.114005 [arXiv:1408.4921 [hep-ph]].

- [29] S. Weinberg, Tetraquark Mesons in Large N Quantum Chromodynamics, Phys. Rev. Lett. **110** (2013) 261601 doi:10.1103/PhysRevLett.110.261601 [arXiv:1303.0342 [hep-ph]].
- [30] R. F. Lebed, Large- N Structure of Tetraquark Mesons, Phys. Rev. D **88** (2013), 057901 doi:10.1103/PhysRevD.88.057901 [arXiv:1308.2657 [hep-ph]].
- [31] T. D. Cohen and R. F. Lebed, Tetraquarks with exotic flavor quantum numbers at large N_c in QCD(AS), Phys. Rev. D **89** (2014) no.5, 054018 doi:10.1103/PhysRevD.89.054018 [arXiv:1401.1815 [hep-ph]].
- [32] T. D. Cohen and R. F. Lebed, Are There Tetraquarks at Large N_c in QCD(F)?, Phys. Rev. D **90** (2014) no.1, 016001 doi:10.1103/PhysRevD.90.016001 [arXiv:1403.8090 [hep-ph]].
- [33] T. Cohen, F. J. Llanes-Estrada, J. R. Pelaez and J. Ruiz de Elvira, Nonordinary light meson couplings and the $1/N_c$ expansion, Phys. Rev. D **90** (2014) no.3, 036003 doi:10.1103/PhysRevD.90.036003 [arXiv:1405.4831 [hep-ph]].
- [34] M. Knecht and S. Peris, Narrow Tetraquarks at Large N , Phys. Rev. D **88** (2013), 036016 doi:10.1103/PhysRevD.88.036016 [arXiv:1307.1273 [hep-ph]].
- [35] L. McLerran and R. D. Pisarski, Phases of cold, dense quarks at large $N(c)$, Nucl. Phys. A **796** (2007), 83-100 doi:10.1016/j.nuclphysa.2007.08.013 [arXiv:0706.2191 [hep-ph]].
- [36] T. Kojo, Y. Hidaka, L. McLerran and R. D. Pisarski, Quarkyonic Chiral Spirals, Nucl. Phys. A **843** (2010), 37-58 doi:10.1016/j.nuclphysa.2010.05.053 [arXiv:0912.3800 [hep-ph]].
- [37] L. McLerran, K. Redlich and C. Sasaki, Quarkyonic Matter and Chiral Symmetry Breaking, Nucl. Phys. A **824** (2009), 86-100 doi:10.1016/j.nuclphysa.2009.04.001 [arXiv:0812.3585 [hep-ph]].
- [38] L. McLerran, The Phase Diagram of QCD and Some Issues of Large $N(c)$, Nucl. Phys. B Proc. Suppl. **195** (2009), 275-280 doi:10.1016/j.nuclphysbps.2009.10.020 [arXiv:0906.2651 [hep-ph]].
- [39] A. Heinz, F. Giacosa and D. H. Rischke, Restoration of chiral symmetry in the large- N_c limit, Phys. Rev. D **85** (2012), 056005 doi:10.1103/PhysRevD.85.056005 [arXiv:1110.1528 [hep-ph]].
- [40] Y. Hidaka, T. Kojo, L. McLerran and R. D. Pisarski, The Dichotomous Nucleon: Some Radical Conjectures for the Large- N_c Limit, Nucl. Phys. A **852** (2011), 155-174 doi:10.1016/j.nuclphysa.2011.01.008 [arXiv:1004.2261 [hep-ph]].
- [41] L. McLerran and S. Reddy, Quarkyonic Matter and Neutron Stars Phys. Rev. Lett. **122** (2019) no.12, 122701 doi:10.1103/PhysRevLett.122.122701 [arXiv:1811.12503 [nucl-th]].
- [42] F. Giacosa and G. Pagliara, Neutron stars in the large- N_c limit, Nucl. Phys. A **968** (2017), 366-378 doi:10.1016/j.nuclphysa.2017.08.006 [arXiv:1707.02644 [nucl-th]].
- [43] F. Giacosa, "Mesons beyond the quark-antiquark picture," Acta Phys. Polon. B **47** (2016), 7 doi:10.5506/APhysPolB.47.7 [arXiv:1511.04605 [hep-ph]].

- [44] Y. Chen, A. Alexandru, S. J. Dong, T. Draper, I. Horvath, F. X. Lee, K. F. Liu, N. Mathur, C. Morningstar and M. Peardon, *et al.* Glueball spectrum and matrix elements on anisotropic lattices, *Phys. Rev. D* **73** (2006), 014516 doi:10.1103/PhysRevD.73.014516 [arXiv:hep-lat/0510074 [hep-lat]].
- [45] R. L. Jaffe, K. Johnson and Z. Ryzak, Qualitative Features of the Glueball Spectrum, *Annals Phys.* **168** (1986), 344 doi:10.1016/0003-4916(86)90035-7
- [46] V. Mathieu, N. Kochelev and V. Vento, The Physics of Glueballs, *Int. J. Mod. Phys. E* **18** (2009), 1-49 doi:10.1142/S0218301309012124 [arXiv:0810.4453 [hep-ph]].
- [47] A. Zee, *Group Theory in a Nutshell for Physicists*, Princeton University Press, 2016, ISBN 978-1-4008-8118-5, 978-0-691-16269-0
- [48] K. Fukushima and V. Skokov, Polyakov loop modeling for hot QCD,” *Prog. Part. Nucl. Phys.* **96** (2017), 154-199 doi:10.1016/j.ppnp.2017.05.002 [arXiv:1705.00718 [hep-ph]].
- [49] A. Deur, S. J. Brodsky and G. F. de Teramond, The QCD Running Coupling,” *Nucl. Phys.* **90** (2016), 1 doi:10.1016/j.ppnp.2016.04.003 [arXiv:1604.08082 [hep-ph]].
- [50] H. Gies, *Phys. Rev. D* **66** (2002), 025006 doi:10.1103/PhysRevD.66.025006 [arXiv:hep-th/0202207 [hep-th]].
- [51] S. R. Coleman and E. Witten, Chiral Symmetry Breakdown in Large N Chromodynamics, *Phys. Rev. Lett.* **45** (1980), 100 doi:10.1103/PhysRevLett.45.100
- [52] E. Witten, Current Algebra Theorems for the U(1) Goldstone Boson, *Nucl. Phys. B* **156** (1979), 269-283 doi:10.1016/0550-3213(79)90031-2
- [53] J. F. Donoghue, The Gluon ‘Mass’ in the Bag Model, *Phys. Rev. D* **29** (1984), 2559 doi:10.1103/PhysRevD.29.2559
- [54] D. Binosi, D. Ibanez and J. Papavassiliou, The all-order equation of the effective gluon mass, *Phys. Rev. D* **86** (2012), 085033 doi:10.1103/PhysRevD.86.085033 [arXiv:1208.1451 [hep-ph]]. S. Strauss, C. S. Fischer and C. Kellermann, Analytic structure of the Landau gauge gluon propagator, *Phys. Rev. Lett.* **109** (2012), 252001 doi:10.1103/PhysRevLett.109.252001 [arXiv:1208.6239 [hep-ph]].
- [55] S. Godfrey and N. Isgur, Mesons in a Relativized Quark Model with Chromodynamics, *Phys. Rev. D* **32** (1985), 189-231 doi:10.1103/PhysRevD.32.189 See also the summary on ‘quark model’ in Ref. [1].
- [56] P. Kovács, Z. Szép and G. Wolf, Existence of the critical endpoint in the vector meson extended linear sigma model, *Phys. Rev. D* **93** (2016) no.11, 114014 doi:10.1103/PhysRevD.93.114014 [arXiv:1601.05291 [hep-ph]].
- [57] R. A. Tripolt, N. Strodthoff, L. von Smekal and J. Wambach, Spectral Functions for the Quark-Meson Model Phase Diagram from the Functional Renormalization Group, *Phys. Rev. D* **89** (2014) no.3, 034010 doi:10.1103/PhysRevD.89.034010 [arXiv:1311.0630 [hep-ph]].
- [58] H. J. Lipkin, The OZI Rule in Charmonium Decays Above $D\bar{D}$ Threshold, *Phys. Lett. B* **179** (1986), 278 doi:10.1016/0370-2693(86)90580-0

- [59] M. K. Volkov, A. A. Osipov, A. A. Pivovarov and K. Nurlan, $1/N_c$ approximation and universality of vector mesons, *Phys. Rev. D* **104** (2021) no.3, 034021 doi:10.1103/PhysRevD.104.034021 [arXiv:2105.02160 [hep-ph]].
- [60] F. Giacosa and G. Pagliara, On the spectral functions of scalar mesons, *Phys. Rev. C* **76** (2007), 065204 doi:10.1103/PhysRevC.76.065204 [arXiv:0707.3594 [hep-ph]].
- [61] F. Giacosa, A. Okopińska and V. Shastry, A simple alternative to the relativistic Breit–Wigner distribution, *Eur. Phys. J. A* **57** (2021) no.12, 336 doi:10.1140/epja/s10050-021-00641-2 [arXiv:2106.03749 [hep-ph]].
- [62] F. Giacosa, Multichannel decay law, *Phys. Lett. B* **831** (2022), 137200 doi:10.1016/j.physletb.2022.137200 [arXiv:2108.07838 [quant-ph]].
- [63] P. Ko and S. Rudaz, Phenomenology of scalar and vector mesons in the linear sigma model, *Phys. Rev. D* **50** (1994), 6877-6894 doi:10.1103/PhysRevD.50.6877 J. K. Kim, P. Ko, K. Y. Lee and S. Rudaz, $A_1(1260)$ contribution to photon and dilepton productions from hot hadronic matter: Revisited, *Phys. Rev. D* **53** (1996), 4787-4792 doi:10.1103/PhysRevD.53.4787 [arXiv:hep-ph/9602293 [hep-ph]].
- [64] M. Urban, M. Buballa and J. Wambach, Vector and axial vector correlators in a chirally symmetric model, *Nucl. Phys. A* **697** (2002), 338-371 doi:10.1016/S0375-9474(01)01248-9 [arXiv:hep-ph/0102260 [hep-ph]].
- [65] D. Parganlija, F. Giacosa and D. H. Rischke, Vacuum Properties of Mesons in a Linear Sigma Model with Vector Mesons and Global Chiral Invariance, *Phys. Rev. D* **82** (2010), 054024 doi:10.1103/PhysRevD.82.054024 [arXiv:1003.4934 [hep-ph]].
- [66] A. H. Fariborz, R. Jora and J. Schechter, A. H. Fariborz, R. Jora and J. Schechter, Toy model for two chiral nonets, *Phys. Rev. D* **72** (2005), 034001 doi:10.1103/PhysRevD.72.034001 [arXiv:hep-ph/0506170 [hep-ph]]. A. H. Fariborz, Isosinglet scalar mesons below 2-GeV and the scalar glueball mass, *Int. J. Mod. Phys. A* **19** (2004), 2095-2112 doi:10.1142/S0217751X04018695 [arXiv:hep-ph/0302133 [hep-ph]]. M. Napsuciale and S. Rodriguez, A Chiral model for anti- q q and anti- qq qq mesons, *Phys. Rev. D* **70** (2004), 094043 doi:10.1103/PhysRevD.70.094043 [arXiv:hep-ph/0407037 [hep-ph]].
- [67] W. Bietenholz *et al.* Pion in a Box, *Phys. Lett. B* **687** (2010), 410-414 doi:10.1016/j.physletb.2010.03.063 [arXiv:1002.1696 [hep-lat]].
- [68] K. Langfeld and C. Kettner, The Quark condensate in the GMOR relation, *Mod. Phys. Lett. A* **11** (1996), 1331-1338 doi:10.1142/S0217732396001338 [arXiv:hep-ph/9601370 [hep-ph]].
- [69] P. Kovács and G. Wolf, Meson Vacuum Phenomenology in a Three-flavor Linear Sigma Model with (Axial-)Vector Mesons: Investigation of the $U(1)_A$ Anomaly Term, *Acta Phys. Polon. Supp.* **6** (2013) no.3, 853-858 doi:10.5506/APhysPolBSupp.6.853 [arXiv:1304.5362 [hep-ph]].
- [70] F. Giacosa, A. Koenigstein and R. D. Pisarski, How the axial anomaly controls flavor mixing among mesons, *Phys. Rev. D* **97** (2018) no.9, 091901 doi:10.1103/PhysRevD.97.091901 [arXiv:1709.07454 [hep-ph]].

- [71] F. Giacosa, S. Jafarzade and R. Pisarski, “Anomalous interactions for heterochiral mesons with $J^{PC} = 1^{+-}$ and 2^{-+} , [arXiv:2309.00086 [hep-ph]].
- [72] J. Gasser and H. Leutwyler, Chiral Perturbation Theory to One Loop, *Annals Phys.* **158** (1984), 142 doi:10.1016/0003-4916(84)90242-2 See also S. Scherer, Introduction to chiral perturbation theory, *Adv. Nucl. Phys.* **27** (2003) 277 [arXiv:hep-ph/0210398] and refs. therein.
- [73] A. Koenigstein and F. Giacosa, Phenomenology of pseudotensor mesons and the pseudotensor glueball, *Eur. Phys. J. A* **52** (2016) no.12, 356 doi:10.1140/epja/i2016-16356-x [arXiv:1608.08777 [hep-ph]].
- [74] S. Jafarzade, A. Koenigstein and F. Giacosa, Phenomenology of $J^{PC} = 3^{--}$ tensor mesons, *Phys. Rev. D* **103** (2021) no.9, 096027 doi:10.1103/PhysRevD.103.096027 [arXiv:2101.03195 [hep-ph]].
- [75] A. Athenodorou and M. Teper, The glueball spectrum of SU(3) gauge theory in $3 + 1$ dimensions, *JHEP* **11** (2020), 172 doi:10.1007/JHEP11(2020)172 [arXiv:2007.06422 [hep-lat]].
- [76] E. Trotti, S. Jafarzade and F. Giacosa, Thermodynamics of the glueball resonance gas, *Eur. Phys. J. C* **83** (2023) no.5, 390 doi:10.1140/epjc/s10052-023-11557-0 [arXiv:2212.03272 [hep-ph]].
- [77] H. X. Chen, W. Chen, X. Liu, Y. R. Liu and S. L. Zhu, An updated review of the new hadron states, *Rept. Prog. Phys.* **86** (2023) no.2, 026201 doi:10.1088/1361-6633/aca3b6 [arXiv:2204.02649 [hep-ph]].
- [78] G. J. Gounaris, J. E. Paschalis and R. Kogerler, The 0 Spin Glueballs: A New Approach to Relativistic Bound States, *Z. Phys. C* **31** (1986), 277 [erratum: *Z. Phys. C* **33** (1987), 474] doi:10.1007/BF01479537
- [79] V. A. Novikov, L. B. Okun, M. A. Shifman, A. I. Vainshtein, M. B. Voloshin and V. I. Zakharov, Charmonium and Gluons: Basic Experimental Facts and Theoretical Introduction, *Phys. Rept.* **41** (1978), 1-133 doi:10.1016/0370-1573(78)90120-5 M. Campostrini, A. Di Giacomo and Y. Gunduc, Gluon Condensation in SU(3) Lattice Gauge Theory, *Phys. Lett. B* **225** (1989), 393-397 doi:10.1016/0370-2693(89)90588-1
- [80] F. Giacosa, A. Pilloni and E. Trotti, Glueball–glueball scattering and the glueballonium, *Eur. Phys. J. C* **82** (2022) no.5, 487 doi:10.1140/epjc/s10052-022-10403-z [arXiv:2110.05582 [hep-ph]].
- [81] W. J. Lee and D. Weingarten, *Phys. Rev. D* **61** (2000), 014015 doi:10.1103/PhysRevD.61.014015 [arXiv:hep-lat/9910008 [hep-lat]].
- [82] F. Giacosa, T. Gutsche, V. E. Lyubovitskij and A. Faessler, Scalar nonet quarkonia and the scalar glueball: Mixing and decays in an effective chiral approach, *Phys. Rev. D* **72** (2005), 094006 doi:10.1103/PhysRevD.72.094006 [arXiv:hep-ph/0509247 [hep-ph]].
- [83] H. Y. Cheng, C. K. Chua and K. F. Liu, Scalar glueball, scalar quarkonia, and their mixing, *Phys. Rev. D* **74** (2006), 094005 doi:10.1103/PhysRevD.74.094005 [arXiv:hep-ph/0607206 [hep-ph]].
- [84] F. Br  nner, D. Parganlija and A. Rebhan, Glueball Decay Rates in the Witten-Sakai-Sugimoto Model, *Phys. Rev. D* **91** (2015)

- no.10, 106002 [erratum: Phys. Rev. D **93** (2016) no.10, 109903] doi:10.1103/PhysRevD.91.106002 [arXiv:1501.07906 [hep-ph]].
- [85] L. C. Gui *et al.* [CLQCD], Scalar Glueball in Radiative J/ψ Decay on the Lattice, Phys. Rev. Lett. **110** (2013) no.2, 021601 doi:10.1103/PhysRevLett.110.021601 [arXiv:1206.0125 [hep-lat]].
 - [86] W. I. Eshraim, S. Janowski, F. Giacosa and D. H. Rischke, Decay of the pseudoscalar glueball into scalar and pseudoscalar mesons, Phys. Rev. D **87** (2013) no.5, 054036 doi:10.1103/PhysRevD.87.054036 [arXiv:1208.6474 [hep-ph]].
 - [87] M. Ablikim *et al.* [(BESIII Collaboration)* and BESIII], Observation of a State $X(2600)$ in the $\pi^+\pi^-\eta'$ System in the Process $J/\psi \rightarrow \gamma\pi^+\pi^-\eta'$, Phys. Rev. Lett. **129** (2022) no.4, 042001 doi:10.1103/PhysRevLett.129.042001 [arXiv:2201.10796 [hep-ex]].
 - [88] F. Giacosa, J. Sammet and S. Janowski, Decays of the vector glueball, Phys. Rev. D **95** (2017) no.11, 114004 doi:10.1103/PhysRevD.95.114004 [arXiv:1607.03640 [hep-ph]].
 - [89] A. Vereijken, S. Jafarzade, M. Piotrowska and F. Giacosa, Is $f_2(1950)$ the tensor glueball?, Phys. Rev. D **108** (2023) no.1, 014023 doi:10.1103/PhysRevD.108.014023 [arXiv:2304.05225 [hep-ph]].
 - [90] F. Hechenberger, J. Leutgeb and A. Rebhan, Radiative meson and glueball decays in the Witten-Sakai-Sugimoto model, Phys. Rev. D **107** (2023) no.11, 114020 doi:10.1103/PhysRevD.107.114020 [arXiv:2302.13379 [hep-ph]].
 - [91] F. Hechenberger, J. Leutgeb and A. Rebhan, Spin-1 Glueballs in the Witten-Sakai-Sugimoto Model, [arXiv:2401.17986 [hep-ph]].
 - [92] C. A. Meyer and E. S. Swanson, Hybrid Mesons, Prog. Part. Nucl. Phys. **82** (2015), 21-58 doi:10.1016/j.ppnp.2015.03.001 [arXiv:1502.07276 [hep-ph]].
 - [93] J. J. Dudek, R. G. Edwards, M. J. Peardon, D. G. Richards and C. E. Thomas, Toward the excited meson spectrum of dynamical QCD, Phys. Rev. D **82** (2010), 034508 doi:10.1103/PhysRevD.82.034508 [arXiv:1004.4930 [hep-ph]]. J. J. Dudek *et al.* [Hadron Spectrum], Toward the excited isoscalar meson spectrum from lattice QCD, Phys. Rev. D **88** (2013) no.9, 094505 doi:10.1103/PhysRevD.88.094505 [arXiv:1309.2608 [hep-lat]].
 - [94] V. Shastry, C. S. Fischer and F. Giacosa, The phenomenology of the exotic hybrid nonet with $\pi_1(1600)$ and $\eta_1(1855)$, Phys. Lett. B **834** (2022), 137478 doi:10.1016/j.physletb.2022.137478 [arXiv:2203.04327 [hep-ph]]; V. Shastry and F. Giacosa, Radiative production and decays of the exotic $\eta_1'(1855)$ and its siblings, Nucl. Phys. A **1037** (2023), 122683 doi:10.1016/j.nuclphysa.2023.122683 [arXiv:2302.07687 [hep-ph]].
 - [95] W. I. Eshraim, C. S. Fischer, F. Giacosa and D. Parganlija, Hybrid phenomenology in a chiral approach, Eur. Phys. J. Plus **135** (2020) no.12, 945 doi:10.1140/epjp/s13360-020-00900-z [arXiv:2001.06106 [hep-ph]].
 - [96] V. Baru, J. Haidenbauer, C. Hanhart, Y. Kalashnikova and A. E. Kudryavtsev, Evidence that the $a(0)(980)$ and $f(0)(980)$ are not elementary particles, Phys. Lett. B **586** (2004), 53-61 doi:10.1016/j.physletb.2004.01.088 [arXiv:hep-ph/0308129 [hep-ph]].

- [97] T. Branz, T. Gutsche and V. E. Lyubovitskij, Strong and radiative decays of the scalars $f_0(980)$ and $a_0(980)$ in a hadronic molecule approach, *Phys. Rev. D* **78** (2008), 114004 doi:10.1103/PhysRevD.78.114004 [arXiv:0808.0705 [hep-ph]].
- [98] A. A. Petrov, Glueball-meson molecules, *Phys. Lett. B* **843** (2023), 138030 doi:10.1016/j.physletb.2023.138030 [arXiv:2204.11269 [hep-ph]].
- [99] M. Boglione and M. R. Pennington, Dynamical generation of scalar mesons, *Phys. Rev. D* **65** (2002), 114010 doi:10.1103/PhysRevD.65.114010 [arXiv:hep-ph/0203149 [hep-ph]].
- [100] T. Wolkanowski, F. Giacosa and D. H. Rischke, $a_0(980)$ revisited, *Phys. Rev. D* **93** (2016) no.1, 014002 doi:10.1103/PhysRevD.93.014002 [arXiv:1508.00372 [hep-ph]].
- [101] J. R. Peláez, On the Nature of light scalar mesons from their large $N(c)$ behavior, *Phys. Rev. Lett.* **92** (2004), 102001 doi:10.1103/PhysRevLett.92.102001 [arXiv:hep-ph/0309292 [hep-ph]].
- [102] J. R. Peláez, From controversy to precision on the sigma meson: a review on the status of the non-ordinary $f_0(500)$ resonance, *Phys. Rept.* **658** (2016), 1 doi:10.1016/j.physrep.2016.09.001 [arXiv:1510.00653 [hep-ph]].
- [103] J. R. Peláez, A. Rodas and J. Ruiz de Elvira, *Eur. Phys. J. C* **77** (2017) no.2, 91 doi:10.1140/epjc/s10052-017-4668-1 [arXiv:1612.07966 [hep-ph]].
- [104] T. Wolkanowski, M. Soltysiak and F. Giacosa, $K_0^*(800)$ as a companion pole of $K_0^*(1430)$, *Nucl. Phys. B* **909** (2016), 418-428 doi:10.1016/j.nuclphysb.2016.05.025 [arXiv:1512.01071 [hep-ph]].
- [105] F. Giacosa, M. Piotrowska and S. Coito, $X(3872)$ as virtual companion pole of the charm-anticharm state $\chi_{c1}(2P)$, *Int. J. Mod. Phys. A* **34** (2019) no.29, 1950173 doi:10.1142/S0217751X19501732 [arXiv:1903.06926 [hep-ph]].
- [106] E. van Beveren, T. A. Rijken, K. Metzger, C. Dullemond, G. Rupp and J. E. Ribeiro, A Low Lying Scalar Meson Nonet in a Unitarized Meson Model, *Z. Phys. C* **30** (1986), 615-620 doi:10.1007/BF01571811 [arXiv:0710.4067 [hep-ph]].
 E. van Beveren, D. V. Bugg, F. Kleefeld and G. Rupp, *Phys. Lett. B* **641** (2006), 265-271 doi:10.1016/j.physletb.2006.08.051 [arXiv:hep-ph/0606022 [hep-ph]].
 J. A. Oller and E. Oset, Chiral symmetry amplitudes in the S wave isoscalar and isovector channels and the σ , $f_0(980)$, $a_0(980)$ scalar mesons, *Nucl. Phys. A* **620** (1997), 438-456 [erratum: *Nucl. Phys. A* **652** (1999), 407-409] doi:10.1016/S0375-9474(97)00160-7 [arXiv:hep-ph/9702314 [hep-ph]].
 J. A. Oller, E. Oset and J. R. Peláez, Meson meson interaction in a non-perturbative chiral approach, *Phys. Rev. D* **59** (1999), 074001 [erratum: *Phys. Rev. D* **60** (1999), 099906; erratum: *Phys. Rev. D* **75** (2007), 099903] doi:10.1103/PhysRevD.59.074001 [arXiv:hep-ph/9804209 [hep-ph]].
- [107] F. Giacosa, Dynamical generation and dynamical reconstruction, *Phys. Rev. D* **80** (2009), 074028 doi:10.1103/PhysRevD.80.074028 [arXiv:0903.4481 [hep-ph]].

- [108] Z. H. Guo, L. Y. Xiao and H. Q. Zheng, Is the $f_0(600)$ meson a dynamically generated resonance? A Lesson learned from the $O(N)$ model and beyond, *Int. J. Mod. Phys. A* **22** (2007), 4603-4616 doi:10.1142/S0217751X0703710X [arXiv:hep-ph/0610434 [hep-ph]].
- [109] R. L. Jaffe, Multi-Quark Hadrons. 1. The Phenomenology of (2 Quark 2 anti-Quark) Mesons, *Phys. Rev. D* **15** (1977), 267 doi:10.1103/PhysRevD.15.267
- [110] R. L. Jaffe, Exotica, *Phys. Rept.* **409** (2005), 1-45 doi:10.1016/j.physrep.2004.11.005 [arXiv:hep-ph/0409065 [hep-ph]].
- [111] L. Maiani, F. Piccinini, A. D. Polosa and V. Riquer, A New look at scalar mesons, *Phys. Rev. Lett.* **93** (2004), 212002 doi:10.1103/PhysRevLett.93.212002 [arXiv:hep-ph/0407017 [hep-ph]].
- [112] F. Giacosa, Strong and electromagnetic decays of the light scalar mesons interpreted as tetraquark states, *Phys. Rev. D* **74** (2006), 014028 doi:10.1103/PhysRevD.74.014028 [arXiv:hep-ph/0605191 [hep-ph]].
- [113] F. Giacosa, Mixing of scalar tetraquark and quarkonia states in a chiral approach, *Phys. Rev. D* **75** (2007), 054007 doi:10.1103/PhysRevD.75.054007 [arXiv:hep-ph/0611388 [hep-ph]].
- [114] L. Olbrich, M. Zétényi, F. Giacosa and D. H. Rischke, Influence of the axial anomaly on the decay $N(1535) \rightarrow N\eta$, *Phys. Rev. D* **97** (2018) no.1, 014007 doi:10.1103/PhysRevD.97.014007 [arXiv:1708.01061 [hep-ph]].
- [115] V. Koch, Aspects of chiral symmetry, *Int. J. Mod. Phys. E* **6** (1997), 203-250 doi:10.1142/S0218301397000147 [arXiv:nucl-th/9706075 [nucl-th]].
- [116] C. E. Detar and T. Kunihiro, Linear σ Model With Parity Doubling, *Phys. Rev. D* **39** (1989), 2805 doi:10.1103/PhysRevD.39.2805
- [117] D. Zschesche, L. Tolos, J. Schaffner-Bielich and R. D. Pisarski, Cold, dense nuclear matter in a $SU(2)$ parity doublet model, *Phys. Rev. C* **75** (2007), 055202 doi:10.1103/PhysRevC.75.055202 [arXiv:nucl-th/0608044 [nucl-th]].
- [118] S. Gallas, F. Giacosa and D. H. Rischke, Vacuum phenomenology of the chiral partner of the nucleon in a linear sigma model with vector mesons, *Phys. Rev. D* **82** (2010), 014004 doi:10.1103/PhysRevD.82.014004 [arXiv:0907.5084 [hep-ph]].
- [119] S. Gallas, F. Giacosa and G. Pagliara, Nuclear matter within a dilatation-invariant parity doublet model: the role of the tetraquark at nonzero density, *Nucl. Phys. A* **872** (2011), 13-24 doi:10.1016/j.nuclphysa.2011.09.008 [arXiv:1105.5003 [hep-ph]].
- [120] R. A. Tripolt, C. Jung, L. von Smekal and J. Wambach, Vector and axial-vector mesons in nuclear matter, *Phys. Rev. D* **104** (2021) no.5, 054005 doi:10.1103/PhysRevD.104.054005 [arXiv:2105.00861 [hep-ph]].
- [121] P. Lakaschus, J. L. P. Mauldin, F. Giacosa and D. H. Rischke, *Phys. Rev. C* **99** (2019) no.4, 045203 doi:10.1103/PhysRevC.99.045203 [arXiv:1807.03735 [hep-ph]].
- [122] L. Olbrich, M. Zétényi, F. Giacosa and D. H. Rischke, Three-flavor chiral effective model with four baryonic multiplets within the mirror assignment, *Phys. Rev. D* **93** (2016) no.3, 034021 doi:10.1103/PhysRevD.93.034021 [arXiv:1511.05035 [hep-ph]].

- [123] H. Satz, The Thermodynamics of Quarks and Gluons, Lect. Notes Phys. **785** (2010), 1-21 doi:10.1007/978-3-642-02286-9_1 [arXiv:0803.1611 [hep-ph]].
H. Satz, The Quark-Gluon Plasma: A Short Introduction, Nucl. Phys. A **862-863** (2011), 4-12 doi:10.1016/j.nuclphysa.2011.05.014 [arXiv:1101.3937 [hep-ph]].
- [124] J. T. Lenaghan, D. H. Rischke and J. Schaffner-Bielich, Chiral symmetry restoration at nonzero temperature in the $SU(3)_c \times SU(3)_L$ linear sigma model, Phys. Rev. D **62** (2000), 085008 doi:10.1103/PhysRevD.62.085008 [arXiv:nucl-th/0004006 [nucl-th]].
- [125] N. K. Glendenning, Compact stars: Nuclear physics, particle physics, and general relativity, Springer Verlag, 2000.
- [126] A. Heinz, S. Struber, F. Giacosa and D. H. Rischke, Role of the tetraquark in the chiral phase transition, Phys. Rev. D **79** (2009), 037502 doi:10.1103/PhysRevD.79.037502 [arXiv:0805.1134 [hep-ph]].
- [127] R. D. Pisarski and F. Rennecke, The chiral phase transition and the axial anomaly, [arXiv:2401.06130 [hep-ph]].
- [128] M. Gazdzicki, M. Gorenstein and P. Seyboth, Onset of deconfinement in nucleus-nucleus collisions: Review for pedestrians and experts, Acta Phys. Polon. B **42** (2011), 307-351 doi:10.5506/APhysPolB.42.307 [arXiv:1006.1765 [hep-ph]].
- [129] H. Adhikary *et al.* [NA61/SHINE], Search for the critical point of strongly-interacting matter in $^{40}\text{Ar} + ^{45}\text{Sc}$ collisions at 150A Ge V /c using scaled factorial moments of protons, Eur. Phys. J. C **83** (2023) no.9, 881 doi:10.1140/epjc/s10052-023-11942-9 [arXiv:2305.07557 [nucl-ex]]. M. I. Gorenstein, M. Gazdzicki and W. Greiner, Critical line of the deconfinement phase transitions,” Phys. Rev. C **72** (2005), 024909 doi:10.1103/PhysRevC.72.024909 [arXiv:nucl-th/0505050 [nucl-th]].
- [130] G. Pagliara and J. Schaffner-Bielich, Stability of CFL cores in Hybrid Stars, Phys. Rev. D **77** (2008), 063004 doi:10.1103/PhysRevD.77.063004 [arXiv:0711.1119 [astro-ph]].